

Chinook Salmon Passage in the Kenai River at River Mile 13.7 Using Adaptive Resolution Imaging Sonar, 2013

by

James D. Miller

Debby L. Burwen

Brandon H. Key

and

Steven J. Fleischman

July 2016

Alaska Department of Fish and Game

Divisions of Sport Fish and Commercial Fisheries



Symbols and Abbreviations

The following symbols and abbreviations, and others approved for the Système International d'Unités (SI), are used without definition in the following reports by the Divisions of Sport Fish and of Commercial Fisheries: Fishery Manuscripts, Fishery Data Series Reports, Fishery Management Reports, and Special Publications. All others, including deviations from definitions listed below, are noted in the text at first mention, as well as in the titles or footnotes of tables, and in figure or figure captions.

Weights and measures (metric)		General		Mathematics, statistics		
centimeter	cm	Alaska Administrative Code	AAC	<i>all standard mathematical signs, symbols and abbreviations</i>		
deciliter	dL	all commonly accepted abbreviations	e.g., Mr., Mrs., AM, PM, etc.	alternate hypothesis	H _A	
gram	g	all commonly accepted professional titles	e.g., Dr., Ph.D., R.N., etc.	base of natural logarithm	<i>e</i>	
hectare	ha			catch per unit effort	CPUE	
kilogram	kg			coefficient of variation	CV	
kilometer	km	at compass directions:	@	common test statistics	(F, t, χ^2 , etc.)	
liter	L			confidence interval	CI	
meter	m			correlation coefficient (multiple)	R	
milliliter	mL			correlation coefficient (simple)	r	
millimeter	mm			covariance	cov	
Weights and measures (English)				east	E	degree (angular)
		north	N	degrees of freedom	df	
	cubic feet per second	ft ³ /s	south	S	expected value	<i>E</i>
	foot	ft	west	W	greater than	>
	gallon	gal	copyright	©	greater than or equal to	≥
	inch	in	corporate suffixes:		harvest per unit effort	HPUE
	mile	mi	Company	Co.	less than	<
	nautical mile	nmi	Corporation	Corp.	less than or equal to	≤
	ounce	oz	Incorporated	Inc.	logarithm (natural)	ln
	pound	lb	Limited	Ltd.	logarithm (base 10)	log
quart	qt	District of Columbia	D.C.	logarithm (specify base)	log ₂ , etc.	
yard	yd	et alii (and others)	et al.	minute (angular)	'	
Time and temperature		et cetera (and so forth)	etc.	not significant	NS	
		exempli gratia		null hypothesis	H ₀	
	day	d	(for example)	e.g.	percent	%
	degrees Celsius	°C	Federal Information Code	FIC	probability	P
	degrees Fahrenheit	°F	id est (that is)	i.e.	probability of a type I error (rejection of the null hypothesis when true)	α
	degrees kelvin	K	latitude or longitude	lat or long	probability of a type II error (acceptance of the null hypothesis when false)	β
	hour	h	monetary symbols (U.S.)	\$, ¢	second (angular)	"
	minute	min	months (tables and figures): first three letters	Jan,...,Dec	standard deviation	SD
	second	s	registered trademark	®	standard error	SE
	Physics and chemistry		trademark	™	variance	
all atomic symbols				population sample	Var var	
alternating current		AC	United States (adjective)	U.S.		
ampere		A	United States of America (noun)	USA		
calorie		cal	U.S.C.	United States Code		
direct current		DC	U.S. state	use two-letter abbreviations (e.g., AK, WA)		
hertz		Hz				
horsepower		hp				
hydrogen ion activity (negative log of)		pH				
parts per million		ppm				
parts per thousand	ppt, ‰					
vols	V					
watts	W					

FISHERY DATA SERIES NO. 16-15

**CHINOOK SALMON PASSAGE IN THE KENAI RIVER AT RIVER MILE
13.7 USING ADAPTIVE RESOLUTION IMAGING SONAR, 2013**

by
James D. Miller
Debby L. Burwen (retired)
Brandon H. Key
and
Steven J. Fleischman

Alaska Department of Fish and Game
Division of Sport Fish, Research and Technical Services
333 Raspberry Road, Anchorage, Alaska, 99518-1565

July 2016

This investigation was partially financed by the Federal Aid in Sport Fish Restoration Act
(16 U.S.C. 777-777K) under Project F-10-14 Job No. S-2-5b.

ADF&G Fishery Data Series was established in 1987 for the publication of Division of Sport Fish technically oriented results for a single project or group of closely related projects, and in 2004 became a joint divisional series with the Division of Commercial Fisheries. Fishery Data Series reports are intended for fishery and other technical professionals and are available through the Alaska State Library and on the Internet: <http://www.adfg.alaska.gov/sf/publications/>. This publication has undergone editorial and peer review.

*James D. Miller,
Alaska Department of Fish and Game, Division of Sport Fish
333 Raspberry Road, Anchorage, Alaska 99518-1599, USA*

*Debby L. Burwen (retired),
Alaska Department of Fish and Game, Division of Sport Fish
333 Raspberry Road, Anchorage, Alaska 99518-1599, USA*

*Brandon H. Key,
Alaska Department of Fish and Game, Division of Sport Fish
43961 Kalifornsky Beach Road Suite B, Soldotna Alaska 99669-8276, USA*

and

*Steven J. Fleischman
Alaska Department of Fish and Game, Division of Sport Fish, Research and Technical Services
333 Raspberry Road, Anchorage, Alaska 99518-1599, USA*

This document should be cited as follows:

Miller, J. D., D. L. Burwen, B. H. Key, and S. J. Fleischman. 2016. Chinook salmon passage in the Kenai River at River Mile 13.7 using adaptive resolution imaging sonar, 2013. Alaska Department of Fish and Game, Fishery Data Series No. 16-15, Anchorage.

The Alaska Department of Fish and Game (ADF&G) administers all programs and activities free from discrimination based on race, color, national origin, age, sex, religion, marital status, pregnancy, parenthood, or disability. The department administers all programs and activities in compliance with Title VI of the Civil Rights Act of 1964, Section 504 of the Rehabilitation Act of 1973, Title II of the Americans with Disabilities Act (ADA) of 1990, the Age Discrimination Act of 1975, and Title IX of the Education Amendments of 1972.

If you believe you have been discriminated against in any program, activity, or facility please write:

ADF&G ADA Coordinator, P.O. Box 115526, Juneau, AK 99811-5526
U.S. Fish and Wildlife Service, 4401 N. Fairfax Drive, MS 2042, Arlington, VA 22203
Office of Equal Opportunity, U.S. Department of the Interior, 1849 C Street NW MS 5230, Washington DC 20240

The department's ADA Coordinator can be reached via phone at the following numbers:
(VOICE) 907-465-6077, (Statewide Telecommunication Device for the Deaf) 1-800-478-3648,
(Juneau TDD) 907-465-3646, or (FAX) 907-465-6078

For information on alternative formats and questions on this publication, please contact:
ADF&G, Division of Sport Fish, Research and Technical Services, 333 Raspberry Rd, Anchorage AK 99518 (907) 267-2375

TABLE OF CONTENTS

	Page
LIST OF TABLES.....	ii
LIST OF FIGURES	iii
LIST OF APPENDICES	iv
ABSTRACT	1
INTRODUCTION.....	1
METHODS.....	3
Study Area.....	3
Site Description	3
Acoustic Sampling.....	3
Sonar System Configuration and River Coverage	4
Sampling Procedure.....	5
Data Collection Parameters	5
Manual ARIS Fish Length Measurements.....	7
Netted Fish Length Measurements	8
Data Analysis.....	8
Fish Passage.....	8
Chinook Salmon Passage.....	9
Tethered Fish Data Collection	10
RESULTS.....	11
Size Distribution and Species Composition.....	11
Spatial and Temporal Distribution.....	12
Direction of Travel	12
Medium and Large Fish Passage	13
Chinook Salmon Passage.....	13
Small Fish Passage	13
Tethered Fish Measurements	13
DISCUSSION.....	14
Chinook Salmon Abundance	14
Tethered Fish Measurements	16
Recommendations	17
ACKNOWLEDGEMENTS.....	18
REFERENCES CITED	19
TABLES	23
FIGURES	41
APPENDIX A: COMPARISON OF DIDSON AND ARIS CONFIGURATIONS	65
APPENDIX B: INSTRUCTIONS AND SETTINGS FOR MANUAL FISH LENGTH MEASUREMENTS.....	87
APPENDIX C: ARIS LENGTH MIXTURE MODEL AND ASSOCIATED BUGS PROGRAM CODE	99
APPENDIX D: SPATIAL AND TEMPORAL DISTRIBUTION OF FISH BY SIZE AS MEASURED BY ARIS, RM 13.7 KENAI RIVER, 2013.....	107

TABLE OF CONTENTS (Continued)

	Page
APPENDIX E: DIRECTION OF TRAVEL OF MEDIUM AND LARGE FISH DETECTED BY ARIS, RM 13.7 KENAI RIVER, 2013.....	115

LIST OF TABLES

Table	Page
1. On-site components of the ARIS systems used in 2013.....	24
2. Summary of sonar stratum range changes by date at RM 13.7 Kenai River, 2013.	25
3. Sampling schedule and parameter values on 19 July 2013 for each range stratum sampled by 5 ARIS systems in 2013.	26
4. Select user-configurable parameters in Sound Metrics Corporation ARIScope data collection software and their corresponding values in DIDSON.....	27
5. Spatial and temporal distribution of upstream-bound medium and large fish, by river bank, transducer, and time at RM 13.7 for the Kenai River early and late runs, 2013.....	28
6. Percentage of all fish migrating downstream, by river bank, transducer, and fish size at RM 13.7 for the 2013 Kenai River early and late runs.	29
7. Estimates of net upstream daily passage of medium and large Chinook salmon at RM 13.7 Kenai River, early run 2013.....	30
8. Estimates of net upstream daily passage of medium and large Chinook salmon at RM 13.7 Kenai River, late run 2013.....	31
9. ARIS-length mixture model net upstream passage estimates for Chinook salmon and for small Chinook salmon, RM 13.7 Kenai River, early run 2013.....	33
10. ARIS-length mixture model net upstream passage estimates for Chinook salmon and for small Chinook salmon, RM 13.7 Kenai River, late run 2013.	34
11. Daily estimates of Chinook salmon age composition derived from fitting a mixture model to length measurements from ARIS at RM 13.7 and midriver gillnet catches from RM 8.6, Kenai River early run 2013.....	35
12. Daily estimates of Chinook salmon age composition derived from fitting a mixture model to length measurements from ARIS at RM 13.7 and midriver gillnet catches from RM 8.6, Kenai River late run 2013.....	37
13. ARIS-based length measurements at low and high frequency for 3 tethered salmon at RM 8.6 Kenai River on 17 July 2013.	39
14. ARIS-based length measurements for 2 tethered salmon sampled at close and far range.....	40

LIST OF FIGURES

Figure	Page
1. Cook Inlet showing the location of the Kenai River.	42
2. Map of Kenai River showing location of Chinook salmon sonar sites at river miles 8.6 and 13.7.	43
3. Sonar sites showing approximate beam coverage at RM 8.6 and RM 13.7 of the Kenai River.	44
4. Location of 9 transects conducted at the RM 13.7 site on 9 July 2012.	45
5. Corresponding profiles for 8 transects conducted near RM 13.7 of the Kenai River with respect to Figure 4.	46
6. Approximate coverage by nearshore and offshore sonars for the right bank and left bank main channel at RM 13.7 of the Kenai River.	47
7. Sonar coverage of the minor channel at the RM 13.7 sonar site was achieved using an ARIS 1200 deployed on a tripod mount combined with a fixed weir.	48
8. An ARIS 1200 with a high-resolution lens mounted on a steel tripod for offshore deployment and on an aluminum H-mount for nearshore deployment.	49
9. ARIS data collection schematic for the RM 13.7 site on the Kenai River.	50
10. Diagram showing components required on the right bank for wireless transmission of ARIS data to a data-collection computer located in the left-bank sonar tent.	51
11. Schematic for 4 left-bank and 5 right-bank range strata on the main channel of the Kenai River at RM 13.7.	52
12. Example images from each of the 4 left-bank and 5 right-bank range strata taken at RM 13.7 Kenai River on 8 August 2013.	53
13. ARISFish display window showing an echogram with traces of migrating fish that can be simultaneously displayed in video mode where fish images can be enlarged and measured.	54
14. Frequency distributions of ARIS lengths by bank at RM 13.7, DIDSON lengths by bank at RM 8.6, and mid eye to tail fork (METF) lengths by species from an onsite netting project, Kenai River early and late runs, 2013.	55
15. Horizontal distribution, in 5 m increments from the left-bank main channel shore to the right-bank minor channel shore, of medium and large early- and late-run fish, measured from ARIS, RM 13.7 Kenai River, 2013.	56
16. Weekly proportions of fish greater than 75 cm AL migrating upstream at night, compared to relative night duration in Kenai, Alaska.	57
17. Estimated net upstream passage of Chinook salmon based on an ARIS-length mixture model and estimated net upstream passage of medium and large Chinook salmon greater than or equal to 75 cm ARIS length and large Chinook salmon greater than or equal to 90 cm, for early-run and late-run Kenai River Chinook salmon, 2013.	58
18. Daily discharge rates collected at the Soldotna Bridge and Secchi disk readings taken at the RM 13.7 sonar site; ARIS-length mixture model estimates of net upstream Chinook salmon passage at RM 13.7, inriver gillnet Chinook salmon CPUE at RM 8.6, and sport fishery CPUE; and spatially expanded DIDSON-length mixture model (DLMM) upstream-only Chinook salmon passage at RM 8.6 compared to ALMM, Kenai River early run, 2013.	59
19. Daily discharge rates collected at the Soldotna Bridge and Secchi disk readings taken at the RM 13.7 sonar site; ARIS-length mixture model estimates of net upstream Chinook salmon passage at RM 13.7, inriver gillnet Chinook salmon CPUE at RM 8.6, and Chinook salmon sport fishery CPUE; RM 19 sockeye salmon sonar passage and inriver gillnet sockeye salmon CPUE at RM 8.6; and spatially expanded DIDSON-length mixture model upstream-only Chinook salmon passage at RM 8.6 compared to ALMM, late run Kenai River, 2013.	60
20. Images from 3 tethered salmon, collected at RM 8.6 Kenai River on 17 July 2013.	61
21. Three images collected at low frequency from a 116 cm tethered Chinook salmon.	62
22. Images from a 68.5 cm sockeye salmon tethered at far range that show a strong 4-pixel image, an ambiguous 5-pixel image where the tail is not yet distinct, and a strong 5-pixel image.	63
23. Images from a 68.5 cm sockeye salmon tethered at close range.	64

LIST OF APPENDICES

Appendix	Page
A1. Comparison of DIDSON and ARIS configurations including an overview of features that affect resolution and range capabilities.	66
A2. Summary of manufacturer specifications for maximum range, individual beam dimensions, and spacing for DIDSON SV, DIDSON LR, ARIS 1800, and ARIS 1200 systems at 2 frequencies, with and without the addition of a high resolution lens.....	71
A3. Manufacturer specifications for models ARIS 1200, ARIS 1800, DIDSON SV, and DIDSON LR.	72
A4. Diagram showing the horizontal plane of a DIDSON LR or ARIS 1200 with a high-resolution lens.	76
A5. Relationships between focal length and lens position for ARIS.	77
A6. An enlargement of a tethered Chinook salmon showing the individual pixels that compose a DIDSON image contrasted with an ARIS image of a free-swimming Chinook salmon.....	78
A7. Downrange resolution for ARIS images is set using the “Detail” slider under the expanded “Sonar Control” dialog window or by setting the “Sample Period” under the “Advanced Sonar Settings” dialog window.	79
A8. Summary of ARIScope data acquisition parameters that affect downrange resolution.....	80
A9. Images from a close-range tethered fish at 2 different range windows demonstrate the advantage of a shorter range window and higher sample period for close-range sampling.	82
A10. Images from a 68.5 cm sockeye salmon demonstrate a measurement bias at ranges less than 3.5 m, even with the short 5 m range window.	83
A11. Data collected from tethered fish provided the opportunity to compare the effects and inter-relationship between 2 parameters affecting image resolution: transmitted pulse length and sample period.	84
A12. Images of a tethered fish taken at 2 different aims	85
B1. Instructions and settings for manual length measurements from ARIS images generated in 2013 using SMC ARISFish software Version 1.5 REV 575.	88
B2. To avoid counting this fish in both Stratum 2 and Stratum 3, the fish will only be counted in Stratum 3 where it crosses the centerline of the beam.	94
B3. Specific examples for applying the “centerline” rule when selecting fish for counting and measurements.	95
C1. Mixture model description.	100
C2. Flow chart of a mixture model.	102
C3. Methodology used for fitting the mixture model.....	103
C4. WinBUGS code for ARIS length mixture model.	104
C6. Abridged tethered fish data set used to provide a mildly informative prior distribution for the relationship between fork length and ARIS length.....	105
C7. Methodological details of ARIS length mixture models compared to DIDSON length mixture models at RM 8.6, Kenai River, 2013.	106
D1. Spatial and temporal distribution of small (ARIS length [AL] < 75 cm), medium (75 cm ≤ AL < 90 cm), and large fish (AL ≥ 90 cm), RM 13.7 Kenai River, 17–29 May 2013.....	108
D2. Spatial and temporal distribution of small (ARIS length [AL] < 75 cm), medium (75 cm ≤ AL < 90 cm), and large fish (AL ≥ 90 cm), RM 13.7 Kenai River, 30 May–12 June 2013.	109
D3. Spatial and temporal distribution of small (ARIS length [AL] < 75 cm), medium (75 cm ≤ AL < 90 cm), and large fish (AL ≥ 90 cm), RM 13.7 Kenai River, 13–26 June 2013.....	110
D4. Spatial and temporal distribution of small (ARIS length [AL] < 75 cm), medium (75 cm ≤ AL < 90 cm), and large fish (AL ≥ 90 cm), RM 13.7 Kenai River, 27 June–10 July 2013.	111
D5. Spatial and temporal distribution of small (ARIS length [AL] < 75 cm), medium (75 cm ≤ AL < 90 cm), and large fish (AL ≥ 90 cm), RM 13.7 Kenai River, 11–24 July 2013.	112
D6. Spatial and temporal distribution of small (ARIS length [AL] < 75 cm), medium (75 cm ≤ AL < 90 cm), and large fish (AL ≥ 90 cm), RM 13.7 Kenai River, 25 July–7 August 2013.....	113
D7. Spatial and temporal distribution of small (ARIS length [AL] < 75 cm), medium (75 cm ≤ AL < 90 cm), and large fish (AL ≥ 90 cm), RM 13.7 Kenai River, 8–17 August 2013.	114
E1. Daily count and proportion of fish greater than or equal to 75 cm ARIS length moving upstream and downstream for the early run, RM 13.7 Kenai River, 2013.	116
E2. Daily count and proportion of fish greater than or equal to 75 cm ARIS length moving upstream and downstream for the late run, RM 13.7 Kenai River, 2013.....	118

ABSTRACT

In 2013, Kenai River Chinook salmon (*Oncorhynchus tshawytscha*) passage was estimated using Adaptive Resolution Imaging Sonar (ARIS) at a newly established site at river mile 13.7. Medium and large Chinook salmon (greater than or equal to 75 cm as measured by ARIS) were directly assessed by the sonar, yielding net upstream passage estimates of 1,724 (SE 93) during the early run (17 May–30 June) and 12,656 (SE 282) during the late run (1 July–17 August). Smaller Chinook salmon (less than 75 cm ARIS length) overlap in size with other species; thus, a combination of sonar, netting, telemetry, and weir data from this and other projects are required for assessing the abundance of all Kenai River Chinook salmon regardless of size. During the 2013 early run, telemetry and weir data were used to obtain a net upstream passage estimate of 2,806 (SE 341) small Chinook salmon; this estimate was combined with the ARIS estimate of medium and large Chinook salmon for a total of 4,530 (SE 353) Chinook salmon regardless of size. During the late run, a mixture model was fitted to sonar and netting data to obtain a net upstream passage estimate of 19,373 (SE 583) Chinook salmon regardless of size.

Key words: ARIS, Chinook salmon, *Oncorhynchus tshawytscha*, acoustic assessment, Kenai River, riverine sonar

INTRODUCTION

Chinook salmon (*Oncorhynchus tshawytscha*) returning to the Kenai River (Figure 1) are managed as 2 distinct runs (Burger et al. 1985): early (mid-May–30 June) and late (1 July–mid-August). Early-run Chinook salmon are harvested primarily by sport anglers, and late-run Chinook salmon are harvested by commercial, sport, subsistence, and personal use fisheries. These fisheries may be restricted or liberalized if the projected escapement falls below or above goals adopted by the Alaska Board of Fisheries (BOF). These goals are defined by Alaska Administrative Codes 5 AAC 56.070 (*Kenai River and Kasilof River Early-Run King Salmon Conservation Management Plan*) and 5 AAC 21.359 (*Kenai River Late-Run King Salmon Management Plan*) and are intended to ensure sustainable Chinook salmon stocks. Escapement goals have evolved over the years as stock assessment and our understanding of stock dynamics have improved (McBride et al. 1989; Hammarstrom and Hasbrouck 1998-1999; Bosch and Burwen 1999). During the 2013 season, goals of 5,300–9,000 early-run and 15,000–30,000 late-run Chinook salmon were in effect, as assessed by DIDSON-based sonar estimates at river mile (RM) 8.6. Sonar estimates of inriver Chinook salmon passage provide the basis for estimating spawning escapement and implementing management plans that regulate harvest in the competing fisheries for this stock.

From 1987 through 2011, the Alaska Department of Fish and Game (ADF&G) used dual-beam (1987–1994) and split-beam (1995–2011) side-looking sonar technology to estimate Chinook salmon passage in the Kenai River at RM 8.6. These technologies relied on target strength (loudness of returning echoes) and range (distance from shore) thresholds to differentiate between sockeye (*O. nerka*) and Chinook salmon. These criteria were based on the premise that sockeye salmon are smaller and migrate primarily near shore, whereas Chinook salmon are larger and tend to migrate up the middle of the river. However, subsequent studies showed that these criteria can lead to inaccurate estimates (Burwen et al. 1998; Hammarstrom and Hasbrouck 1999). Extensive research was conducted at the Kenai RM 8.6 Chinook salmon sonar site toward improving our ability to identify species from split-beam sonar data (Burwen and Fleischman 1998; Burwen et al. 2003; Miller et al. 2010). Beginning in 2002, ADF&G evaluated the potential for dual-frequency identification sonar (DIDSON) to provide improved discrimination of larger Chinook salmon from smaller species of salmon based on size measurements taken directly from high-resolution images of migrating salmon (Burwen et al. 2007). Split-beam estimates were found to be inaccurate (Miller et al. 2013), and they were discontinued following

the 2011 season (Miller et al. 2015). DIDSON-based estimates continued to be produced at the RM 8.6 site.

The RM 8.6 site was originally selected in 1985 (Eggers et al. 1995), based primarily on its suitability for operating a dual-beam (and subsequently a split-beam) sonar system, which required a near-perfect linear bottom profile over the entire insonified zone or, in this case, from the nearshore region to the thalweg. See Key et al. (2016a) for a comprehensive history of sonar research and development at the Kenai River RM 8.6 site. The RM 8.6 site, however, has many disadvantages, primarily related to its location within tidal influence: 1) incomplete coverage of the river during high tides that flood the region behind the transducers, 2) milling fish behavior related to tidal flux, 3) physical risk to gear by large debris carried by extreme tidal fluxes, and 4) lack of legal access to the property on one bank. It became evident that relocating the site farther upriver could improve the estimates of Chinook salmon passage by minimizing or eliminating these negative factors. In 1999, ADF&G evaluated a second sonar site at RM 13.2 for use of split-beam sonar to assess fish passage, but the bottom topography was less acoustically favorable, and fish were more difficult to detect due to increased background noise levels from bottom irregularities and boat traffic (Burwen et al. 2000).

Because DIDSON multibeam technology was better able to insonify irregular bottom profiles, the search for a site above tidal influence was resumed in 2011. A potential new site at RM 13.7 (Figure 2) was identified and evaluated during a 2-week period in 2012 using the newest generation of DIDSON technology, referred to as Adaptive Resolution Imaging Sonar (ARIS). One of the main advantages of the RM 13.7 site is the potential to achieve bank-to-bank coverage of the river with sonar, which is not possible at the RM 8.6 site (Figure 3). ADF&G operated a full-scale experimental project at the RM 13.7 site using ARIS during 17 May–17 August 2013 while continuing to operate DIDSON at the RM 8.6 site.

Estimates of Chinook salmon abundance require information on Chinook salmon size, which has historically been obtained from an inriver gillnetting program operated at RM 8.6 (Perschbacher 2012a-d, 2014). Until recently, netting at RM 8.6 has been restricted to a midriver corridor in order to approximately match the cross-sectional area insonified by the DIDSON. In 2012, Chinook salmon sampled at the RM 8.6 netting project and at upstream tributary weirs differed in size, raising the possibility that Chinook salmon sampled midriver at RM 8.6 were not representative of the entire run. Auxiliary nearshore sonar deployments at RM 8.6 in 2011 and 2012 confirmed that some Chinook salmon were migrating between the DIDSON transducers and shore (Miller et al. 2014-2015). In response, the netting program at RM 8.6 was expanded to include experimental nearshore drifts in 2013 (Perschbacher 2015).

In addition, following the 2012 season, a state space model (SSM) was fitted to sonar, netting, catch-rate, and capture–recapture data; historical abundance was reconstructed; and escapement goals (3,800–8,500 fish for the early run; 15,000–30,000 fish for the late run) were recommended in preparation for the 2013 season (Fleischman and McKinley 2013; McKinley and Fleischman 2013). This modeling exercise, which synthesized information from all applicable data, estimated that the proportion of Chinook salmon migrating midriver (pMR) and detected by sonar and nets at RM 8.6 was 0.65 during the early run and 0.78 during the late run. In 2013 and 2014, to account for incomplete detection at RM 8.6, DIDSON estimates of inriver abundance were expanded by 1.55 ($1/0.65$) during the early run and 1.28 ($1/0.78$) during the late run, and used inseason to assess achievement of the new escapement goals.

This report documents data collection methods, analyses, and results from sonar operations at RM 13.7 in 2013. Daily estimates are reported for net upstream Chinook salmon passage. The estimates reported here represent the first full season of operation at RM 13.7, and constitute exploratory data (i.e., data that are not currently being used for management decisions) that will be considered in plans for future assessments of Kenai River Chinook salmon. DIDSON-derived estimates from the RM 8.6 sonar site (Key et al. 2016a) were used to manage Kenai River fisheries in 2013.

METHODS

STUDY AREA

The Kenai River drainage is approximately 2,150 square miles. It is glacially influenced, with discharge rates lowest during winter (less than 1,800 ft³/s), increasing throughout the summer, and peaking in August (greater than 14,000 ft³/s; Benke and Cushing 2005). The Kenai River has 10 major tributaries, many of which provide important spawning and rearing habitat for salmon. Tributaries include the Russian, Killey, Moose, and Funny rivers.

The Kenai River drainage is located in a transitional zone between a maritime climate and a continental climate (USDA 1992). The geographic position and local topography influence both rainfall and temperature throughout the drainage. Average annual (1981–2010) precipitation for the City of Kenai, located at the mouth of the Kenai River, is 48 cm. Average minimum and maximum summer (June, July, and August) temperatures for the City of Kenai range from 8°C to 16°C¹.

SITE DESCRIPTION

The sonar site is located 22 km (13.7 miles) from the mouth of the Kenai River (Figure 2). This location was identified during bathymetric surveys conducted in 2012 and was selected for its location above tidal influence, its favorable physical characteristics for deploying ARIS multibeam technology, its accessibility via an adjacent boat launch facility, and legal access to property on either bank of the main channel. The main channel on the west side of the river is approximately 90 m wide and the minor channel located along the east side is approximately 30 m wide (Figure 3). The minor channel has sufficient water for fish passage at higher water levels, from approximately mid-June through August. Tidal fluctuation at this site is minimal (less than 1 ft) and is observable only during the large spring tide sequence. The substrate in both the main channel and the minor channel is composed of small cobble, rocks, and gravel.

ACOUSTIC SAMPLING

Acoustic sampling was conducted using Sound Metrics Corporation (SMC) ARIS systems². Daily abundance estimates were generated from 17 May through 17 August 2013. Components of the ARIS systems are listed in Table 1. Appendices A1–A12 provide greater detail on ARIS technology and a comparison with DIDSON technology.

¹ WRCC (Western Region Climate Center). 2015. Kenai FAA Airport, Alaska. Website Western U.S. Climate Historical Summaries, Climatological Data Summaries, Alaska, accessed March 21, 2016. <http://www.wrcc.dri.edu/cgi-bin/cliMAIN.pl?ak4546>.

² Product names used in this publication are included for completeness but do not constitute product endorsement.

Sonar System Configuration and River Coverage

Site characteristics at RM 13.7 allow for near complete sonar coverage of the river cross-section. A bathymetric survey conducted in 2012 included 9 bottom profile transects that showed several promising areas for deploying sonars (Figures 4–5). Transects 5 and 6 in Figure 5 were chosen for the right- and left-bank main channel sonar deployments in 2013.

A total of 5 sonars were required to provide coverage: a nearshore and offshore sonar on each bank of the main channel (Figure 6) plus 1 sonar on the minor channel (Figure 7). During the early part of the season, when the water level was low, 1 sonar on each bank was sufficient to insonify most of the 60–70 m of river cross-section in the main channel (Table 2), but later in the season, as water levels rose, a second sonar was deployed on each bank to insonify the nearshore zone and the first 3–5 m in front of the offshore sonars (Figure 6). The nearshore sonars were first deployed on 6 June (Table 2) and were moved closer to shore as the water level rose. At its highest water stage, the main channel increased to approximately 90 m in width. In the main channel, the original (now offshore) sonars were not moved closer to shore as water levels rose because they were already insonifying the maximum range recommended for operation in high-frequency mode (approximately 30 m; Appendix A2). The minor channel was dry when the project began in mid-May, but it had sufficient water for fish passage starting in early June and the sonar was deployed on 6 June (Table 2). This channel was approximately 30 m wide at high water and was covered by a single sonar combined with a fixed weir, both deployed on the left bank of the minor channel (Figures 3 and 7).

Two different ARIS models were used to provide optimal cross-river coverage of the main channel (Figures 3 and 6, Table 1). ARIS 1200 models with high-resolution lenses (+HRL) were used as offshore sonars because they have the longer range capabilities (up to about 33 m in high frequency mode) needed to insonify most of the main channel at lower water levels as well as the offshore region of the main channel during higher water levels. An ARIS model 1200 +HRL was also used to cover the right-bank³ nearshore region (Figure 6) and on the minor channel due to the longer (~25 m) range requirements. An ARIS 1800 with a standard lens was deployed as the nearshore sonar on the left bank of the main channel because of the limited range that needed to be covered and the advantages of this sonar model for covering close-range targets. The ARIS 1800 is more advantageous for insonifying close-range targets and nearshore areas because it operates at a higher frequency, yielding higher resolution without the use of a large (high-resolution) lens. The standard lens has the advantage of better focusing capabilities at closer ranges (Appendix A5) and wider beam dimensions ($14^\circ \times 28^\circ$ versus $3^\circ \times 15^\circ$) to provide better coverage in both vertical and horizontal dimensions at short ranges. Finally, using sonars with different operating frequencies allowed nearshore and offshore strata to be sampled simultaneously without crosstalk interference.

All sampling was controlled by computers housed in a tent located on the left (west) bank of the river (Figure 3). The ARIS units were mounted on SMC X2 pan-and-tilt units for remote aiming in the horizontal and vertical axes. The sonar and rotator units were deployed in the river using either a tripod-style mount (capable of being deployed from a boat at higher water levels) or an H-style mount (used for nearshore deployment; Figure 8). In the horizontal plane, the sonars were aimed perpendicular to the flow of the river current to maximize the probability of

³ The right bank is on the right-hand side of the river as one faces downstream.

insonifying migrating salmon from a lateral aspect. In the vertical plane, the sonars were aimed to insonify the near-bottom region of the river (Figure 6). Internal sensors in the ARIS units provided measurements of compass heading, pitch, and roll, as well as water temperature.

Communication cables from the left-bank ARIS units fed directly into the left-bank ARIS Command Modules and data collection computers (Figure 9). On the right bank, data from the 3 ARIS systems were transmitted via 3 wireless bridges to 3 data collection computers on the left bank (Figures 9 and 10). Two battery banks, charged daily using generators, provided power to the right-bank sonar electronics and wireless bridges.

Sampling Procedure

Dividing the total insonified range into shorter range strata allowed the aim of each sonar to be optimized for sampling a given river section (i.e., generally, the aim must be raised in the vertical dimension as strata are sampled farther from shore). The ARIS can be programmed to automatically sample each range stratum using the software interface “ARIScope.” At the start of the season, 2 sonars were deployed on the mainstem, each sampling 3 strata. Table 2 summarizes the range coverage by each range stratum along with the changes in range parameters throughout the season as the water level rose and aims were refined. By 7 June, when all 5 sonars were deployed, a total of 12 strata were sampled, each with a unique set of data collection parameters (Table 3, Figure 11). By 19 July, water levels were more or less stable and no further changes were made to any parameters or to the positions of the sonars through the end of the season on 17 August. A systematic sample design (Cochran 1977) was used to sample each stratum for 10 minutes each hour following the schedule in Table 3. This routine was followed 24 hours per day and 7 days per week unless a transducer was inoperable.

A test of the systematic sample design at the RM 8.6 sonar site in 1999 found no significant difference between estimates of Chinook salmon passage obtained using 1-hour counts and estimates obtained by extrapolating 20-minute counts to 1 hour (Miller et al. 2002). Systematic 10-minute counts have been used for decades at counting towers elsewhere in Alaska (Seibel 1967).

Data Collection Parameters

In designing ARIS, the manufacturers separated the data collection (ARIScope) and data processing (ARISFish) software components. Unlike the DIDSON Control and Display interface, ARIScope has several data collection parameters that are now user selectable rather than fixed or limited to a few discrete values (Table 4). User-selectable parameters for ARIScope include “Window Length,” transmit “Pulse” width, “Sample Period,” number of “Samples/Beam,” and “Detail” (Tables 3 and 4, Appendix A1). The downrange resolution capability is particularly improved with ARIS; DIDSON was limited to 512 samples per beam to define the downrange resolution, but ARIS can collect up to 4,000 samples per beam. The user-selectable parameters are described in Appendix A1 along with the corresponding fixed values in the DIDSON system.

A consultant from Sound Metrics Corporation was on site from 12 to 20 May to assist project personnel with selecting the initial sampling strata and optimizing the aim and data collection parameters for each stratum. Parameters that varied with each stratum were frame rate, frequency, window length, sample period (which controls samples per beam and “Detail”), and transmit pulse width (Table 3).

Frame Rate

The maximum allowable frame rate was used for each stratum (Table 3). In practice, frame rates for each stratum were arrived at empirically by first fixing the parameters for start and end ranges and sample period for each stratum and then finding the maximum achievable frame rate. Frame rate is dependent on the number of beams used (96 beams for ARIS 1800, 48 beams for ARIS 1200), the end range of each stratum, and the frame size. The farther the end range, the longer the return time for the number of pings that builds an individual frame (16 pings for ARIS 1800, 3 pings for the ARIS 1200). Higher-resolution images with large frame sizes will also restrict the maximum frame rate. On the right bank, frame rates were also limited by the bandwidth of the wireless radios.

Window Length

The range interval covered by each of the 5 sonars was divided into 1 to 3 discrete strata primarily based on the need to change the vertical aim to better cover the near-bottom region of the river as the slope of the river changed with range from the sonar (Figures 6 and 11). Window lengths for the first strata sampled by the ARIS 1200 sonars were always set to 5 m to minimize the bias due to focal length caused by the high-resolution lens (Appendix A1). Window lengths for the other strata were selected to optimize bottom coverage while still considering frame rates. For example, the right-bank offshore Stratum 2 and Stratum 3 could be combined based on aiming criteria only (note the similar vertical aiming angles or pitch in Figure 12). However the frame rate of 5 frames per second (fps) needed to extend the range to approximately 35 m is too slow for ranges close to 10 m, where the beam width is narrow and the number of frames per fish would not provide good measurements. At longer ranges, where the beam is wide and fish spend a longer time transiting the beam, getting a sufficient number of frames is not an issue.

Frequency

All strata were sampled at high frequency (1.2 MHz) to optimize the cross-range resolution (Appendix A1) with 2 exceptions. First, the last strata on the right- and left-bank offshore sonars were sampled at low frequency (0.7 MHz) from 16 May to 6 June 2013 because colder water temperatures (as low as 5°C on 16 May) caused enough transmission loss that low-frequency mode was required to achieve the desired range of approximately 35 m when sampling the farthest stratum on each bank. Second, the right-bank offshore sonar experienced high background noise from an unknown source when sampling at high frequency but not low frequency. Although the noise was present in the first 2 strata as well, it was not sufficiently strong to warrant the change to low frequency mode.

By 6 June (0950 hours), water temperatures had warmed to 9°C and high-frequency mode was used to achieve the desired maximum range of about 34 m by the left-bank offshore sonar. However, the extreme noise interference experienced by the right-bank offshore ARIS unit continued throughout the season, requiring data to be collected at low frequency (Table 3).

Sample Period

In combination with transmit pulse width, the parameter “Sample Period” (or equivalently “Detail”) controls the downrange resolution for the image. Sample period was not necessarily set at the maximum resolution for a stratum because of the costs in terms of frame rate and frame or file size. With DIDSON, the sample period was fixed at 27 μ s with a transmit pulse width of 50 μ s. All ARIS strata were collected at shorter sample periods that varied from 4 to 11 μ s

(Table 3) or at least twice the downrange resolution as DIDSON. Shorter sample periods were generally used with close-range strata and paired with shorter transmit pulse widths, providing exceptionally high resolution. For example, the sample periods for the first stratum of each ARIS 1200 varied from 4 to 6 μ s. With increasing range, longer transmit pulse widths are generally required for sufficient power to achieve greater ranges. As a general rule, the manufacturer recommends setting the transmit pulse width long enough to get 2 samples within the transmit pulse. However, at ranges less than about 10 m, a transmit pulse long enough for 1 sample will suffice (Bill Hanot, personal communication, Sound Metrics Corporation, Seattle, WA).

Other Settings

The autofocus feature was enabled for all data collection so that the sonar automatically set the lens focus to the midrange of the selected range window. The transmit pulse width for each stratum was set to “Auto,” which sets the pulse width to the end range in microseconds. “Transmit Level” was set to maximum and “Gain” was set to 24 dB for all strata.

MANUAL ARIS FISH LENGTH MEASUREMENTS

Estimates of total length were made from fish images using ARISFish V1.5 software supplied by SMC. Detailed instructions for taking manual measurements and the software settings and parameters that were used for this project are given in Appendix B1. Electronic echograms similar to those generated with the DIDSON software (Miller et al. 2015) provided a system to manually count, track, and size individual fish (Figure 13).

Measured fish were subjected to a “centerline rule” (Appendices B2–B3). Only those fish that crossed the longitudinal central axis of the ARIS video image were candidates for measuring. Fish that did not cross the centerline were ignored. This removed the opportunity for fish to be counted in multiple spatial strata, which would create a positive bias in the passage estimates. Note that the 2010–2014 DIDSON-based abundance estimates at the RM 8.6 site (Miller et al. 2013–2015; Key et al. 2016a, 2016b) were not subjected to a centerline rule.

For the purpose of this study, fish size was divided into 3 categories based on ARIS length (AL) measurements. Fish with AL measurements greater than or equal to 40 cm and less than 75 cm are referred to as “small fish.” Fish with AL measurements greater than or equal to 75 cm and less than 90 cm are referred to as “medium fish.” Fish with AL measurements greater than or equal to 90 cm are referred to as “large fish.”

Estimates of medium- and large-fish abundance were produced by the sonar alone. Throughout the season, all medium and large fish were counted and measured, and travel direction (upstream or downstream) was recorded. The sampling protocol, where a sample is defined as a specific spatial stratum monitored for 10 minutes, is described below:

- 1) During samples without dense aggregations of fish, length and direction of travel were recorded for all salmon-shaped fish greater than or equal to 40 cm AL that met the centerline rule (Appendix B3).
- 2) During individual samples with dense aggregations of fish, length and direction of travel were recorded for all fish greater than or equal to 75 cm AL. However, length was recorded for only a subsample of fish with ARIS length greater than or equal to 40 cm and less than 75 cm. The first F fish in the sampled period were measured, where choice of F depended on daily staff time constraints. For the remainder of the sample (after the first F fish), only fish appearing to be greater than or equal to 75 cm AL were measured,

and only those fish that actually measured greater than or equal to 75 cm AL were recorded. During these times, fish measuring less than 75 cm AL were not recorded in any way, including fish chosen for measurement that turned out to be less than 75 cm.

3) Direction of travel was recorded for all measured targets.

Additional detail on procedures and software settings used to obtain manual fish length measurements can be found in Appendices A1–A12.

NETTED FISH LENGTH MEASUREMENTS

An established test gillnetting project at RM 8.6 (Perschbacher 2015) provided information on fish length, by species, which was needed for some of the estimates produced in this report. Length measurements of fish netted from the midriver insonified zone made up 1 source of input data required for mixture model estimates of Chinook salmon abundance (see below). Nearshore gillnetting data from a 2013 pilot program at RM 8.6 (Perschbacher 2015) were not used here.

DATA ANALYSIS

Estimates of fish passage are detailed below. Unlike the DIDSON sonar estimates at RM 8.6, which applied to all fish migrating upstream in a midriver corridor (Miller et al. 2013-2015; Key et al. 2016a, 2016b), the RM 13.7 ARIS estimates reported here assess net upstream (upstream minus downstream) passage, and are germane to the entire river cross-section.

Fish Passage

The ARIS sonar system was composed of multiple individual transducers scheduled to operate 10 minutes per hour for each spatial stratum, 24 hours per day. There were 1–3 spatial strata sampled per transducer and 2–5 transducers deployed in the river at any given time. The number of fish y that satisfied the set X of criteria under investigation (e.g., fish with ARIS length equal to or greater than 75 cm and that migrated in an upstream direction) during day i was estimated as follows:

$$\hat{y}_i = \sum_k \sum_s \hat{y}_{iks} \quad (1)$$

where y_{iks} is net fish passage in stratum s of transducer k during day i and is estimated by

$$\hat{y}_{iks} = \frac{24}{h_{iks}} \sum_{j=1}^4 \hat{y}_{ijks} \quad (2)$$

where h_{iks} is the number of hours during which fish passage was estimated for stratum s of transducer k during day i , and y_{ijks} is hourly fish passage for stratum s of transducer k during hour j of day i , which is estimated by

$$\hat{y}_{ijks} = \frac{60}{m_{ijks}} c_{ijks} \quad (3)$$

where

m_{ijks} = number of minutes (usually 10) sampled for stratum s of transducer k during hour j of day i , and

c_{ijks} = number of fish satisfying criteria X in stratum s of transducer k during hour j of day i .

The variance of the daily estimates of y , due to systematic sampling in time, was approximated (successive difference model⁴; Wolter 1985) with adjustments for missing data as follows:

$$\hat{V}[\hat{y}_i] \cong 24^2(1-f) \frac{\sum_{j=2}^{24} \phi_{ij} \phi_{i(j-1)} (\hat{y}_{ij} - \hat{y}_{i(j-1)})^2}{2 \sum_{j=1}^{24} \phi_{ij} \sum_{j=2}^{24} \phi_{ij} \phi_{i(j-1)}} \quad (4)$$

where

f = is the sampling fraction (temporal sampling fraction, usually 0.17),

ϕ_{ij} = is 1 if \hat{y}_{ij} exists for hour j of day i , or 0 if not, and

$$\hat{y}_{ij} = \sum_k \sum_s \hat{y}_{ijks} \cdot \quad (5)$$

Other estimates of passage were obtained by changing the criteria X for fish counts c_{ijks} in Equation 3. For example, estimates of medium and large fish were obtained by setting criteria to upstream travel with ARIS lengths greater than or equal to 75 cm and less than 90 cm or ARIS lengths greater than or equal to 90 cm, respectively. Estimates of daily net upstream passage were obtained by calculating separate estimates of upstream and downstream passage (Equations 1–3) and subtracting the downstream estimate from the upstream estimate. The estimated variance of net upstream daily passage was the sum of the upstream and downstream variances.

Chinook Salmon Passage

Upstream Chinook salmon passage, regardless of size, was estimated by fitting a mixture model to upstream ARIS length and midriver RM 8.6 netting data. Upstream Chinook salmon passage on day i was estimated as follows:

$$\hat{z}_i = \hat{w}_i \hat{\pi}_{Ci} \cdot \quad (8)$$

where

w_i = upstream passage of measured fish on day i , obtained by applying Equations 1–3 for measured upstream fish greater than or equal to 40 cm AL, and

π_{Ci} = the proportion of measured fish that are Chinook salmon on day i , derived by fitting an ARIS length mixture model (ALMM) to upstream ARIS lengths from RM 13.7 and midriver netting data from RM 8.6 (Perschbacher 2015) as described in Appendices C1–C6.

⁴ This is an assessment of the uncertainty due to subsampling (counting fish for 10 minutes per hour and expanding). The formulation in Equation 8 is conservative in the sense that it has been shown to overestimate the true uncertainty when applied to salmon passage data (Reynolds et al. 2007; Xie and Martens 2014).

The variance estimate followed Goodman (1960):

$$\text{var}(\hat{z}_i) = \hat{y}_i^2 \text{var}(\hat{\pi}_{Ci}) + \hat{\pi}_{Ci}^2 \text{var}(\hat{w}_i) - \text{var}(\hat{\pi}_{Ci}) \text{var}(\hat{w}_i). \quad (9)$$

Upstream ARIS data were used to be consistent with the drift gillnetting data, which presumably capture only upstream-bound fish. Only netting data obtained from standardized midriver drifts (not nearshore drifts conducted as part of a pilot study) were used for ALMM estimates in 2013.

Daily net upstream Chinook salmon passage was approximated as

$$\hat{N}_i \approx \hat{z}_i \frac{u_i - d_i}{u_i}, \quad (10)$$

where u_i and d_i are daily estimates of upstream and downstream passage of fish greater than or equal to 75 cm AL, respectively, obtained using Equations 1–3.

Note that estimates of w_i and π_{Ci} are intermediate quantities only, in the sense that they are required in order to estimate z_i and N_i but have no biological interpretation themselves because not all small fish (40–75 cm AL) were measured and counted. Estimates of z_i and N_i remain valid. A subsequent test conducted on 26 days of July 2014 data found good agreement between Chinook salmon abundance estimates obtained with complete sampling versus those obtained without complete sampling of small fish. The relationship had a slope of 0.96 and a coefficient of determination of 0.99.

TETHERED FISH DATA COLLECTION

Because of noise interference, low frequency was needed to sample the farthest stratum on the right bank (17 May–17 August 2013) and left bank (May 16–June 6 2013) offshore sonars. The need to collect data at low frequency on the right-bank offshore sonar due to noise interference was unexpected because no interference had been documented on either bank during the 2012 trials at this site. There were concerns over whether length measurements taken from low- and high-frequency images were comparable. To determine whether substantial differences in length measurements from data collected at the different frequencies existed, limited data were collected on tethered fish of known size (measured in fork length, tip of snout to fork of tail) at each frequency. Methods for tethering the fish were similar to those described in Burwen et al. (2010), and a more detailed explanation on the effects of frequency and beam width on cross-range resolution can be found in Appendix A1.

Data were collected using an ARIS 1200 +HRL at the RM 8.6 site on 17 July 2013. Data were collected at the lower river site rather than at RM 13.7 because there was no noise interference, and because a netting study conducted near the RM 8.6 site provided live salmon to tether. A total of 4 fish were captured and tethered. Two stations were set up at ranges approximately 10 m and 30 m from the sonar. The primary goal was to collect data at ranges similar to the RM 13.7 right bank offshore sonar Stratum 3 where low frequency was used (Table 3). However, it was also an opportunity to compare measurements at 2 different ranges, so the nearshore station was added. Unfortunately, 1 fish escaped before it could be moved to the offshore station at 30 m. Also, a large Chinook salmon, appearing fatigued, was released after being tethered at the offshore station and was never moved to the nearshore station. This resulted in 3 fish with offshore measurements and 3 fish with nearshore measurements. Only 2 fish were measured at both near- and offshore stations. Acoustic data were collected at high (1.2 MHz) and low (0.7 MHz) frequencies at the offshore station. Data were collected at high frequency only on fish

tethered at the nearshore station because low frequency was never needed to collect data at close range.

For each fish at each range and at each frequency, 3 individual ARIS-based measurements were made from 3 different frames that were selected based on image quality (Burwen et al. 2010). The 3 individual measurements were then averaged. It was not practical to conduct the study blindly. In general, frequency was known by the observer, partly because this information is freely available in the file headers and partly because the observer was experienced and knew at which frequency the data were collected; trained observers can generally tell which frequency is used by the brightness of the image (low frequency produces far brighter images than high frequency). Furthermore, the observer had some idea of the fish lengths. Although the observer was not given access to the true lengths, this observer had also participated in tethering the fish, which were so few in number that the lengths of the fish, particularly the single large Chinook salmon, could be recalled. This was not considered a serious disadvantage because the primary goal of this study was to determine whether methods could be developed to measure fish similarly at each frequency with an experienced and trained observer, using the knowledge that images collected at low frequency can differ from those collected at high frequency. For example, crosstalk between beams is more visible in low-frequency mode due to reduced transmission loss at the lower frequency, which can be minimized by reducing the gain setting. Also, with the increased energy at low frequency, there is greater potential for saturating the image, causing the image to look too bright or “washed out” if the appropriate gain setting is not used. The image “Threshold” and “Intensity” controls may also be employed to better match the image characteristics (brightness, apparent crosstalk) of a fish at high versus low frequency.

RESULTS

Data collection began on 17 May for the main channel offshore transducers, 6 June for the main channel nearshore transducers, and 8 June for the minor channel transducer. All sampling ended after 17 August.

SIZE DISTRIBUTION AND SPECIES COMPOSITION

Small fish (presumably sockeye salmon) predominated in both early and late runs, as evidenced by large left-hand modes in the ARIS length (AL) frequency distributions (Figure 14, top panels). The modes of the AL distributions line up well⁵ with mid eye to tail fork (METF) length distributions from salmon measured by the inriver netting project (Figure 14, bottom panels). The AL distributions are broader than the corresponding METF distributions because there is greater error associated with measuring length from ARIS images.

Non-Chinook salmon captured in the RM-8.6 gillnets rarely exceeded 65–70 cm METF (Figure 14, bottom panels). From inspection of AL frequency distributions (Figure 14, top panels), it is evident that the right tail of the left-hand mode (presumably non-Chinook salmon) very rarely exceeded 75 cm AL. From inspection of DIDSON length (DL) frequency distributions (Figure 14, middle panels), it is also evident that the right tail of the left-hand mode (presumably non-Chinook salmon) very rarely exceeded 75 cm DL. Thus, DIDSON and ARIS

⁵ Lengths from the netting data are not representative across species because non-Chinook salmon were sampled (measured) at only one-half the rate of Chinook salmon. Chinook salmon are therefore disproportionately represented in the netting length data.

length measurements were very nearly equivalent, at least for fish approximately 65 cm to 75 cm METF.

The frequency distribution of early-run ARIS lengths was more complex than the early-run DIDSON length distribution, possessing a small separate mode near 45 cm (Figure 14, top left panel). This mode probably consists of resident fish (e.g., rainbow trout [*O. mykiss*] and Dolly Varden [*Salvelinus malma*]) rather than sockeye salmon.⁶ No mode was present at 45 cm in the late-run ARIS length frequency distribution (Figure 14, top right panel), when much larger numbers of sockeye salmon could have obscured any such resident fish.

SPATIAL AND TEMPORAL DISTRIBUTION

Spatial and temporal patterns of migration are displayed for medium ($75 \text{ cm} \leq \text{AL} < 90 \text{ cm}$) and large ($\text{AL} \geq 90 \text{ cm}$) fish in Appendices D1–D7. Small ($40 \text{ cm} \leq \text{AL} < 75 \text{ cm}$) fish that were measured are also displayed, although they are underrepresented, especially during the late run. In general, small fish migrated closer to the river bank than did medium and large fish, although fish of all sizes were present in midriver.

During both the early and late runs, a majority (57–64%) of upstream-bound medium and large ($\text{AL} \geq 75 \text{ cm}$) fish migrated past the sonar site on the right bank of the main channel, especially during the late run. (Table 5, Figure 15). Only 2% of early run and 3% of late run upstream bound medium and large ($\text{AL} \geq 75 \text{ cm}$) fish were found migrating in the minor channel.

A greater fraction of medium and large fish migrated closer to shore in the early run than in the late run (Table 5, Figure 15, Appendices D1–D7). For instance, 59% of fish greater than or equal to 75 cm AL were observed from the nearshore main channel transducers in the early run, versus only 36% in the late run (values in Table 5 summed over left- and right-bank nearshore transducers).

A diurnal cycle in migration was often evident at RM 13.7; i.e., migration slowed during hours of darkness (Table 5). When upstream-bound medium and large fish were classified as day (sunrise to sunset) versus night (sunset to sunrise) migrators, the number migrating at night was disproportionately small compared to the relative length of night and day (Figure 16). The relative ratio of day to night migrators was 86:14 in the early run and 83:17 in the late run (Table 5); but the relative length of day and night at the latitude of Kenai, Alaska, ranged from 80:20 (at the 21 June solstice) to 65:35 (15 August; Figure 16)⁷.

DIRECTION OF TRAVEL

Relative upstream and downstream passage rates differed by run, spatial location, and size of fish. Among medium and large fish ($\text{AL} \geq 75 \text{ cm}$), a greater fraction were traveling downstream in the late run (7.1%) than in the early run (2.5%) (Table 6). For both runs, the downstream fraction was similar between left and right banks of the main channel, but higher in the minor channel. Also for both runs, the downstream fraction was higher for fish detected by the offshore transducers than those detected by nearshore transducers. During both runs, large fish ($\text{AL} \geq 90 \text{ cm}$) were more likely to be traveling downstream than were medium-sized fish ($75 \text{ cm} \leq \text{AL} < 90 \text{ cm}$; Table 6).

⁶ Among 2013 Russian River sockeye salmon (the main component of early-run Kenai River sockeye salmon), ocean-age-1 fish averaging 40 cm METF made up only 9% of the escapement (Jason Pawluk, Sport Fish Biologist, ADF&G, Soldotna; personal communication).

⁷ http://aa.usno.navy.mil/data/docs/RS_OneYear.php

During the early run in the main channel, small fish detected by offshore transducers were far more likely (8%, regardless of transducer) to be traveling downstream than were small fish detected by the nearshore transducers (1%, regardless of transducer; Table 6).

Daily percentages of medium and large fish ($AL \geq 75$ cm) that were bound upstream and downstream are tabulated in Appendices E1–E2.

MEDIUM AND LARGE FISH PASSAGE

During the early run (17 May–30 June) in 2013, an estimated 1,724 (SE 93) fish greater than or equal to 75 cm ARIS length passed RM 13.7, including 1,065 (SE 71) medium ($75 \text{ cm} \leq AL < 90 \text{ cm}$) and 659 (SE 60) large ($AL \geq 90 \text{ cm}$) fish (Tables 7 and 8).

During the late run (1 July–17 August), an estimated 12,656 (SE 282) fish greater than or equal to 75 cm ARIS length passed RM 13.7 in 2013, including 4,842 (SE 158) medium ($75 \text{ cm} \leq AL < 90 \text{ cm}$) and 7,814 (SE 216) large ($AL \geq 90 \text{ cm}$) fish (Tables 7 and 8). The ARIS-based estimates of medium and large fish are germane to the entire river cross-section at RM 13.7.

CHINOOK SALMON PASSAGE

Daily proportions of upstream-bound Chinook salmon of all sizes were estimated using an ARIS-length (AL) mixture model. These proportions were multiplied by ARIS estimates of upstream fish passage and corrected for downstream fish to produce ARIS estimates of net upstream Chinook salmon passage: 2,845 (SE 274) Chinook salmon during the early run (17 May–30 June; Table 9) and 19,373 (SE 583) during the late run (1 July–17 August; Table 10). The small fish component of the early-run sonar passage estimate is considered too low (see below).

Daily estimates of net upstream Chinook salmon passage are plotted in Figure 17. Other measures of abundance are plotted for comparison in Figures 18 and 19, including DIDSON-based estimates from RM 8.6. The AL mixture model also produced daily estimates of Chinook salmon age group composition (Tables 11–12). These estimates incorporated length information from ARIS as well as from inriver gillnet catches.

SMALL FISH PASSAGE

ARIS estimates of net upstream small Chinook salmon passage were 1,121 (SE 289) Chinook salmon during the early run (17 May–30 June; Table 9) and 6,717 (SE 647) during the late run (1 July–17 August; Table 10). The early run estimate is considered too low. See below for a discussion of the credibility of the small Chinook salmon estimates during the early run.

TETHERED FISH MEASUREMENTS

Length measurements from images collected at low frequency were similar to those collected at high frequency for each of 3 tethered fish (Table 13). Table 13 shows that the difference (low minus high frequency) of mean length measurements for individual fish ranged from -0.1 to 1.9 cm. Because the increased energy at low frequency results in much brighter images, threshold and intensity settings, which affect the dynamic range in an image, were selected to give a similar visual display for each frequency (see Appendix A1). Figure 20 shows the similarity in images from each of the 3 tethered fish measured at low (panels 1–3, on left) and high (panels 4–6, on right) frequencies after setting appropriate threshold and intensity parameters.

ARIS-based mean lengths of fish tethered at close (<6 m) and far (>27 m) range differed by as much as 4.3 cm (Table 14). Measurements taken at close range differed less from true length than those taken at far range (1.4 cm and 0.6 cm versus 2.9 cm and 2.3 cm, respectively) (Table 14).

DISCUSSION

CHINOOK SALMON ABUNDANCE

Direct estimates of medium and large fish passage from the ARIS at RM 13.7 (Tables 7–8) constitute the most accurate and reliable information to date about Kenai River Chinook salmon abundance. This is true for 2 reasons. First, because ARIS transducers at RM 13.7 are configured to provide nearly 100% spatial coverage, expansion factors and their associated uncertainty are no longer required. Second, fish measuring 75 cm AL or longer do not overlap in length with sockeye and other small salmon (Figure 14), and therefore these fish are Chinook salmon that can be directly assessed by the sonar. Estimates of medium and large Chinook salmon net upstream passage for 2013 were 1,724 (SE 93) during the early run (Table 7) and 12,656 (SE 282) during the late run (Table 8). Chinook salmon measuring 75 cm AL average approximately 75 cm METF (33 inches total length; Miller et al. *In prep*)⁸.

Estimates of small Chinook salmon at either sonar site can be subject to large errors. For example, Key et al. (2016a) noted that counts of small Chinook salmon at the Funny and Killey river weirs totaled 2,095 in 2013 (based on data from Boersma and Gates [2014] and Gates and Boersma [2014]), yet the spatially expanded DLMM estimate of small Chinook salmon passage at RM 8.6 during the 2013 early run was only 682. The ARIS at RM 13.7 did not perform much better—the ALMM estimate of small Chinook salmon passage during the 2013 early run was still far too low (1,121; Table 9). Clearly, early run abundance of small Chinook salmon was greatly underestimated by both sonar projects in 2013.

Estimates of small Chinook salmon are problematic because they rely on auxiliary netting data as well as sonar data (Appendix C2). Small Chinook salmon cannot be distinguished from other salmon with the sonar, and therefore they cannot be directly counted. Supplemental information from the inriver gillnetting project on the relative proportions of small, medium, and large Chinook salmon is required. As an example, if the sonar counts 100 Chinook salmon that are medium or large, and the inriver nets catch 10 Chinook salmon, of which 2 (20% or 0.2 of total) are less than 75 cm (AL or METF) and the remaining 8 (0.8 of total) are larger, then an estimate of total Chinook salmon abundance (regardless of size) is $100/0.8 = 125$. Of these, approximately 20% (25 fish) are small (<75 cm AL) and the remaining 100 are larger⁹. Note that higher proportions of small Chinook salmon in the nets result in higher estimates of small Chinook (and all Chinook) salmon abundance, and vice versa. For example, if the sonar count remained the same (100) but 4 (instead of 2) of the 10 netted fish were small, we would estimate there were 167 Chinook salmon ($100/0.6$), composed of 67 small and 100 large fish.

⁸ Miller, J. D., D. L. Burwen, B. H. Key, and S. J. Fleischman. *In prep*. Estimates of Chinook salmon passage in the Kenai River at river mile 13.7 using adaptive resolution imaging sonar, 2014. Alaska Department of Fish and Game, Fishery Data Series, Anchorage.

⁹ This is a simplified example to illustrate how the netting data affects the abundance estimates. The actual estimates of small Chinook salmon are obtained by fitting a statistical mixture model in order to account for error in the ARIS length measurements and to provide an assessment of uncertainty. See Appendices C1–C3 for an explanation of the ARIS length mixture model (ALMM).

Accurate estimates of Chinook salmon abundance therefore depend upon obtaining representative samples of Chinook salmon with respect to size. If the inriver nets undersample small Chinook salmon, small (and all) Chinook salmon are underestimated, and vice versa. Because migrating Chinook salmon sometimes stratify by size, with smaller fish migrating closer to the river bank and larger fish farther offshore (Miller 2000; Hughes 2004), DLMM and ALMM estimates of Chinook salmon abundance are sensitive to how the netting data are collected. Historically, nets have been deployed at RM 8.6 in a midriver corridor, but in a 2013 pilot study, nets were occasionally (twice weekly) deployed near shore (Perschbacher 2015). During the early run, Chinook salmon were caught at higher rates nearshore than in midriver, and nearshore fish were smaller, on average, than midriver fish. During the late run, nearshore catch rates declined relative to midriver, and the size difference was much smaller and not statistically significant (Perschbacher 2015). Clearly, nets deployed midriver missed many small fish migrating near shore during the early run, leading to the large shortfall of small early-run Chinook salmon as estimated by ALMM. For this reason, the 2013 early-run estimates in Table 9 are considered too low and do not accurately reflect true early-run Chinook salmon abundance.

Based on a combination of sonar, weir, and telemetry data, we believe the 2013 early run numbered between 3,900 and 5,300. A direct estimate of 1,724 (SE 93) fish greater than 75 cm (AL or METF) is available from the ARIS sonar (Table 7). For smaller (<75 cm) Chinook salmon, a capture–recapture estimate of abundance can be derived from telemetry (Eskelin and Reimer *In prep*¹⁰) and weir data (Boersma and Gates 2014; Gates and Boersma 2014). Out of 17 small Chinook salmon tracked successfully by telemetry, 13 (76%) were eventually located above weirs on the Funny and Killey rivers. A total of 2,146 small Chinook salmon were counted passing the 2 weirs in 2013, yielding an estimate $(2,146/0.76)$ of 2,806 (SE 341) early-run small Chinook salmon. For the 2013 early run, the sum of the sonar estimate of large fish and the weir–telemetry estimate of small fish, which is 4,530 (SE 353, 95% CI 3,876–5,294), will be used as the basis for future run reconstructions and forecasts.

The 2013 late-run ALMM estimates (19,373 Chinook salmon regardless of size; 6,717 small Chinook salmon; Table 10) may also have a low bias because these estimates also used midriver netting data, which often under-represent small fish. However, compared to the 2013 early run, the late-run bias was probably much smaller. Perschbacher (2015; Figure 6) found that the fraction of Chinook salmon caught near shore declined many-fold during the late run. Furthermore, although nearshore fish were smaller on average than midriver fish during the late run, the difference was small and not statistically significant (Perschbacher 2015; Figure 8).

Efforts to improve our understanding of small Chinook salmon abundance are ongoing. Because physical conditions are very different near shore than they are midriver, and because sockeye and pink salmon can interfere with netting near shore, it can be difficult to obtain representative samples of Chinook salmon size. Methodology was developed to standardize nearshore drifts in 2013 (Perschbacher 2015). In 2014, the number of nearshore drifts will be increased so as to equalize sampling across spatial strata.

¹⁰ Eskelin, A., and A. M. Reimer. *In prep*. Migratory timing and distribution of Kenai River Chinook salmon, 2014 and 2015, with synthesis of 2010–2013 Studies. Alaska Department of Fish and Game, Division of Sport Fish, Fisheries Data Series, Anchorage.

TETHERED FISH MEASUREMENTS

Because of noise interference, low frequency was needed to sample the farthest stratum on the right-bank (17 May–17 August 2013) and left-bank (May 16–June 6 2013) offshore sonars, and this raised concerns over whether length measurements taken from low- and high-frequency images were comparable. Transmitting at lower frequency increases maximum effective range, but it does so at potentially reduced cross-range image resolution because, although the beam spacing is the same ($\sim 0.3^\circ$), the individual beams are wider at low frequency (0.33°) than at high frequency (0.27°). There were concerns that the wider beam width at low frequency might increase the likelihood of a sub-beam lighting up when the snout or tail of the fish partially projects into an individual beam, causing the fish to have a larger measurement at low frequency than at high frequency.

According to the manufacturer, fish length measurements should be similar in high- or low-frequency mode because the beam spacing is the same (Bill Hanot, personal communication, Sound Metrics Corporation, Seattle, WA). ARIS-based mean lengths of tethered fish closely approximated the true length (TL) for each fish at high and low frequencies (Table 13). However, the increased intensity at low frequency can also increase the visibility of crosstalk in the image. Crosstalk appears as repeated “faint” ghosting from bright targets and can impact length measurements. Figure 21 shows 3 images collected at low frequency from a 116 cm Chinook salmon that demonstrate the potential effect of crosstalk on length measurements. Figure 21, Panel 1 shows crosstalk in the beams adjacent to both the snout and tail. This frame would readily be eliminated from consideration for measurement because the shape of the fish is distorted by the crosstalk. In Panel 2 of Figure 21, the image shows crosstalk adjacent to the tail that could be mistaken for an extension of the tail by 1 or even 2 pixels. Panel 3 of Figure 21 shows an optimal image for measurement with a well-defined unambiguous snout and tail.

Comparing ARIS-based lengths with true lengths from tethered fish at near and far ranges illustrates 2 important concepts regarding the accuracy and precision with which fish can be measured from ARIS images. First, because cross-range resolution decreases (pixels widen) with increasing range, fish closer to the sonar can generally be measured more precisely (Burwen et al. 2007; Appendix A1). Second, the precision with which a fish can be measured depends in large part on how close the actual fish length is to a multiple of the pixel width at the range measured.

As an example, Fish 2 in Tables 13–14 was first tethered at about 28 m (Figure 22) then moved to approximately 5 m (Figure 23) from the sonar. When measuring targets at far range where image pixels are wider, the observer is often making a choice between a fish that is either x or $x+1$ pixels long. In Table 13, “Lower bound” and “Upper bound” show the values of a fish measured at x (lower bound) or $x+1$ (upper bound) pixels for the range given in the “Range” row. The high-frequency measurements for Fish 2 were taken at approximately 27.5 m from the sonar where the pixel width is 14.4 cm (“Crossrange resolution” in Table 13). In this case, the observer was making the choice between a fish that was 4 or 5 pixels long as shown in Figure 22. The measurement would be approximately 57.6 cm (4×14.4 cm) if a 4-pixel image were selected or 72.0 cm (5×14.4 cm) if a 5-pixel image were selected. The individual measurements in Table 13 of 69.7 cm, 72.1 cm, and 70.6 cm were measured closer to the upper bound value of 72.0 cm.

Table 14, which compares the measurements of 2 fish measured at both the close- and far-range tethering stations, shows how much more precisely each fish can be measured at the nearshore station. Figure 23 shows improved resolution when Fish 2 is moved to less than 5 m from the sonar. The higher resolution at this close range provides measured lengths (67.2 cm, 68.7 cm, and 67.9 cm) that are closer to the true length of 68.5 cm than the measurements taken at the 27 m range (Table 13). The fish can be measured more precisely because the pixel width at the 4.1 m range is only 2.1 cm rather than 14.7 cm at the 28 m range (Table 14).

Although these limited results indicate that length measurements at high and low frequency are similar enough to be used interchangeably if the observer is discriminating in selecting an image to measure, a more comprehensive tethered fish experiment is planned for the 2014 season. Also planned for the 2014 season are some modifications to the sonar hardware to decrease sensitivity to the external noise source at high frequency so that use of low frequency will be limited to early in the season, when cooler water temperatures reduce the maximum effective range (signal strength) at high frequency.

RECOMMENDATIONS

Collect at least 1 more year of paired data at the lower and upper sites. Comparison of data from RM 8.6 and RM 13.7 will promote better understanding of fish behavior and of how the abundance estimates from the 2 sites relate to one another.

Conduct an expanded tethered fish study to evaluate optimal parameter settings for data collection. In 2013, length measurements from DIDSON and ARIS appeared to be equivalent (Figure 14), and the few tethered fish data collected in 2013 were consistent with this finding. Additional tethered fish data would be valuable for additional comparisons of high and low frequency size measurements and of various parameter settings that affect downrange resolution. For example, during 2013, RM 13.7 ARIS data were collected using parameter settings that provided high downrange resolution because doing so was not storage or time prohibitive, but at present we do not know if collecting data at higher resolution increases the precision or accuracy of length measurements.

Address noise on right-bank offshore sonar. Extreme noise interference occurred at high frequency on the right bank offshore sonar throughout the season. No noise had been documented on either bank during the 2012 trials at the RM 13.7 site. Although the source of the noise could not be positively identified, 2 cell and radio towers within line-of-site were suspected. A local radio station operating at 1.14 MHz is the most likely source because that frequency is close to the 1.2 MHz operating frequency of the ARIS 1200 in high-frequency mode. Attempts to resolve the problem through additional grounding techniques were unsuccessful. A representative from SMC was optimistic that hardware upgrades to be implemented in early 2014 to both the ARIS and X2 hardware would resolve the noise issue.

Continue to operate the inriver netting project in the same standardized protocol as has been practiced since 2002. Current escapement goals are based on ALMM estimates derived from midriver netting data. Also, consistent data produced by the netting project have proven valuable for reconstructing historical abundance.

Supplement the existing netting protocol with additional drifts or sets designed to sample fish that migrate behind transducers. Netting data that span the river will be valuable in the event that many small fish again migrate near shore, as happened during the 2013 early run.

Use the alternative estimate of 4,530 early-run Chinook salmon (1,724 ARIS estimate of salmon ≥ 75 cm plus 2,806 telemetry–weir estimate of salmon < 75 cm) as the basis for future run reconstructions and forecasts. The standard assessment based on midriver sonar and netting missed substantial numbers of small Chinook salmon migrating near shore during the 2013 early run.

ACKNOWLEDGEMENTS

We would like to thank Michael Friedrich for his assistance in overseeing the day-to-day operation of the project. We thank Cynthia Jaffe and Lindsay Fagrelus for their positive and enthusiastic attitudes during many hours processing DIDSON and ARIS data. Thanks to Kara Bethune for her expert assistance with processing sonar data during the busiest part of the season. We would also like to thank Mike Hopp for his assistance inseason deploying and breaking down the project and postseason measuring fish images. We would like to express our gratitude to Don and John Cho with Riverbend Resort for allowing daily access to the RM 13.7 site via their property, for providing a source of electricity to operate the left-bank electronics, and for the use of their boat launch for project deployment and breakdown. Finally, thanks to Division of Sport Fish staff in Soldotna who provided logistical support throughout the season.

REFERENCES CITED

- Benke, A. C., and C. E. Cushing. 2005. Rivers of North America. Elsevier Academic Press, Burlington, Massachusetts.
- Boersma, J. K., and K. S. Gates. 2014. Abundance and run timing of adult Chinook salmon in the Funny River, Kenai Peninsula, Alaska, 2013. U.S. Fish and Wildlife Service, Alaska Fisheries Data Series Report Number 2014-5, Soldotna. http://www.fws.gov/alaska/fisheries/fish/Data_Series/d_2014_5.pdf
- Bosch, D., and D. Burwen. 1999. Estimates of Chinook salmon abundance in the Kenai River using split-beam sonar, 1997. Alaska Department of Fish and Game, Fishery Data Series No. 99-3, Anchorage. <http://www.adfg.alaska.gov/FedAidPDFs/fds99-03.pdf>
- Burger, C. V., R. L. Wilmot, and D. B. Wangaard. 1985. Comparison of spawning areas and times for two runs of Chinook salmon (*Oncorhynchus tshawytscha*) in the Kenai River, Alaska. Canadian Journal of Fisheries and Aquatic Sciences 42(4):693-700.
- Burwen, D., J. Hasbrouck, and D. Bosch. 2000. Investigations of alternate sites for Chinook salmon sonar on the Kenai River. Alaska Department of Fish and Game, Fishery Data Series No. 00-43, Anchorage. <http://www.adfg.alaska.gov/FedAidPDFs/fds00-43.pdf>
- Burwen, D. L., D. E. Bosch, and S. J. Fleischman. 1998. Evaluation of hydroacoustic assessment techniques for Chinook salmon on the Kenai River, 1995. Alaska Department of Fish and Game, Fishery Data Series No. 98-3, Anchorage. <http://www.adfg.alaska.gov/FedAidPDFs/fds98-03.pdf>
- Burwen, D. L., and S. J. Fleischman. 1998. Evaluation of side-aspect target strength and pulse width as hydroacoustic discriminators of fish species in rivers. Canadian Journal of Fisheries and Aquatic Sciences 55(11):2492-2502.
- Burwen, D. L., S. J. Fleischman, and J. D. Miller. 2007. Evaluation of a dual-frequency imaging sonar for estimating fish size in the Kenai River. Alaska Department of Fish and Game, Fishery Data Series No. 07 44, Anchorage. <http://www.adfg.alaska.gov/FedAidPDFs/fds07-44.pdf>
- Burwen, D. L., S. J. Fleischman, and J. D. Miller. 2010. Accuracy and precision of manual fish length measurements from DIDSON sonar images. Transactions of the American Fisheries Society, 139:1306-1314.
- Burwen, D. L., S. J. Fleischman, J. D. Miller, and M. E. Jensen. 2003. Time-based signal characteristics as predictors of fish size and species for a side-looking hydroacoustic application in a river. ICES Journal of Marine Science 60:662-668.
- Cochran, W. G. 1977. Sampling techniques. 3rd edition. John Wiley and Sons, New York.
- Eggers, D. M., P. A. Skvorc II, and D. L. Burwen. 1995. Abundance estimates of Chinook salmon in the Kenai River using dual-beam sonar. Alaska Fishery Research Bulletin 2(1):1-22. <http://www.adfg.alaska.gov/FedAidpdfs/AFRB.02.1.001-022.pdf>
- Fleischman, S. J., and D. L. Burwen. 2003. Mixture models for the species apportionment of hydroacoustic data, with echo-envelope length as the discriminatory variable. ICES Journal of Marine Science 60:592-598.
- Fleischman, S. J., and T. R. McKinley. 2013. Run reconstruction, spawner–recruit analysis, and escapement goal recommendation for late-run Chinook salmon in the Kenai River. Alaska Department of Fish and Game, Fishery Manuscript Series No. 13-02, Anchorage. <http://www/adfg/alaska.gov/FedAidpdfs/FMS13-02>
- Gates, K. S., and J. K. Boersma. 2014. Abundance and run timing of adult Chinook salmon in the Killey River and Quartz Creek, Kenai Peninsula, Alaska, 2013. U.S. Fish and Wildlife Service, Alaska Fisheries Data Series Report Number 2014-4, Soldotna. http://www.fws.gov/alaska/fisheries/fish/Data_Series/d_2014_4.pdf
- Gelman, A., J. B. Carlin, H. S. Stern, and D. B. Rubin. 2004. Bayesian data analysis. 3rd edition. Chapman and Hall, Boca Raton, Florida.
- Gilks, W. R., A. Thomas, and D. J. Spiegelhalter. 1994. A language and program for complex Bayesian modeling. The Statistician 43:169-178. <http://www.mrc-bsu.cam.ac.uk/bugs> (Accessed January 2010).

REFERENCES CITED (Continued)

- Glick, W. J., and T. M. Willette. 2015. Upper Cook Inlet sockeye salmon escapement studies, 2013. Alaska Department of Fish and Game, Fishery Data Series No. 15-25, Anchorage. <http://www.adfg.alaska.gov/FedAidPDFs/FDS15-25.pdf>
- Goodman, L. A. 1960. On the exact variance of products. *Journal of the American Statistical Association* 55:708-713.
- Hammarstrom, S. L., and J. J. Hasbrouck. 1998. Estimation of the abundance of late-run Chinook salmon in the Kenai River based on exploitation rate and harvest, 1996. Alaska Department of Fish and Game, Fishery Data Series No. 98-6, Anchorage. <http://www.adfg.alaska.gov/FedAidPDFs/fds98-06.pdf>
- Hammarstrom, S. L., and J. J. Hasbrouck. 1999. Estimation of the abundance of late-run Chinook salmon in the Kenai River based on exploitation rate and harvest, 1997. Alaska Department of Fish and Game, Fishery Data Series No. 99-8, Anchorage. <http://www.adfg.alaska.gov/FedAidPDFs/fds99-08.pdf>
- Hughes, N. F. 2004. The wave-drag hypothesis: an explanation for size-based lateral segregation during the upstream migration of salmonids. *Canadian Journal of Fisheries and Aquatic Sciences* 61(1):103-109.
- Key, B. H., J. D. Miller, D. L. Burwen, and S. J. Fleischman. 2016a. Estimates of Chinook salmon passage in the Kenai River at river mile 8.6 using dual-frequency identification sonar, 2013. Alaska Department of Fish and Game, Fishery Data Series No. 16-13, Anchorage. <http://www.adfg.alaska.gov/FedAidPDFs/FDS16-13.pdf>
- Key, B. H., J. D. Miller, D. L. Burwen, and S. J. Fleischman. 2016b. Estimates of Chinook salmon passage in the Kenai River at river mile 8.6 using dual-frequency identification sonar, 2014. Alaska Department of Fish and Game, Fishery Data Series No. 16-14, Anchorage. <http://www.adfg.alaska.gov/FedAidPDFs/FDS16-14.pdf>
- McBride, D. N., M. Alexandersdottir, S. Hammarstrom, and D. Vincent-Lang. 1989. Development and implementation of an escapement goal policy for the return of Chinook salmon to the Kenai River. Alaska Department of Fish and Game, Fishery Manuscript No. 8, Juneau. <http://www.adfg.alaska.gov/FedAidPDFs/fms-008.pdf>
- McKinley, T. R., and S. J. Fleischman. 2013. Run reconstruction, spawner–recruit analysis, and escapement goal recommendation for early-run Chinook salmon in the Kenai River. Alaska Department of Fish and Game, Fishery Manuscript Series No. 13-03, Anchorage. <http://www.adfg.alaska.gov/FedAidPDFs/FMS13-03.pdf>
- Miller, J. D. 2000. Sonar enumeration of Pacific salmon escapement into Nushagak River, 1999. Alaska Department of Fish and Game, Division of Commercial Fisheries, Regional Information Report 2A00-19, Anchorage. <http://www.adfg.alaska.gov/FedAidPDFs/RIR.2A.2000.19.pdf>
- Miller, J. D., D. Bosch, and D. Burwen. 2002. Estimates of Chinook salmon abundance in the Kenai River using split-beam sonar, 1999. Alaska Department of Fish and Game, Fishery Data Series No. 02-24, Anchorage. <http://www.adfg.alaska.gov/FedAidPDFs/fds02-24.pdf>
- Miller, J. D., D. L. Burwen, and S. J. Fleischman. 2010. Estimates of Chinook salmon passage in the Kenai River using split-beam sonar, 2006. Alaska Department of Fish and Game, Fishery Data Series No. 10-40, Anchorage. <http://www.adfg.alaska.gov/FedAidpdfs/FDS10-40.pdf>
- Miller, J. D., D. L. Burwen, and S. J. Fleischman. 2013. Estimates of Chinook salmon passage in the Kenai River using split-beam and dual-frequency identification sonars, 2010. Alaska Department of Fish and Game, Fishery Data Series No. 13-58, Anchorage. <http://www.adfg.alaska.gov/FedAidPDFs/FDS13-58.pdf>
- Miller, J. D., D. L. Burwen, and S. J. Fleischman. 2014. Estimates of Chinook salmon passage in the Kenai River using split-beam and dual-frequency identification sonars, 2011. Alaska Department of Fish and Game, Fishery Data Series No. 14-18, Anchorage. <http://www.adfg.alaska.gov/FedAidpdfs/FDS14-18>
- Miller, J. D., D. L. Burwen, and S. J. Fleischman. 2015. Estimates of Chinook salmon passage in the Kenai River at river mile 8.6 using dual-frequency identification sonar, 2012. Alaska Department of Fish and Game, Fishery Data Series No. 15-09, Anchorage. <http://www.adfg.alaska.gov/FedAidPDFs/FDS15-09.pdf>

REFERENCES CITED (Continued)

- Perschbacher, J. 2012a. Chinook salmon creel survey and inriver gillnetting study, lower Kenai River, Alaska, 2008. Alaska Department of Fish and Game, Fishery Data Series No. 12-70, Anchorage. <http://www.adfg.alaska.gov/FedAidpdfs/FDS12-70>
- Perschbacher, J. 2012b. Chinook salmon creel survey and inriver gillnetting study, lower Kenai River, Alaska, 2009. Alaska Department of Fish and Game, Fishery Data Series No. 12-61, Anchorage. <http://www.adfg.alaska.gov/FedAidpdfs/FDS12-61>
- Perschbacher, J. 2012c. Chinook salmon creel survey and inriver gillnetting study, lower Kenai River, Alaska, 2010. Alaska Department of Fish and Game, Fishery Data Series No. 12-75, Anchorage. <http://www.adfg.alaska.gov/FedAidPDFs/FDS12-75.pdf>
- Perschbacher, J. 2012d. Chinook salmon creel survey and inriver gillnetting study, lower Kenai River, Alaska, 2011. Alaska Department of Fish and Game, Fishery Data Series No. 12-84, Anchorage. <http://www.adfg.alaska.gov/FedAidPDFs/FDS12-84.pdf>
- Perschbacher, J. 2014. Chinook salmon creel survey and inriver gillnetting study, Lower Kenai River, Alaska, 2012. Alaska Department of Fish and Game, Fishery Data Series No. 14-37, Anchorage. <http://www.adfg.alaska.gov/FedAidPDFs/FDS14-37.pdf>
- Perschbacher, J. 2015. Chinook salmon creel survey and inriver gillnetting study, lower Kenai River, Alaska, 2013. Alaska Department of Fish and Game, Fishery Data Series No. 15-46, Anchorage. <http://www.adfg.alaska.gov/FedAidPDFs/FDS15-46.pdf>
- Reynolds, J. H., C. A. Woody, N. E. Gove, and L. F. Fair. 2007. Efficiently estimating salmon escapement uncertainty using systematically sampled data. Pages 121-129 [In] C. A. Woody, editor. Sockeye salmon evolution, ecology, and management. American Fisheries Society, Symposium No. 54, Anchorage.
- Seibel, M. C. 1967. The use of expanded ten-minute counts as estimates of hourly salmon migration past counting towers on Alaskan rivers. Alaska Department of Fish and Game, Division of Commercial Fisheries, Informational Leaflet 101, Juneau., Anchorage. <http://www.adfg.alaska.gov/FedAidPDFs/afrbil.101.pdf>
- USDA (United States Department of Agriculture). 1992. Kenai River landowner's guide. Prepared by the U. S. Department of Agriculture, Soil conservation Service (SCS) for the Kenai Soil and Water Conservation District, Kenai, Alaska.
- Wolter, K. M. 1985. Introduction to variance estimation. Springer-Verlag, New York.
- Xie, Y., and F. J. Martens. 2014. An empirical approach for estimating the precision of hydroacoustic fish counts by systematic hourly sampling. North American Journal of Fisheries Management 34(3):535-545.

TABLES

Table 1.–On-site components of the ARIS systems used in 2013.

System component	Model (number of units)	Description
Sounders	ARIS 1200 (4)	Left bank mainstem offshore Right bank mainstem offshore Right bank mainstem nearshore Right bank minor channel
	ARIS 1800 (1)	Left bank mainstem nearshore
Lens assembly	ARIS 1800 (1)	Standard lens with $\sim 14^{\circ} \times 28^{\circ}$ beam pattern
	ARIS 1200 (4)	High-resolution lens with $\sim 3^{\circ} \times 15^{\circ}$ beam pattern
Data collection computers	Dell Latitude E6430 (5)	One for each sonar
Wireless bridge radio sets	Cisco Aironet 1310 (1)	
	Radiolabs GS2000 (1)	
	EZ-Bridge-5G-Lite EZBR-0519 (1)	
Remote pan and tilts	Sound Metrics X2 rotators (5)	Controlled via ARIScope software
Storage media (on site)	Western Digital 2TB Passport Drives with USB 3.0 (10)	Two per computer
Internet Access	AT&T MiFi Liberate mobile hot spot (1)	
	AT&T Beams 4G (4)	

Table 2.—Summary of sonar stratum range changes by date at RM 13.7 Kenai River, 2013.

Sonar location	Range stratum	Time (min) ^a	Coverage range (m) by date							
			16 May	18 May	6 Jun	8 Jun	19 Jun	20 Jun	24 Jun	19 Jul
Left nearshore	1	:00 / :30	^b	^b	2.5–11.1	2.5–11.1	2.5–11.1	2.5–11.1	2.5–12.1	2.5–15.1
Left offshore	1	:00 / :30	2.0–8.0	2.0–8.0	3.6–8.6	3.6–8.6	3.6–8.6	3.6–8.6	3.6–8.6	3.6–8.6
	2	:10 / :40	8.0–23.4	8–23.4	8.6–24.4	8.6–24.4	8.6–24.4	8.6–24.4	8.6–24.4	8.6–24.4
	3	:20 / :50	23.0–38.0	23.0–38.0	24.4–34.4	24.4–34.4	24.4–34.4	24.4–34.4	24.4–34.4	24.4–34.4
Right offshore	1	:00 / :30	2.0–8.0	2.0–8.0	3.6–8.6	3.6–8.6	3.6–8.6	3.6–8.6	3.6–8.6	3.6–8.6
	2	:10	8.0–35.0	8.0–24.0	8.6–23.0	8.6–23.0	8.6–23.0	8.6–23.0	8.6–23.0	8.6–23.0
	3	:20	^c	24.0–38.0	23.0–36.0	23.0–36.0	23.0–36.0	23.0–36.0	23.0–36.0	23.0–36.0
Right nearshore	1	:40	^b	^b	3.6–6.6	3.6–6.6	3.6–8.7	3.6–8.7	3.6–8.7	3.6–8.7
	2	:50	^b	^b	6.6–14.1	6.6–14.1	8.7–15.9	8.7–15.9	8.7–15.9	8.7–15.9
Minor channel	1	:00	^b	^b	3.0–6.0	3.0–6.0	3.0–6.0	3.0–6.0	3.0–6.0	3.0–6.0
	2	:10	^b	^b	6.0–12.2	6.0–12.2	6.0–12.2	6.0–12.2	6.0–12.2	6.0–12.2
	3	:30	^b	^b	12.2–20.1	12.2–20.1	12.2–20.1	12.2–20.1	12.2–20.1	12.2–20.1

^a Sample start time in number of minutes past the top of the hour. Two samples were made for some strata; start times are separated by “/”.

^b Sonar was not deployed in this stratum until 6 June.

^c Stratum not created until 18 May.

Table 3.–Sampling schedule and parameter values on 19 July 2013 for each range stratum sampled by 5 ARIS systems in 2013.

Sonar location	ARIS serial no.	Range stratum	Time (min) ^a	Frame rate (fps) ^b	Start range (m)	End range (m)	Frequency	Transmit level	Pulse width (μs)	Start delay	Sample period (μs)	Samples per beam	Pitch (°)	Heading (°)
Left nearshore	1096	1	:00 / :30	7	2.11	15.1	High: 1.8 MHz	Max	20	2930	9	2000	−6.8	45
Left offshore	1064	1	:00 / :30	7	3.57	8.57	High :1.2 MHz	Max	8	4980	5	1394	−10	60
		2	:10 / :40	7	8.6	24.38	High: 1.2 MHz	Max	24	11953	11	1992	−6.5	60
		3	:20 / :50	6.55	24.38	34.42	High: 1.2 MHz	Max	35	33868	7	1992	−3.7	60
Right offshore	1063	1	:00 / :30	9	3.58	8.58	High: 1.2 MHz	Max	8	5000	5	1400	−7	276
		2	:10	6.49	8.63	23	High: 1.2 MHz	Max	21	12000	10	2000	−3.5	276
		3	:20	6.05	23	35.94	Low: 0.7 MHz	Max	36	32000	9	2000	−3.5	276
Right nearshore	1098	1	:40	9	3.6	8.61	High: 1.2 MHz	Min	9	5000	4	1739	−8	209
		2	:50	9	8.68	15.86	High: 1.2 MHz	Max	16	12004	7	1418	−7	209
Minor channel	78	1	:00	9	3.01	6.02	High: 1.2 MHz	Max	6	4200	6	700	−10.3	339
		2	:10	9	5.87	12.17	High: 1.2 MHz	Max	12	8200	8	1100	−5.8	339
		3	:30	9	12.17	20.05	High: 1.2 MHz	Max	12	17000	10	1100	−2	339

^a Sample start time in number of minutes past the top of the hour. Two samples were made for some strata; start times are separated by “/”.

^b Frame rate in frames per second.

Table 4.—Select user-configurable parameters in Sound Metrics Corporation ARIScope data collection software and their corresponding values in DIDSON (high-frequency identification mode only).

Parameter	ARIS 1200	ARIS 1800	DIDSON LR (1200)	DIDSON SV (1800)
Transmit pulse length	4–100 μ s	4–100 μ s	7 μ s, 13 μ s, 27 μ s, 54 μ s ^a	4.5 μ s, 9 μ s, 18 μ s, 36 μ s ^a
Detail ^b	3–100 mm ~206–212 dB	3–100 mm ~200–206 dB	5 mm, 10 mm, 20 mm, 40 mm ^a	2.5 mm, 5.0 mm, 10.0 mm, 20.0 mm ^a
Source level	re 1 μ Pa at 1 m	re 1 μ Pa at 1 m		
Window length	Any	Any	2.5 m, 5.0 m, 10.0 m, 20.0 m	1.25 m, 2.50 m, 5.00 m, 10.00 m
Samples/beam	128–4,000	128–4,000	512	512

^a Relative to window length.

^b Window length per number of samples.

Table 5.—Spatial and temporal distribution (percent of total run) of upstream-bound medium and large fish (ARIS length ≥ 75 cm), by river bank, transducer, and time (day or night) at RM 13.7 for the Kenai River early and late runs, 2013.

	Main channel								
		Left-bank transducer		Right-bank transducer					
Run	Time of day	Nearshore	Offshore	Offshore	Nearshore	All left bank	All right bank	Minor channel	All strata
Early									
	Day	22	15	16	32	37	47	2	86
	Night	2	3	6	4	5	9	0	14
	Both	24	17	21	35	41	57	2	100
Late									
	Day	6	22	29	24	28	53	3	83
	Night	1	4	7	5	5	12	1	17
	Both	7	26	36	29	33	64	3	100

Note: Columns may not sum due to rounding.

Table 6.—Percentage of all (upstream and downstream) fish migrating downstream, by river bank, transducer, and fish size at RM 13.7 for the 2013 Kenai River early and late runs.

Run	Fish size	Main channel						Minor channel	All strata
		Left-bank transducer		Right-bank transducer		All left bank	All right bank		
		Nearshore	Offshore	Offshore	Nearshore				
Early									
	Small	1.3	7.9	8.3	0.9	3.0	3.6		3.3
	Medium	0.0	3.6	3.0	0.0	1.4	1.1	0.0	1.2
	Large	0.0	4.8	3.7	2.7	2.3	3.1	50.0	4.5
	Medium and large	0.0	4.1	3.3	1.0	1.7	1.9	25.0	2.5
Late									
	Medium	0.0	4.1	9.2	3.8	3.1	6.4	9.1	5.5
	Large	7.4	9.5	7.6	7.2	9.1	7.4	13.9	8.1
	Medium and large	4.4	7.5	8.1	5.8	6.9	7.1	11.3	7.1

Note: Small fish are $40 \text{ cm} \leq \text{AL} < 75 \text{ cm}$, medium fish are $75 \text{ cm} \leq \text{AL} < 90 \text{ cm}$, and large fish are $\geq 90 \text{ cm AL}$. The only reliable direction of travel information for small fish was from the main channel during the early run.

Table 7.—Estimates of net upstream daily passage of medium ($75 \text{ cm} \leq \text{AL} < 90 \text{ cm}$) and large ($\text{AL} \geq 90 \text{ cm}$) Chinook salmon at RM 13.7 Kenai River, early run 2013.

Date	$75 \text{ cm} \leq \text{AL} < 90 \text{ cm}$		$\text{AL} \geq 90 \text{ cm}$		$\text{AL} \geq 75 \text{ cm}$	
	Passage	SE	Passage	SE	Passage	SE
17 May	0	0	0	0	0	0
18 May	0	0	6	4	6	4
19 May	6	5	12	7	18	7
20 May	0	0	0	0	0	0
21 May	-6	5	6	4	0	6
22 May	0	0	0	0	0	0
23 May	12	7	-11	9	1	11
24 May	12	9	6	5	18	9
25 May	35	14	12	6	47	16
26 May	6	5	0	0	6	5
27 May	12	7	0	0	12	7
28 May	0	0	0	0	0	0
29 May	18	9	6	5	24	10
30 May	06	4	12	7	18	8
31 May	15	9	7	6	22	11
1 Jun	36	13	30	11	66	15
2 Jun	18	7	6	5	24	7
3 Jun	30	10	18	9	49	7
4 Jun	6	5	0	0	6	5
5 Jun	12	7	12	7	24	10
6 Jun	14	8	21	8	34	13
7 Jun	47	14	45	18	93	23
8 Jun	34	17	16	11	50	22
9 Jun	84	19	19	9	103	22
10 Jun	20	10	48	15	68	16
11 Jun	6	5	26	13	32	14
12 Jun	31	13	7	6	38	13
13 Jun	26	8	31	16	57	17
14 Jun	61	16	49	17	110	26
15 Jun	23	14	39	14	63	21
16 Jun	6	5	6	5	12	7
17 Jun	6	4	6	5	12	6
18 Jun	32	12	6	9	37	14
19 Jun	24	9	13	8	37	14
20 Jun	49	10	0	8	49	13
21 Jun	37	9	6	5	43	9
22 Jun	36	8	12	7	48	11
23 Jun	34	11	13	5	47	14
24 Jun	19	9	7	6	26	13
25 Jun	33	15	18	11	52	20
26 Jun	37	8	0	0	37	8
27 Jun	64	21	7	9	71	22
28 Jun	48	23	30	13	78	23
29 Jun	36	13	65	16	101	20
30 Jun	39	14	46	15	85	21
Total	1,065	71	659	60	1,724	93

Table 8.—Estimates of net upstream daily passage of medium ($75 \text{ cm} \leq \text{AL} < 90 \text{ cm}$) and large ($\text{AL} \geq 90 \text{ cm}$) Chinook salmon at RM 13.7 Kenai River, late run 2013.

Date	$75 \text{ cm} \leq \text{AL} < 90 \text{ cm}$		$\text{AL} \geq 90 \text{ cm}$		$\text{AL} \geq 75 \text{ cm}$	
	Passage	SE	Passage	SE	Passage	SE
1 Jul	48	20	79	18	127	29
2 Jul	12	7	48	22	60	23
3 Jul	12	10	48	12	60	15
4 Jul	48	13	64	24	112	24
5 Jul	24	9	54	16	79	20
6 Jul	36	11	42	13	79	18
7 Jul	6	5	51	18	57	18
8 Jul	31	16	54	15	86	28
9 Jul	81	28	105	30	186	51
10 Jul	80	17	109	19	188	29
11 Jul	42	11	170	33	212	35
12 Jul	43	11	79	21	122	20
13 Jul	78	14	127	26	205	26
14 Jul	115	34	193	31	308	53
15 Jul	85	20	236	24	321	30
16 Jul	144	28	335	54	479	68
17 Jul	157	20	151	27	308	40
18 Jul	129	29	297	52	426	69
19 Jul	85	18	212	33	297	42
20 Jul	169	21	145	18	315	25
21 Jul	54	18	67	25	121	36
22 Jul	48	14	103	19	151	29
23 Jul	80	18	163	30	243	43
24 Jul	66	21	79	19	145	29
25 Jul	62	16	205	34	268	36
26 Jul	186	30	153	30	339	48
27 Jul	103	27	151	33	254	51
28 Jul	145	23	163	34	308	39
29 Jul	121	27	278	44	399	62
30 Jul	181	24	248	36	429	44
31 Jul	163	23	308	37	471	48
1 Aug	200	32	275	44	475	39
2 Aug	248	43	248	32	496	62
3 Aug	224	39	291	59	513	71
4 Aug	164	30	230	38	394	45
5 Aug	180	31	239	41	418	49
6 Aug	145	29	168	31	312	38
7 Aug	75	26	156	33	231	38
8 Aug	205	28	278	42	483	59

-continued-

Table 8.–Page 2 of 2.

Date	75 cm \leq AL < 90 cm		AL \geq 90 cm		AL \geq 75 cm	
	Passage	SE	Passage	SE	Passage	SE
9 Aug	135	20	207	39	342	49
10 Aug	111	23	203	39	313	47
11 Aug	86	19	140	21	227	29
12 Aug	40	14	127	25	167	26
13 Aug	60	14	182	23	242	21
14 Aug	91	29	206	29	297	40
15 Aug	87	19	134	20	221	29
16 Aug	91	20	79	24	170	33
17 Aug	66	22	133	18	200	24
Total	4,842	158	7,814	216	12,656	282

Table 9.—ARIS-length mixture model (ALMM) net upstream passage estimates for Chinook salmon (regardless of size) and for small Chinook salmon (AL < 75 cm), RM 13.7 Kenai River, early run 2013. *For reasons explained in the Discussion section, estimates in this table are considered too low and do not accurately reflect true early-run 2013 abundance.*

Date	ALMM Chinook salmon (all sizes)			ALMM Chinook salmon < 75 cm AL		
	Passage	SE	CV	Passage	SE	CV
17 May	7	5	0.75	7	5	0.75
18 May	24	18	0.75	18	19	1.03
19 May	49	28	0.57	31	29	0.93
20 May	1	3	2.89	1	3	2.89
21 May	0	0		0	6	
22 May	1	3	2.96	1	3	2.96
23 May	0	1	2.50	-1	11	15.20
24 May	23	12	0.51	5	15	3.31
25 May	24	19	0.78	-23	25	1.07
26 May	1	3	2.67	-5	6	1.13
27 May	6	11	1.77	-6	13	2.12
28 May	1	2	2.42	1	2	2.42
29 May	33	23	0.7	9	25	2.81
30 May	21	19	0.91	3	21	6.88
31 May	21	18	0.84	-1	21	20.80
1 Jun	147	152	1.03	81	152	1.88
2 Jun	49	39	0.80	25	40	1.59
3 Jun	69	35	0.51	20	36	1.78
4 Jun	1	3	2.50	-5	6	1.12
5 Jun	16	19	1.18	-8	21	2.66
6 Jun	119	63	0.53	85	65	0.76
7 Jun	222	80	0.36	129	84	0.65
8 Jun	116	52	0.44	66	56	0.85
9 Jun	209	71	0.34	106	75	0.70
10 Jun	124	52	0.42	56	55	0.98
11 Jun	72	38	0.53	40	41	1.01
12 Jun	63	32	0.50	25	34	1.36
13 Jun	99	37	0.37	42	41	0.97
14 Jun	165	50	0.30	55	56	1.02
15 Jun	104	48	0.46	41	52	1.28
16 Jun	28	21	0.75	16	22	1.38
17 Jun	24	17	0.71	12	18	1.51
18 Jun	77	35	0.46	40	38	0.94
19 Jun	83	42	0.51	46	45	0.97
20 Jun	111	70	0.63	62	71	1.14
21 Jun	59	24	0.41	16	26	1.60
22 Jun	71	30	0.42	23	32	1.39
23 Jun	70	30	0.43	23	34	1.46
24 Jun	36	20	0.54	10	23	2.34
25 Jun	71	29	0.41	19	35	1.86
26 Jun	50	21	0.43	13	23	1.75
27 Jun	74	26	0.36	3	34	12.30
28 Jun	90	30	0.33	12	37	3.12
29 Jun	118	33	0.28	17	39	2.29
30 Jun	96	29	0.30	11	35	3.22
Total	2,845	274	0.10	1,121	289	0.26

Table 10.—ARIS-length mixture model (ALMM) net upstream passage estimates for Chinook salmon (regardless of size) and for small Chinook salmon (AL < 75 cm), RM 13.7 Kenai River, late run 2013.

Date	ALMM Chinook salmon (all sizes)			ALMM Chinook salmon < 75 cm AL		
	Passage	SE	CV	Passage	SE	CV
1 Jul	169	44	0.26	42	52	1.25
2 Jul	94	34	0.36	34	41	1.20
3 Jul	135	51	0.38	75	53	0.71
4 Jul	201	56	0.28	89	61	0.68
5 Jul	161	51	0.32	82	54	0.67
6 Jul	218	92	0.42	139	94	0.67
7 Jul	132	43	0.32	75	47	0.62
8 Jul	109	50	0.45	23	57	2.47
9 Jul	336	90	0.27	150	104	0.69
10 Jul	326	79	0.24	138	84	0.61
11 Jul	435	133	0.31	223	138	0.62
12 Jul	220	58	0.26	98	61	0.62
13 Jul	357	77	0.22	152	81	0.54
14 Jul	596	112	0.19	288	124	0.43
15 Jul	694	123	0.18	373	126	0.34
16 Jul	890	124	0.14	411	141	0.34
17 Jul	586	112	0.19	278	119	0.43
18 Jul	762	115	0.15	336	134	0.40
19 Jul	468	92	0.20	171	102	0.59
20 Jul	518	105	0.20	203	108	0.53
21 Jul	211	57	0.27	90	68	0.75
22 Jul	270	69	0.25	119	75	0.63
23 Jul	500	111	0.22	257	119	0.46
24 Jul	254	63	0.25	109	69	0.64
25 Jul	477	103	0.22	209	109	0.52
26 Jul	791	183	0.23	452	189	0.42
27 Jul	449	106	0.24	195	118	0.60
28 Jul	471	82	0.17	163	91	0.56
29 Jul	582	103	0.18	183	120	0.66
30 Jul	581	95	0.16	152	105	0.69
31 Jul	653	97	0.15	182	108	0.59
1 Aug	604	82	0.14	129	91	0.70
2 Aug	612	81	0.13	116	102	0.88
3 Aug	646	78	0.12	133	106	0.80
4 Aug	488	69	0.14	94	82	0.87
5 Aug	483	65	0.13	65	81	1.24
6 Aug	389	71	0.18	77	81	1.04
7 Aug	271	48	0.18	40	61	1.55
8 Aug	555	72	0.13	72	93	1.28
9 Aug	446	77	0.17	104	92	0.88
10 Aug	377	64	0.17	64	80	1.25
11 Aug	276	51	0.18	49	58	1.18
12 Aug	198	44	0.22	31	51	1.66
13 Aug	326	68	0.21	84	72	0.85
14 Aug	350	57	0.16	53	70	1.32
15 Aug	271	53	0.20	50	61	1.22
16 Aug	211	38	0.18	41	50	1.23
17 Aug	224	48	0.21	24	54	2.24
Total	19,373	583	0.03	6,717	647	0.10

Table 11.—Daily estimates of Chinook salmon age composition derived from fitting a mixture model to length measurements from ARIS at RM 13.7 and midriver gillnet catches from RM 8.6, Kenai River early run 2013.

Date	Ages 3 and 4		Age 5		Ages 6 and 7	
	Proportion	SE	Proportion	SE	Proportion	SE
17 May	—	—	—	—	—	—
18 May	—	—	—	—	—	—
19 May	—	—	—	—	—	—
20 May	0.26	0.26	0.25	0.26	0.49	0.30
21 May	0.25	0.25	0.16	0.19	0.59	0.27
22 May	0.17	0.19	0.18	0.21	0.64	0.26
23 May	0.13	0.15	0.15	0.17	0.72	0.21
24 May	0.10	0.13	0.16	0.18	0.73	0.20
25 May	0.11	0.13	0.11	0.13	0.79	0.17
26 May	0.10	0.13	0.11	0.13	0.79	0.17
27 May	0.14	0.16	0.18	0.19	0.68	0.23
28 May	0.13	0.15	0.12	0.15	0.75	0.20
29 May	0.19	0.20	0.36	0.25	0.46	0.25
30 May	0.24	0.24	0.22	0.23	0.55	0.28
31 May	0.24	0.24	0.20	0.22	0.56	0.27
1 Jun	0.40	0.34	0.22	0.24	0.38	0.30
2 Jun	0.39	0.31	0.31	0.24	0.30	0.21
3 Jun	0.21	0.21	0.38	0.30	0.40	0.29
4 Jun	0.17	0.19	0.18	0.20	0.65	0.25
5 Jun	0.17	0.19	0.21	0.23	0.62	0.26
6 Jun	0.50	0.19	0.16	0.16	0.33	0.18
7 Jun	0.49	0.14	0.46	0.15	0.06	0.08
8 Jun	0.56	0.14	0.33	0.13	0.11	0.08
9 Jun	0.49	0.13	0.35	0.12	0.16	0.07
10 Jun	0.48	0.13	0.18	0.10	0.34	0.11
11 Jun	0.46	0.13	0.29	0.13	0.25	0.12
12 Jun	0.47	0.12	0.32	0.12	0.21	0.09
13 Jun	0.37	0.12	0.34	0.13	0.28	0.12
14 Jun	0.37	0.13	0.38	0.13	0.25	0.09
15 Jun	0.40	0.16	0.33	0.16	0.27	0.12
16 Jun	0.42	0.16	0.38	0.19	0.20	0.13
17 Jun	0.46	0.15	0.27	0.16	0.28	0.13
18 Jun	0.50	0.16	0.30	0.18	0.19	0.12

-continued-

Table 11.–Page 2 of 2.

Date	Ages 3 and 4		Age 5		Ages 6 and 7	
	Proportion	SE	Proportion	SE	Proportion	SE
19 Jun	0.47	0.17	0.39	0.19	0.14	0.12
20 Jun	0.62	0.19	0.29	0.18	0.09	0.08
21 Jun	0.32	0.14	0.51	0.16	0.18	0.12
22 Jun	0.28	0.15	0.46	0.21	0.26	0.17
23 Jun	0.31	0.17	0.51	0.18	0.19	0.13
24 Jun	0.20	0.18	0.59	0.20	0.21	0.14
25 Jun	0.19	0.16	0.64	0.20	0.17	0.14
26 Jun	0.13	0.13	0.66	0.16	0.22	0.13
27 Jun	0.07	0.09	0.62	0.15	0.31	0.14
28 Jun	0.08	0.10	0.58	0.14	0.34	0.12
29 Jun	0.13	0.10	0.43	0.13	0.44	0.13
30 Jun	0.13	0.09	0.51	0.15	0.37	0.14
Weighted mean	0.36	0.06	0.36	0.06	0.25	0.05

Note: Proportions are not available for 17–19 May. Mean proportions are weighted by daily ALMM estimates in Table 9.

Table 12.—Daily estimates of Chinook salmon age composition derived from fitting a mixture model to length measurements from ARIS at RM 13.7 and midriver gillnet catches from RM 8.6, Kenai River late run 2013.

Date	Ages 3 and 4		Age 5		Ages 6 and 7	
	Proportion	SE	Proportion	SE	Proportion	SE
1 Jul	0.19	0.11	0.42	0.15	0.39	0.14
2 Jul	0.36	0.12	0.22	0.12	0.42	0.12
3 Jul	0.52	0.11	0.22	0.12	0.25	0.11
4 Jul	0.48	0.10	0.28	0.11	0.25	0.09
5 Jul	0.54	0.10	0.07	0.06	0.39	0.10
6 Jul	0.67	0.10	0.03	0.04	0.30	0.10
7 Jul	0.59	0.09	0.02	0.03	0.39	0.09
8 Jul	0.59	0.10	0.02	0.03	0.39	0.09
9 Jul	0.59	0.08	0.02	0.03	0.39	0.08
10 Jul	0.47	0.09	0.02	0.03	0.50	0.08
11 Jul	0.52	0.09	0.01	0.02	0.46	0.09
12 Jul	0.49	0.09	0.02	0.03	0.49	0.08
13 Jul	0.46	0.08	0.03	0.03	0.51	0.08
14 Jul	0.49	0.08	0.04	0.04	0.47	0.07
15 Jul	0.53	0.07	0.07	0.06	0.40	0.06
16 Jul	0.40	0.08	0.09	0.06	0.52	0.06
17 Jul	0.46	0.09	0.10	0.07	0.45	0.08
18 Jul	0.43	0.07	0.04	0.04	0.53	0.06
19 Jul	0.40	0.08	0.07	0.06	0.53	0.08
20 Jul	0.41	0.09	0.10	0.08	0.49	0.09
21 Jul	0.41	0.11	0.07	0.08	0.52	0.11
22 Jul	0.42	0.10	0.03	0.04	0.54	0.10
23 Jul	0.44	0.09	0.02	0.03	0.54	0.09
24 Jul	0.39	0.10	0.05	0.05	0.56	0.10
25 Jul	0.45	0.10	0.03	0.04	0.52	0.09
26 Jul	0.51	0.11	0.11	0.11	0.38	0.12
27 Jul	0.44	0.10	0.07	0.08	0.49	0.10
28 Jul	0.37	0.08	0.08	0.10	0.54	0.10
29 Jul	0.36	0.09	0.08	0.07	0.57	0.09
30 Jul	0.24	0.09	0.25	0.13	0.51	0.14
31 Jul	0.26	0.08	0.12	0.09	0.62	0.10
1 Aug	0.22	0.07	0.20	0.11	0.57	0.11
2 Aug	0.18	0.06	0.22	0.14	0.61	0.14
3 Aug	0.18	0.06	0.22	0.13	0.59	0.13

-continued-

Table 12.–Page 2 of 2.

Date	Ages 3 and 4		Age 5		Ages 6 and 7	
	Proportion	SE	Proportion	SE	Proportion	SE
4 Aug	0.16	0.06	0.15	0.12	0.69	0.13
5 Aug	0.17	0.06	0.11	0.13	0.72	0.14
6 Aug	0.22	0.08	0.17	0.12	0.62	0.13
7 Aug	0.18	0.07	0.06	0.07	0.76	0.09
8 Aug	0.12	0.07	0.12	0.11	0.75	0.12
9 Aug	0.18	0.09	0.16	0.10	0.66	0.12
10 Aug	0.13	0.08	0.18	0.11	0.69	0.12
11 Aug	0.14	0.08	0.27	0.15	0.59	0.15
12 Aug	0.18	0.09	0.15	0.10	0.68	0.11
13 Aug	0.24	0.10	0.12	0.14	0.64	0.15
14 Aug	0.13	0.08	0.22	0.13	0.66	0.13
15 Aug	0.13	0.09	0.47	0.17	0.40	0.16
16 Aug	0.07	0.08	0.45	0.16	0.48	0.15
17 Aug	0.09	0.10	0.21	0.15	0.70	0.15
Weighted mean	0.34	0.02	0.12	0.02	0.54	0.03

Note: Mean proportions are weighted by daily ALMM estimates in Table 10.

Table 13.—ARIS-based length measurements at low and high frequency for 3 tethered salmon at RM 8.6 Kenai River on 17 July 2013.

	Fish 1 (sockeye salmon) ^a			Fish 2 (sockeye salmon) ^b			Fish 3 (Chinook salmon) ^c		
	Low	High	Difference ^d	Low	High	Difference ^d	Low	High	Difference ^d
Frequency (MHz)	0.7	1.2	−0.5	0.7	1.2	−0.5	0.7	1.2	−0.5
Window length (m)	10	10		10	10		17.4	17.4	
Sample period (μs)	7	7		7	7		12	12	
Samples per beam	2000	2000		2000	2000		2000	2000	
Pulse width (μs)	22	22		33	33		36	36	
Detail (mm)	5.1	5.1		5.1	5.1		5.1	5.1	
Range (m)	29.6	29.4	0.2	28	27.5	0.5	27.8	28	−0.2
Cross-range resolution (cm)	15.3	15.4	−0.1	14.7	14.4	0.3	14.6	14.7	−0.1
True length (cm) ^e	60	60		68.5	68.5		116	116	
ARIS length 1 (cm) ^f	61.7	63.4		73.1	69.7		118.7	116.3	
ARIS length 2 (cm) ^f	63.8	63.1		71.9	72.1		120.3	120.4	
ARIS length 3 (cm) ^f	62.8	62.2		73.2	70.6		119.8	119.8	
Mean ARIS length (cm)	62.8	62.9	−0.1	72.7	70.8	1.9	119.6	118.8	0.8
Variance ARIS length	1.1	0.6		0.7	1.2		0.8	2.2	
Lower bound (cm) ^g	62	61.6		58.6	57.6		116.4	117.3	
Upper bound (cm) ^g	77.5	77		73.3	72		131	131.9	
Mean ARIS length minus true length (cm)	−2.8	−2.9	0.1	−4.2	−2.3	−1.9	−3.6	−2.8	−0.8

Note: ARIScope data-collection parameters are also listed.

^a Fish 1 files: 2_TetheredFar_2013-07-17_172107_F07_B48_S2000_T22_R21-31.aris, 2_TetheredFar_2013-07-17_172337_F12_B48_S2000_T22_R21-31.aris, measured by BHK

^b Fish 2 files: 3_TetheredFar_2013-07-17_174008_F07_B48_S2000_T33_R22-33.aris, 3_TetheredFar_2013-07-17_173823_F12_B48_S2000_T33_R22-33.aris, measured by BHK

^c Fish 3 files: 4_KingNear_2013-07-17_190703_F12_B48_S2000_T36_R17-34_HF.aris, 4_KingNear_2013-07-17_190703_F12_B48_S2000_T36_R17-34_LF.aris, measured by BHK

^d Difference equals low frequency minus high frequency values.

^e True length (fork length) was measured on the fish.

^f Measurements of a given fish were taken from 3 different frames that were selected based on image quality.

^g Upper and lower bounds are based on the minimum and maximum number of pixels composing the fish image.

Table 14.—ARIS-based length measurements for 2 tethered salmon sampled at close (<6 m) and far (>27 m) range.

	Fish 1 (sockeye salmon) ^a			Fish 2 (sockeye salmon) ^b		
	Close	Far	Difference ^c	Close	Far	Difference ^c
Range (m)	5.4	29.4	−24.0	4	27.5	−23.5
Cross-range resolution (cm)	2.8	15.4	−12.6	2.1	14.4	−12.3
Frequency (MHz)	1.2	1.2		1.2	1.2	
Window length (m)	5.8	10	−4.2	5	10	−5
Sample period (μs)	4	7	−3	4	7	−3
Samples per beam	2000	2000		1771	2000	−229
Pulse width (μs)	10	22	−12	8	33	−25
Detail (mm)	2.9	5.1	−2.2	2.9	5.1	−2.2
Actual length (cm) ^d	60	60		68.5	68.5	
ARIS length 1 (cm) ^e	56.6	63.4		68.7	69.7	
ARIS length 2 (cm) ^e	59.7	63.1		68.7	72.1	
ARIS length 3 (cm) ^e	59.4	62.2		69.9	70.6	
Mean ARIS length (cm)	58.6	62.9	−4.3	69.1	70.8	−1.7
ARIS length variance	1.7	0.6		0.7	1.2	
Lower bound (cm) ^f	56.5	61.6		67	57.6	
Upper bound (cm) ^f	59.4	77		69.1	72	
Mean ARIS length minus actual length (cm)	1.4	−2.9	4.3	−0.6	−2.3	1.7

^a Fish 1 files: 2_TetheredNear_2013-07-17_174535_F12_B48_S2000_T10_R3-8.aris, 2_TetheredFar_2013-07-17_172337_F12_B48_S2000_T22_R21-31.aris, measured by BHK.

^b Fish 2 files: 3_TetheredNear_2013-07-17_182746_F12_B48_S1724_T08_R3-8.aris, 3_TetheredFar_2013-07-17_173823_F12_B48_S2000_T33_R22-33.aris, measured by BHK.

^c Difference = low frequency minus high frequency values.

^d True length (fork length) was measured on the fish.

^e Measurements of a given fish were taken from 3 different frames that were selected based on image quality.

^f Upper and lower bounds are based on the minimum and maximum number of pixels composing the fish image.

FIGURES

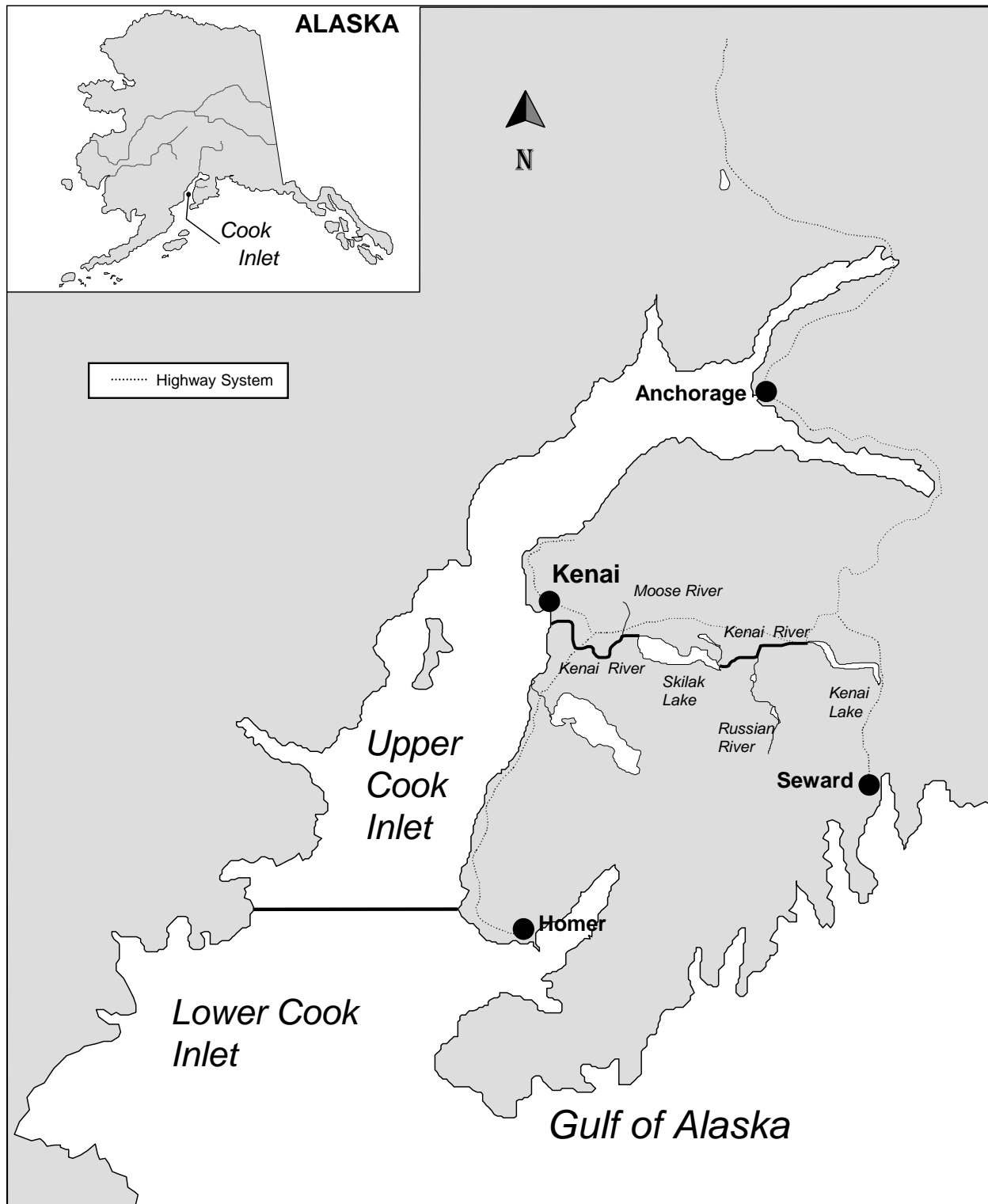


Figure 1.—Cook Inlet showing the location of the Kenai River.

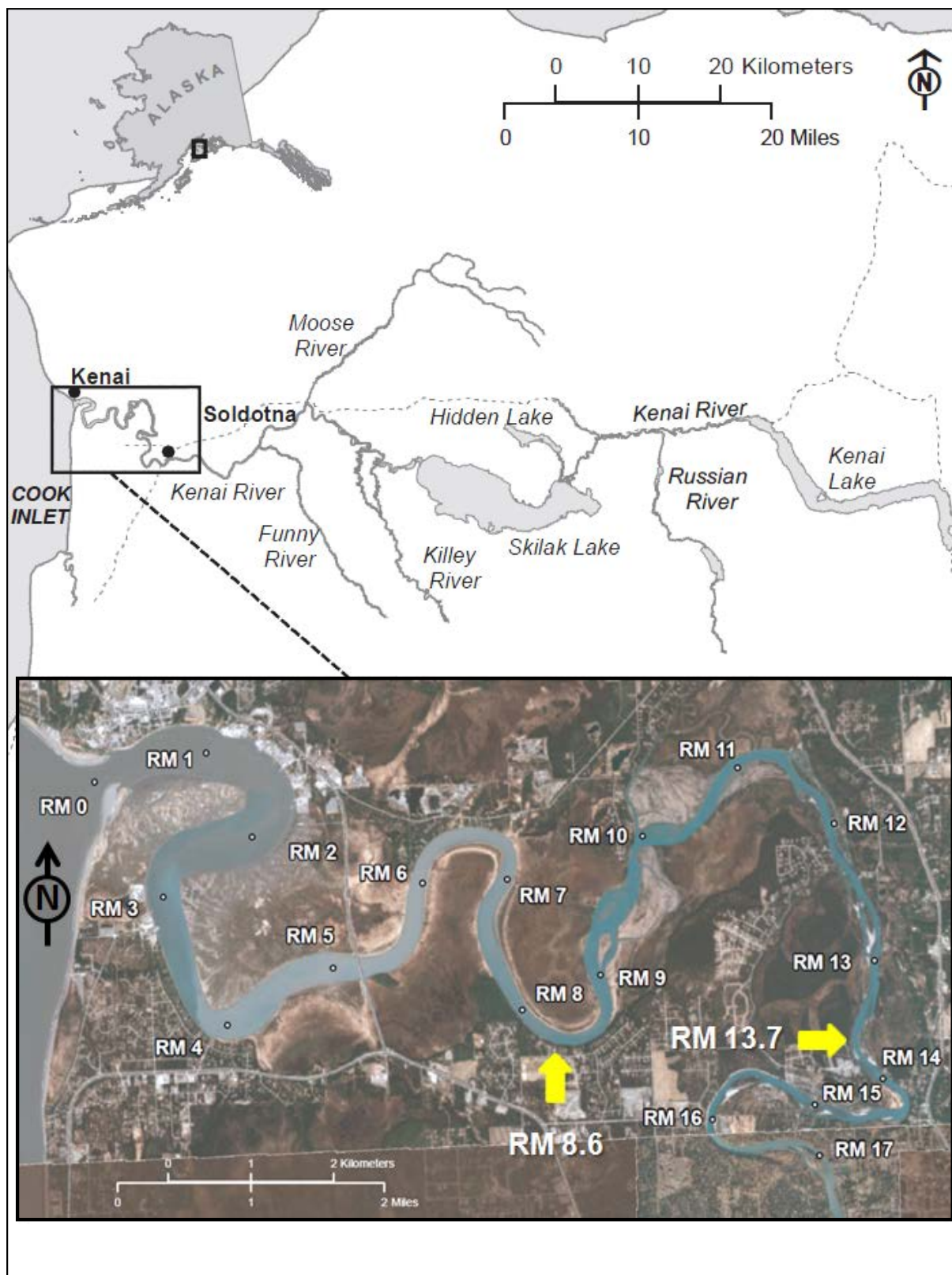


Figure 2.—Map of Kenai River showing location of Chinook salmon sonar sites at river miles 8.6 and 13.7.

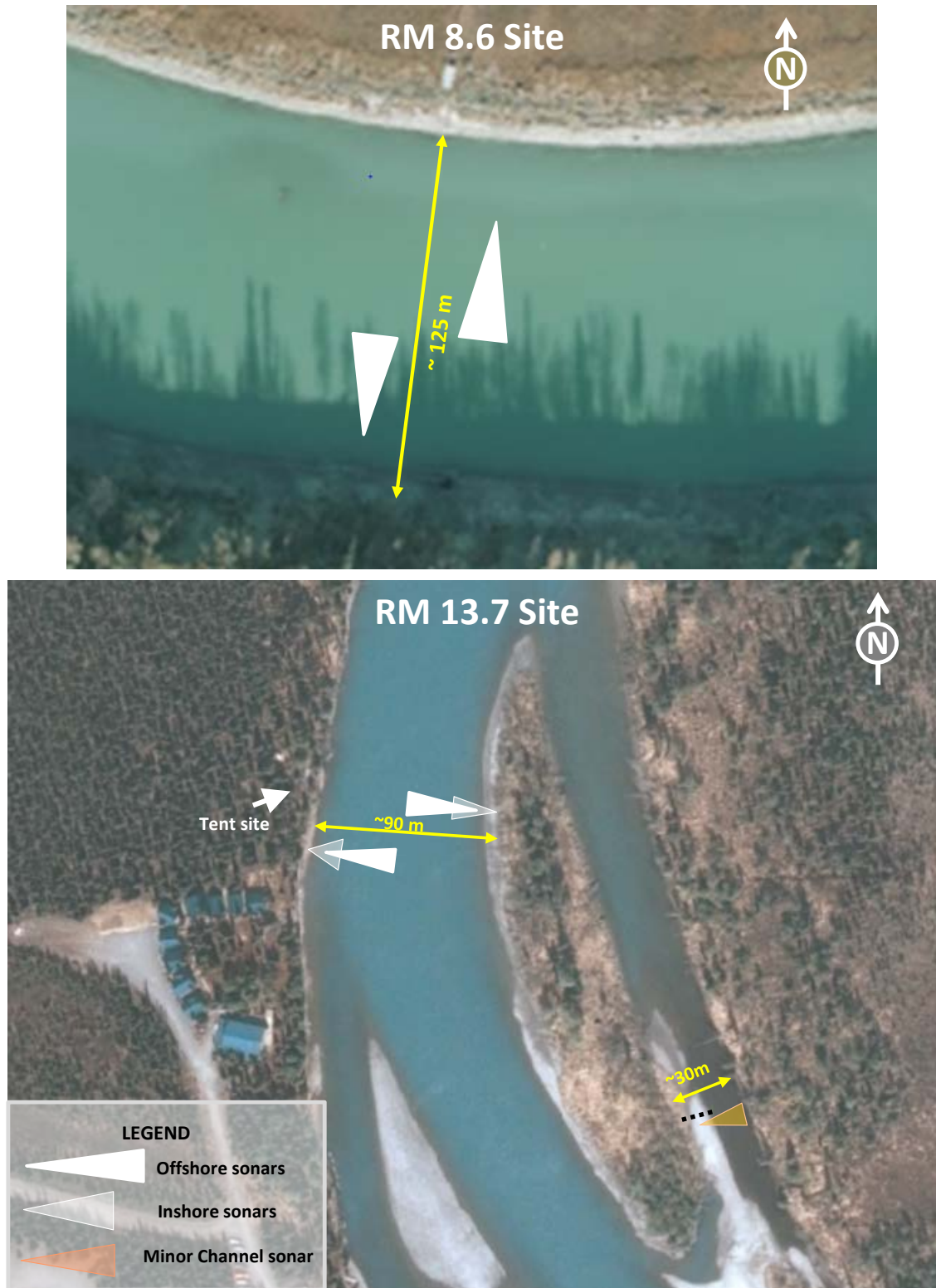


Figure 3.—Sonar sites showing approximate beam coverage at RM 8.6 (top) and RM 13.7 (bottom) of the Kenai River.

Note: Diagrams are not to scale. Tent site indicates location where sonar electronics are housed.



Figure 4.—Location of 9 transects conducted at the RM 13.7 site on 9 July 2012.

Note: Yellow arrows indicate preferred locations for sonars on each bank of the main channel. Red arrow indicates approximate location for sonar in the minor channel.

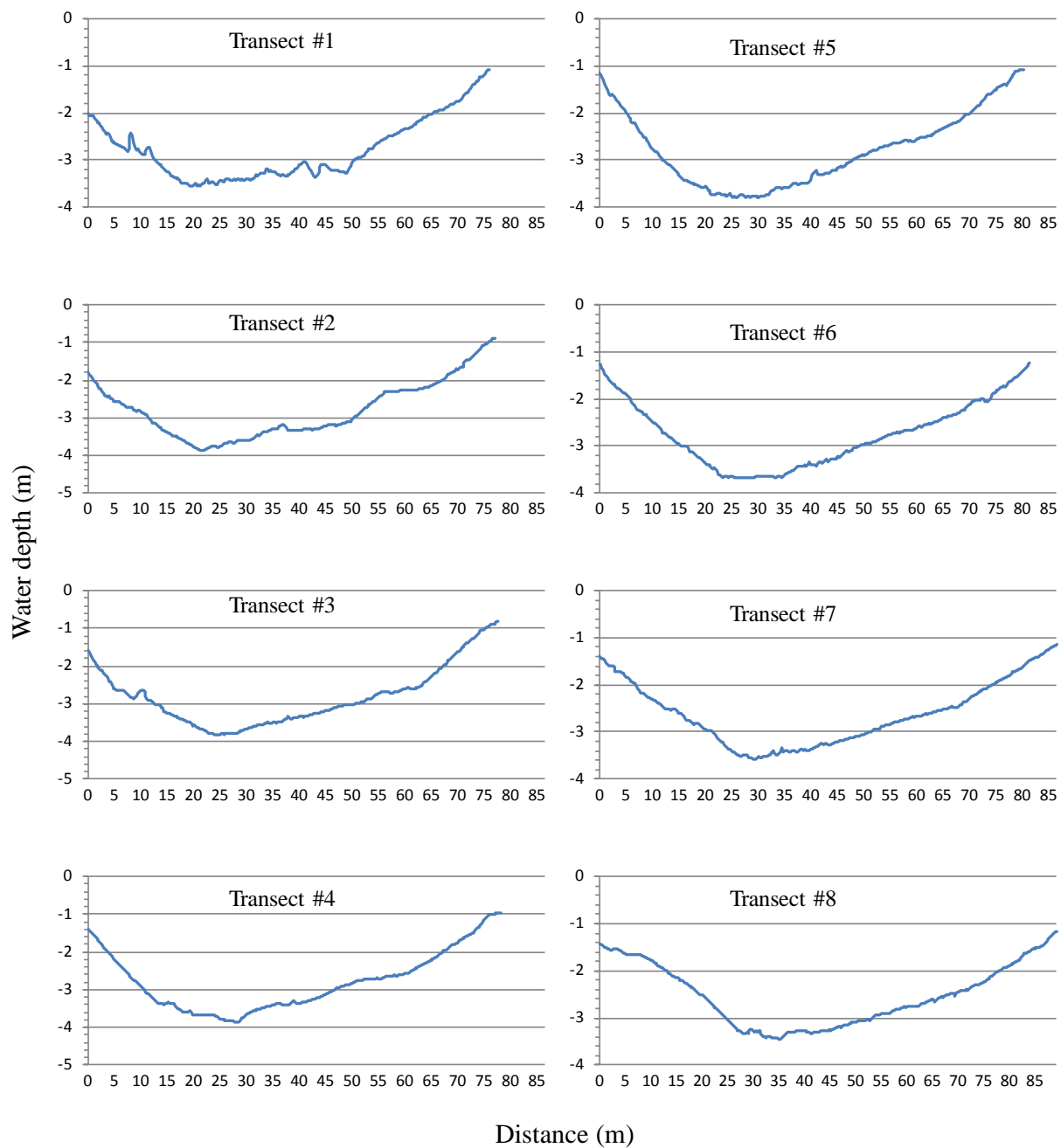


Figure 5.—Corresponding profiles for 8 transects conducted near RM 13.7 of the Kenai River with respect to Figure 4.

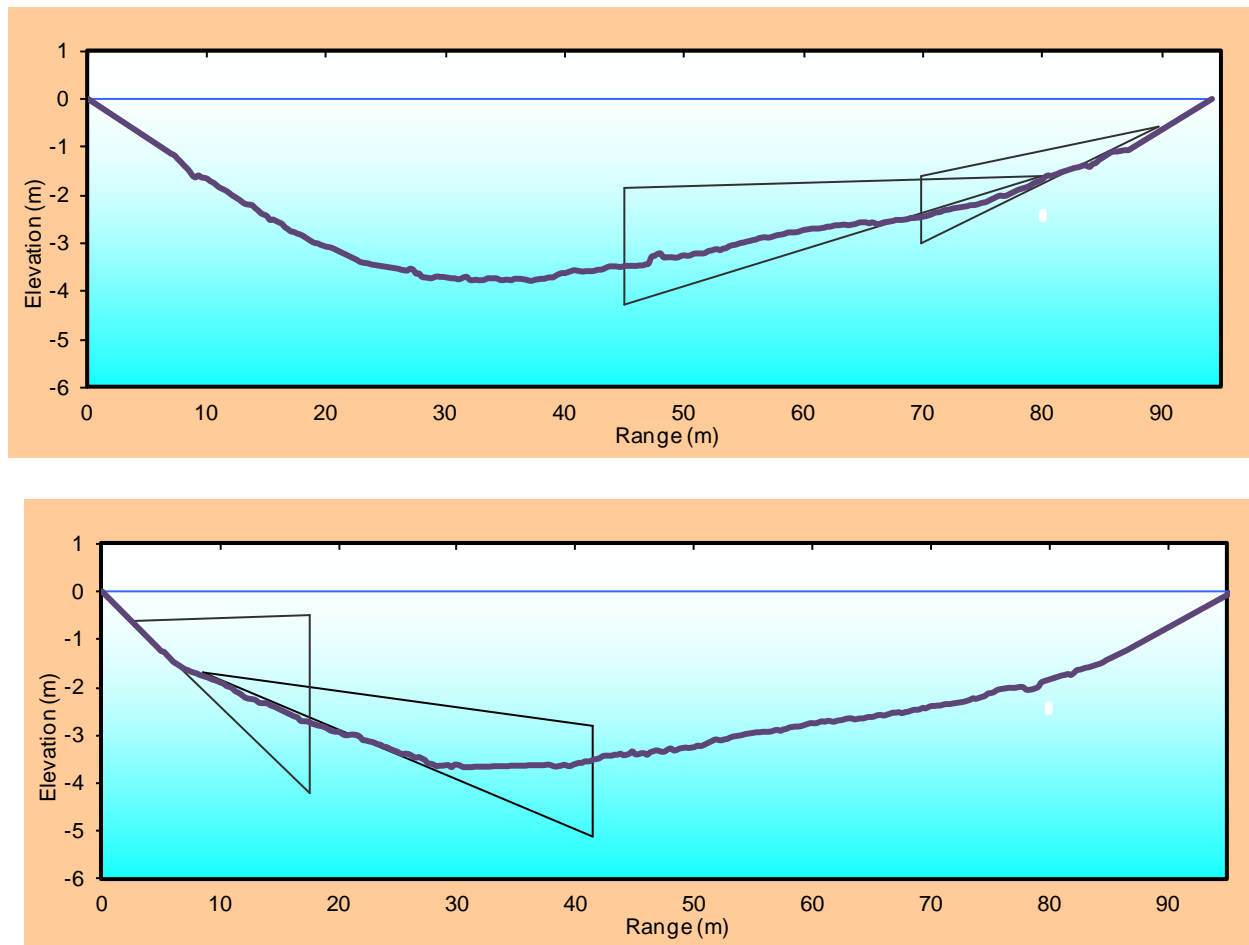


Figure 6.—Approximate coverage by nearshore and offshore sonars for the right bank (top; Transect 5 in Figure 5) and left bank (bottom; Transect 6 in Figure 5) main channel at RM 13.7 of the Kenai River.

Note: Aims are approximate because the actual aims were adjusted for each sample stratum.



Figure 7.—Sonar coverage of the minor channel at the RM 13.7 sonar site was achieved using an ARIS 1200 deployed on a tripod mount combined with a fixed weir.



Figure 8.—An ARIS 1200 with a high-resolution lens mounted on a steel tripod for offshore deployment (A) and on an aluminum H-mount for nearshore deployment (B).

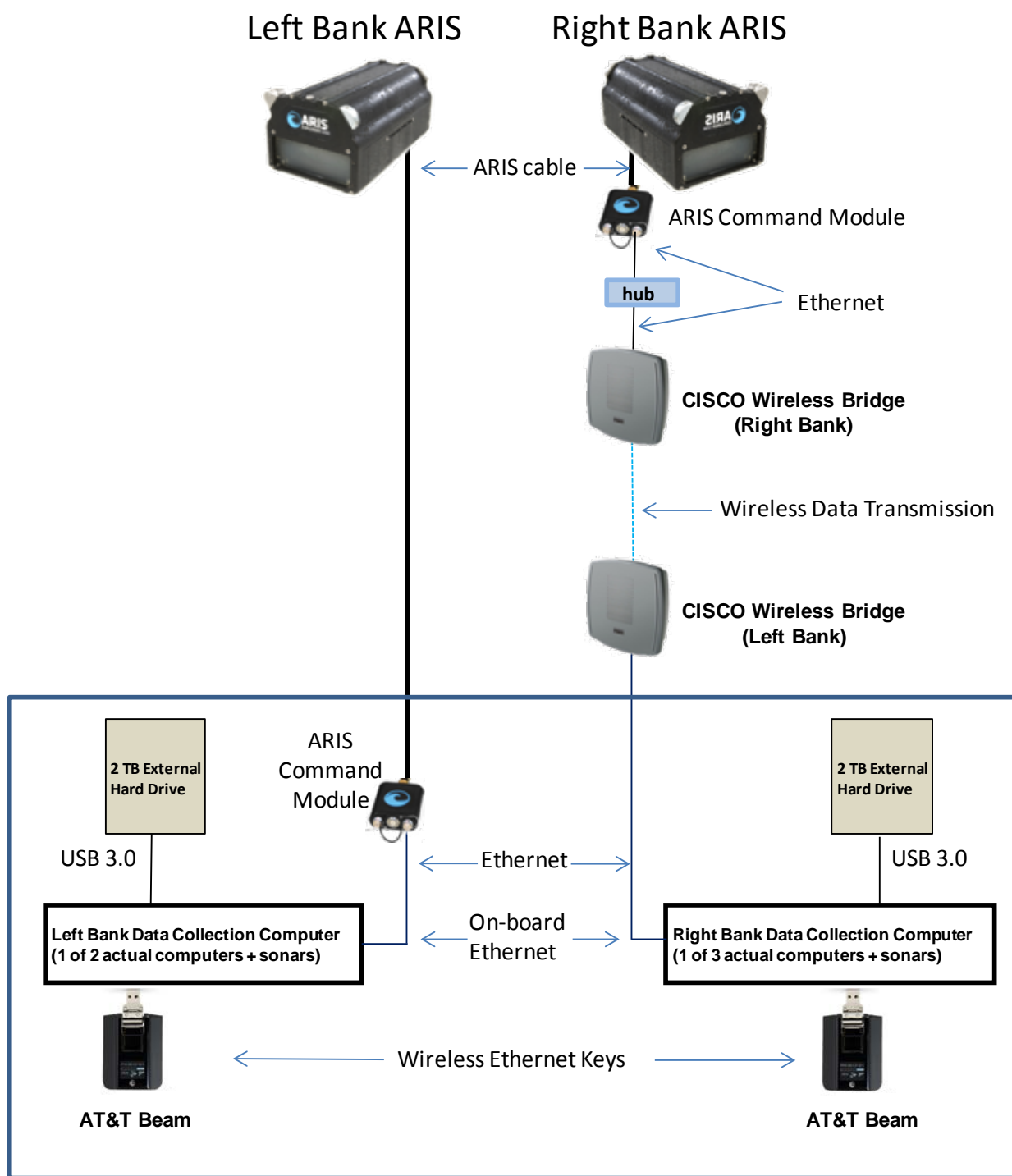


Figure 9.—ARIS data collection schematic for the RM 13.7 site on the Kenai River.

Note: For simplicity, this diagram shows only 1 of 3 right-bank data-collection computer–sonar pairs and 1 of 2 left-bank data-collection computer–sonar pairs. Each computer is equipped with wireless Ethernet through AT&T Beams (providing 4G LTE service) and can be accessed remotely using GoToMyPC accounts.

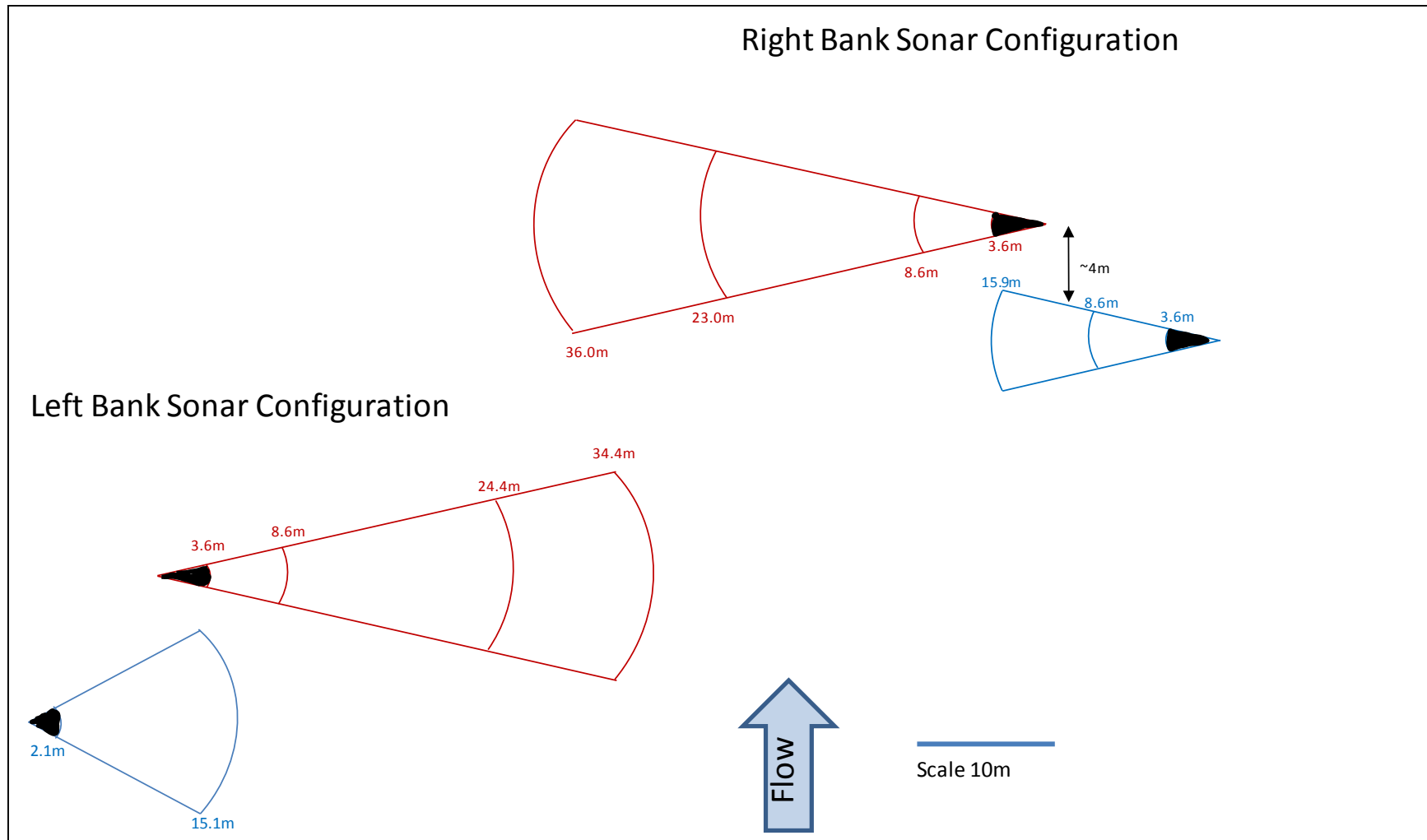
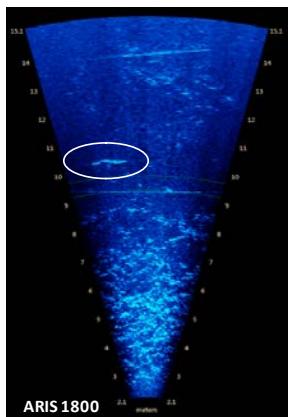


Figure 11.—Schematic for 4 left-bank (1 nearshore range [blue], 3 offshore ranges [red]) and 5 right-bank (2 nearshore ranges [blue], 3 offshore ranges [red]) range strata on the main channel of the Kenai River at RM 13.7.

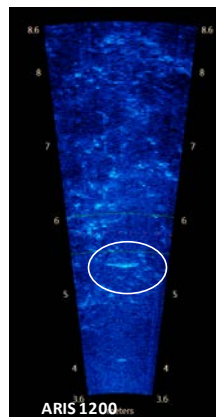
Note: No data are collected between the face of the transducer and the start of the first range stratum in order to avoid range-related size bias caused by poor focal resolution at such close ranges (see Appendix A1).

Left bank Nearshore (1 stratum)

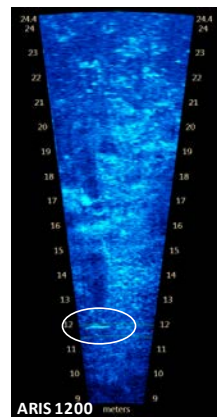


Stratum 1
Range = 2.1–15.1 m
Pitch = -6.7°

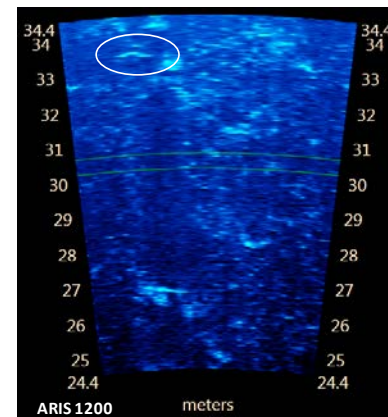
Left bank Offshore (3 strata)



Stratum 1
Range = 3.6–8.6 m
Pitch = -10.0°

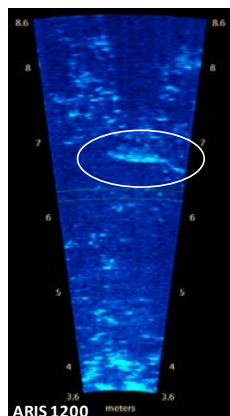


Stratum 2
Range = 8.6–24.4 m
Pitch = -6.9°

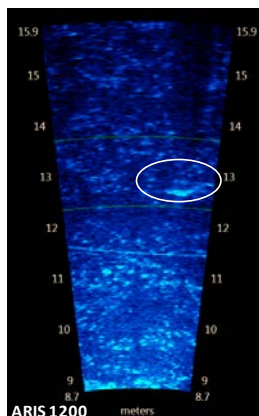


Stratum 3
Range = 24.4–34.4 m
Pitch = -4.0°

Right bank Nearshore (2 strata)

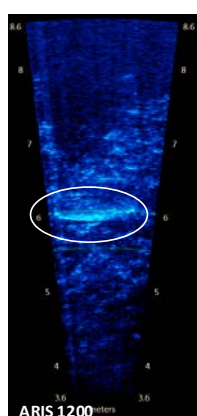


Stratum 1
Range = 3.6–8.6 m
Pitch = -8.1°

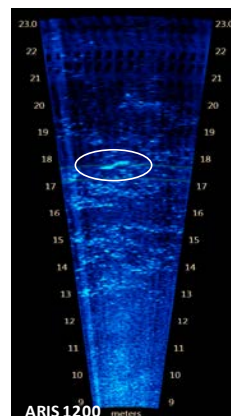


Stratum 2
Range = 8.6–15.9 m
Pitch = -7.2°

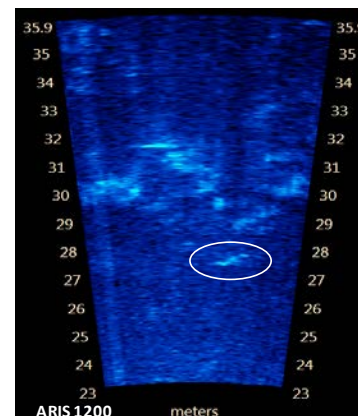
Right bank Offshore (3 strata)



Stratum 1
Range = 3.6–8.6 m
Pitch = -6.3°



Stratum 2
Range = 8.63–23.0 m
Pitch = -3.0°



Stratum 3
Range = 23.0–35.9 m
Pitch = -2.7°

Figure 12.—Example images from each of the 4 left-bank (top) and 5 right-bank (bottom) range strata taken at RM 13.7 Kenai River on 8 August 2013.

Note: Fish swimming through the beams are circled on each image.

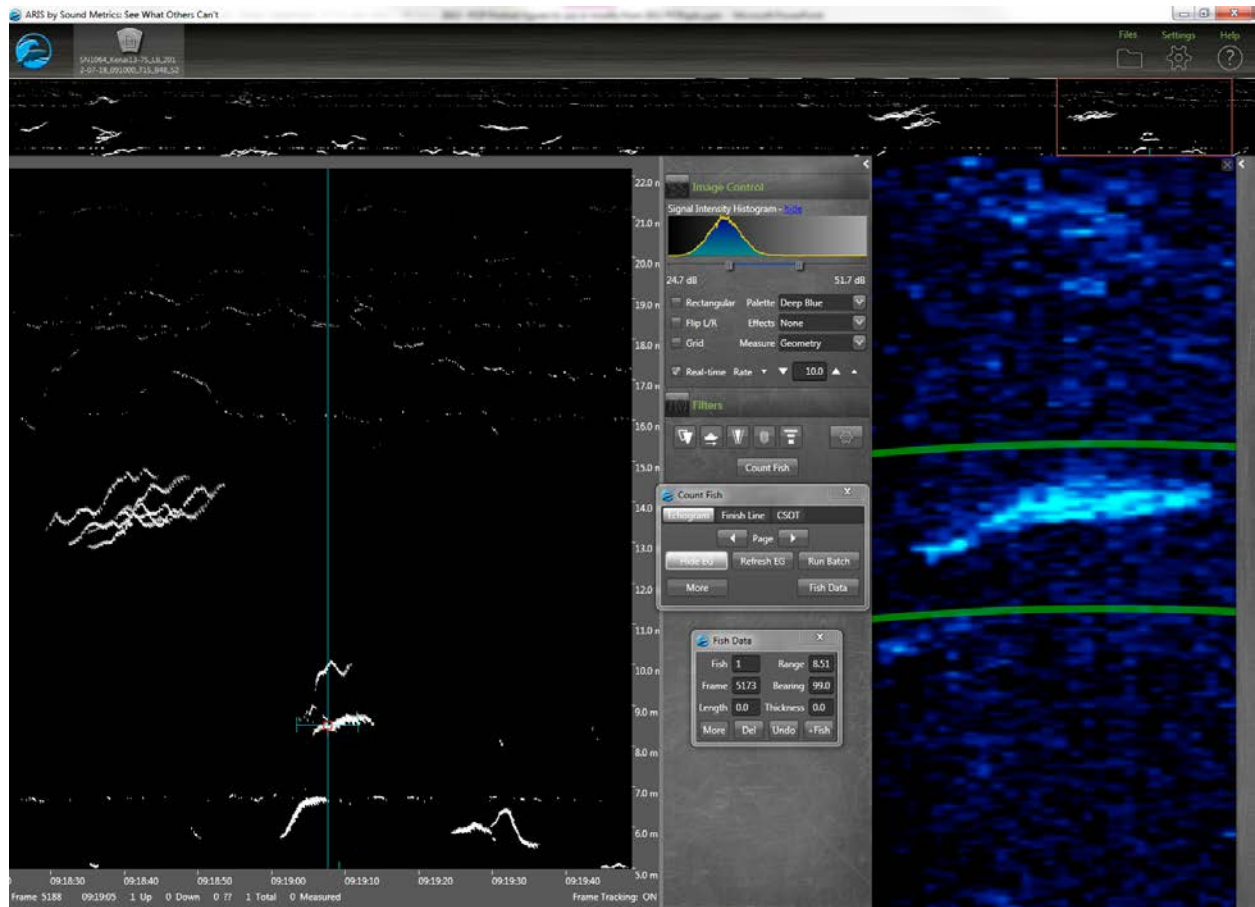


Figure 13.—ARISFish display window showing an echogram (at left) with traces of migrating fish that can be simultaneously displayed in video mode (at right) where fish images can be enlarged and measured.

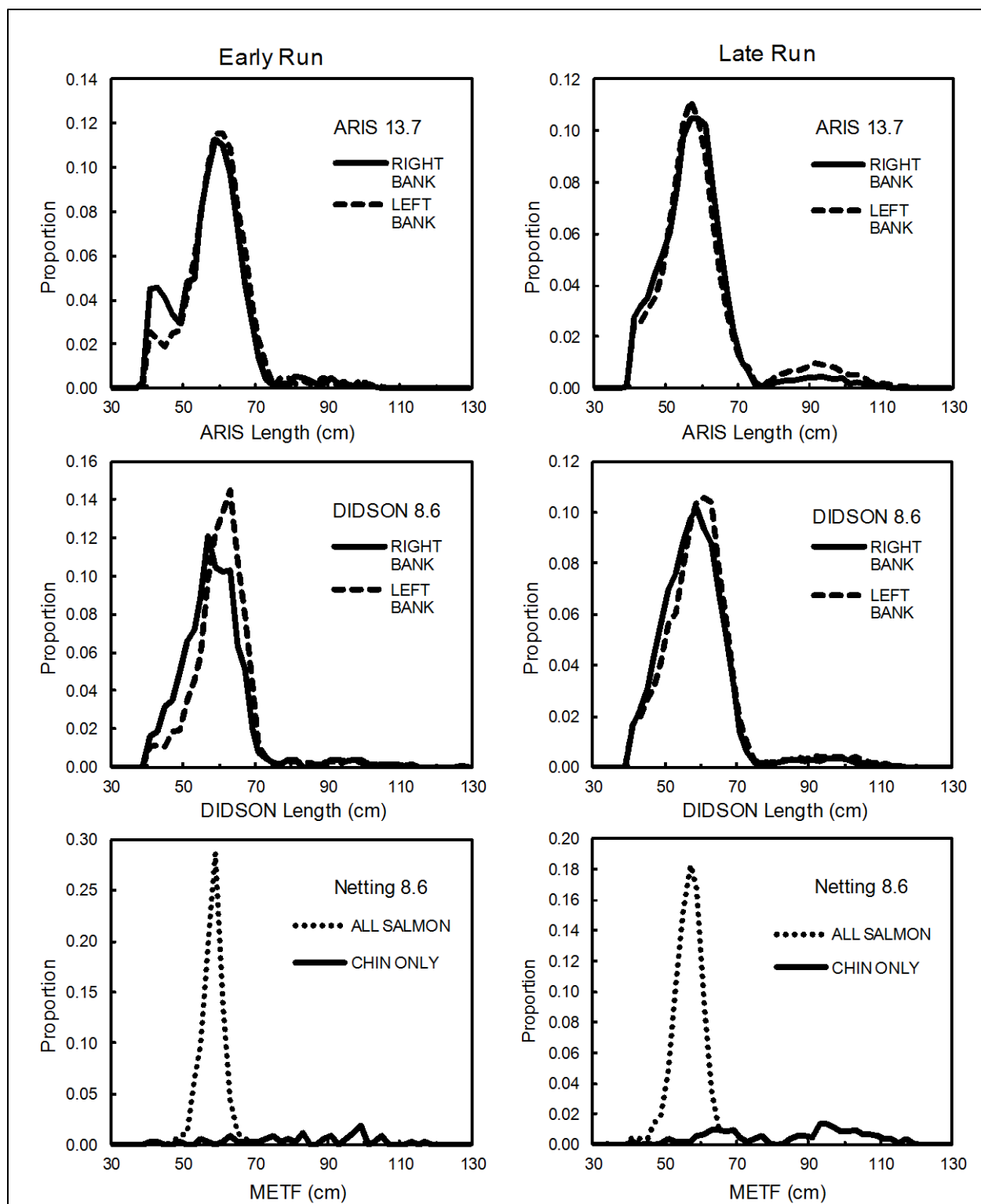


Figure 14.—Frequency distributions of ARIS lengths by bank at RM 13.7 (top), DIDSON lengths by bank at RM 8.6 (middle), and mid eye to tail fork (METF) lengths by species (all salmon vs. Chinook salmon only) from an onsite netting project (bottom; midriver drifts only), Kenai River early and late runs, 2013.

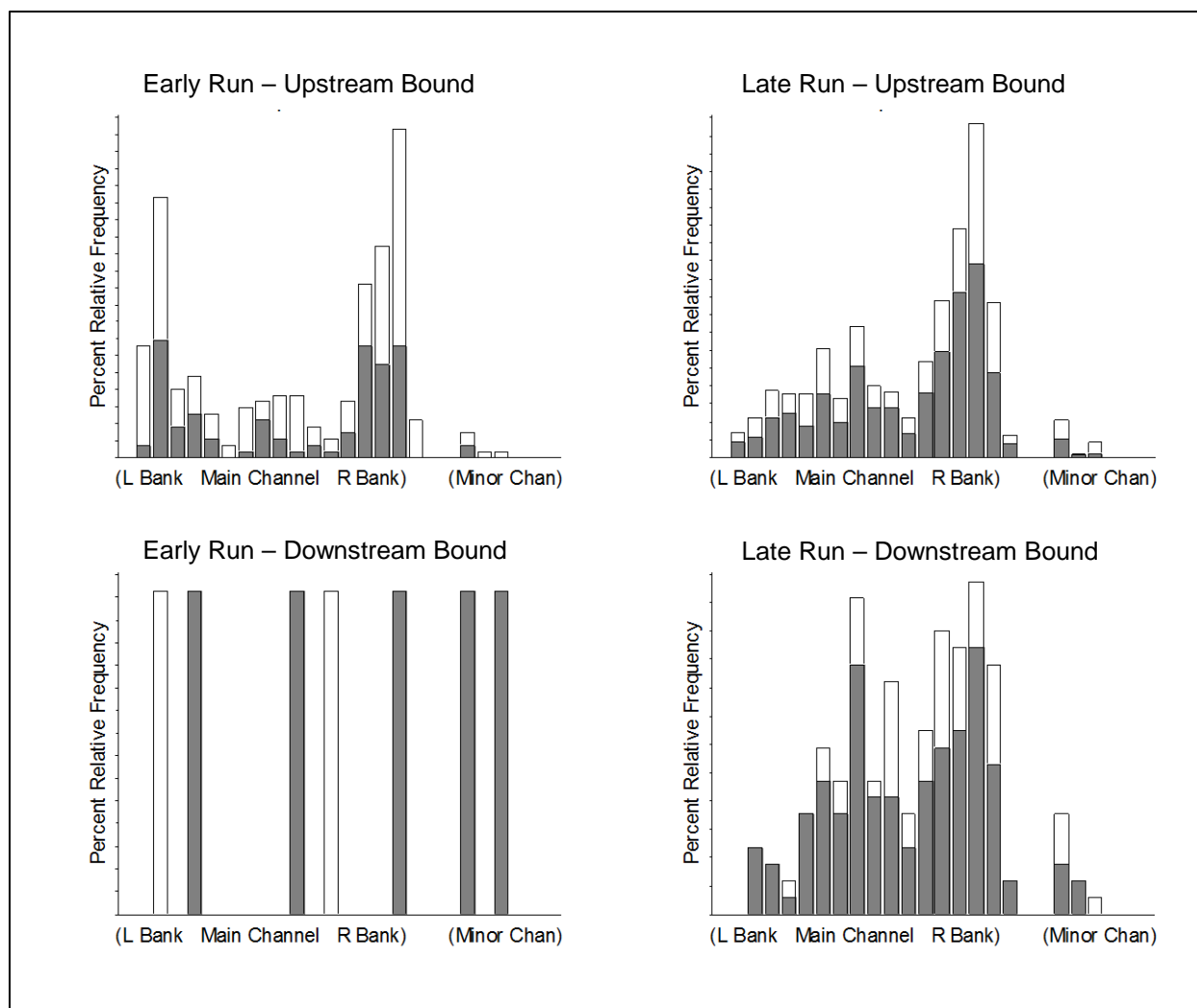


Figure 15.—Horizontal distribution, in 5 m increments from the left-bank main channel shore to the right-bank minor channel shore, of medium ($75 \text{ cm} \leq \text{AL} < 90 \text{ cm}$, open bars) and large ($\text{AL} \geq 90 \text{ cm}$, solid bars) early- and late-run fish, measured from ARIS, RM 13.7 Kenai River, 2013.

Note: Vertical axis shows percent relative frequency by run and direction of travel. Bar lengths sum to 1 for each panel.

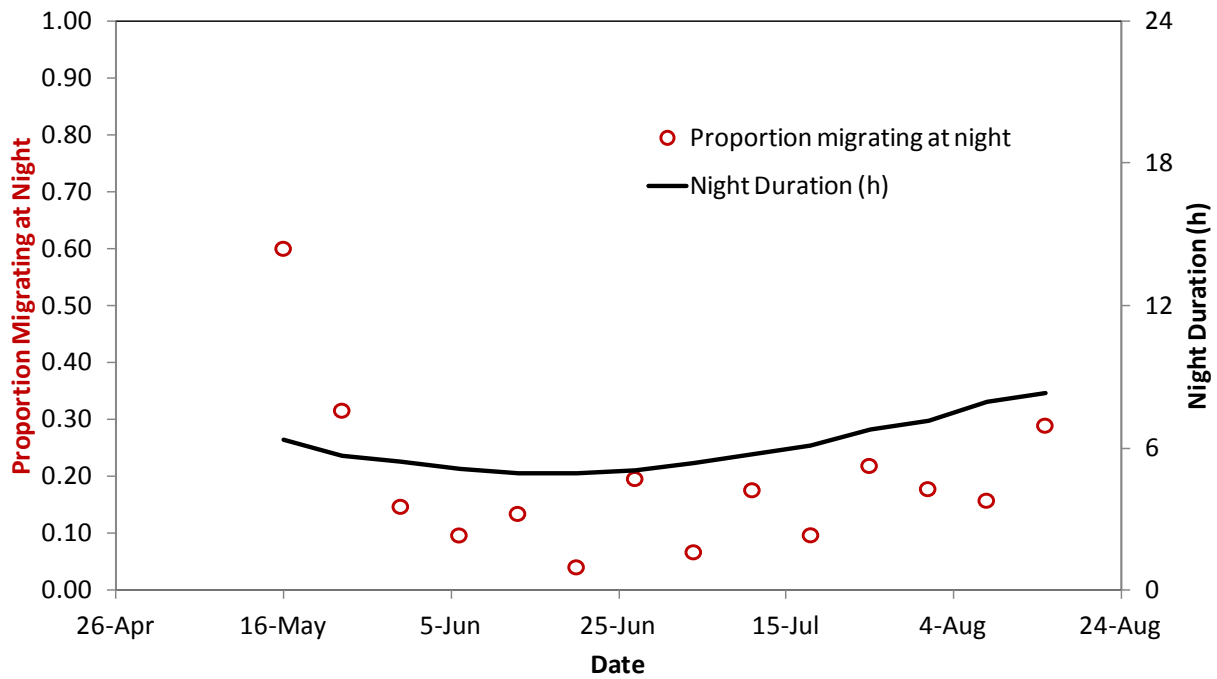


Figure 16.—Weekly proportions of fish greater than 75 cm AL migrating upstream at night (between sunset and sunrise; red circles), compared to relative night duration (solid line) in Kenai, Alaska.

Note: Proportions falling along the solid line are expected if there is no difference in the relative numbers of fish migrating between night and day. Proportions below the solid line indicate relatively fewer fish migrants at night; proportions above the solid line indicate relatively more.

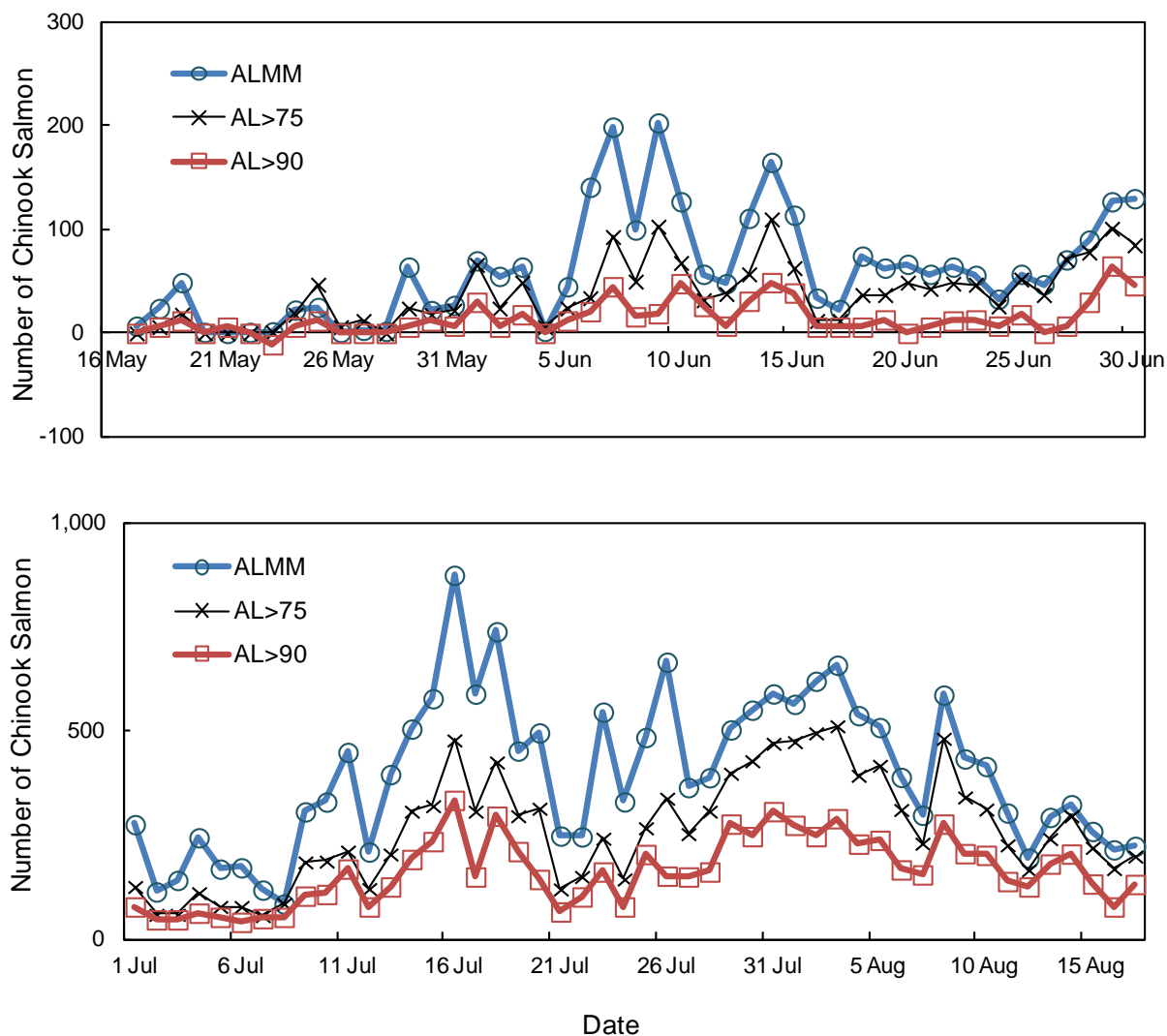


Figure 17.—Estimated net upstream passage of Chinook salmon based on an ARIS-length mixture model (ALMM) and estimated net upstream passage of medium and large Chinook salmon greater than or equal to 75 cm ARIS length ($AL \geq 75$ cm) and large Chinook salmon greater than or equal to 90 cm ($AL \geq 90$ cm), for early-run (top) and late-run (bottom) Kenai River Chinook salmon, 2013.

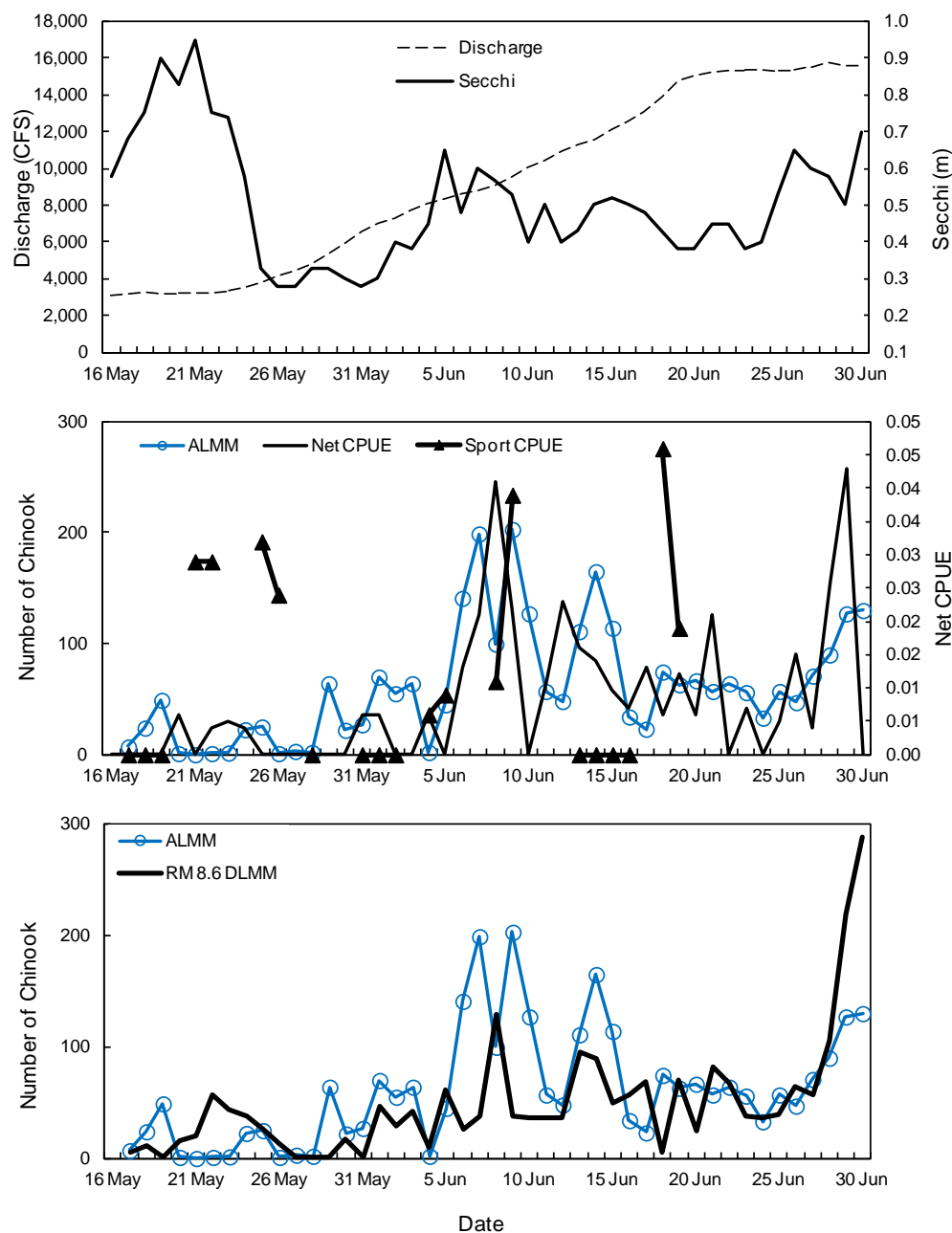


Figure 18.—Daily discharge rates collected at the Soldotna Bridge and Secchi disk readings taken at the RM 13.7 sonar site (top); ARIS-length mixture model (ALMM) estimates of net upstream Chinook salmon passage at RM 13.7, inriver gillnet Chinook salmon CPUE at RM 8.6, and sport fishery CPUE (middle); and spatially expanded DIDSON-length mixture model (DLMM) upstream-only Chinook salmon passage at RM 8.6¹¹ compared to ALMM (bottom), Kenai River early run, 2013.

Note: River discharge taken from USGS¹². Net CPUE and sport fish CPUE taken from Perschbacher (2015). DLMM estimates¹³ were multiplied by 1.55 to account for Chinook salmon passage shoreward of the RM 8.6 transducers. The sport fishery closed after 19 July.

¹¹ Derived by multiplying 1.55 times the daily midriver passage estimates presented in Table 4 in Key et al. (2016a).

¹² USGS Water resource data, Alaska, water year 2013. Website Daily Streamflow for Alaska, Soldotna gauging station, site #15266300, accessed September 8, 2015. <http://water.usgs.gov/ak/nwis/discharge>.

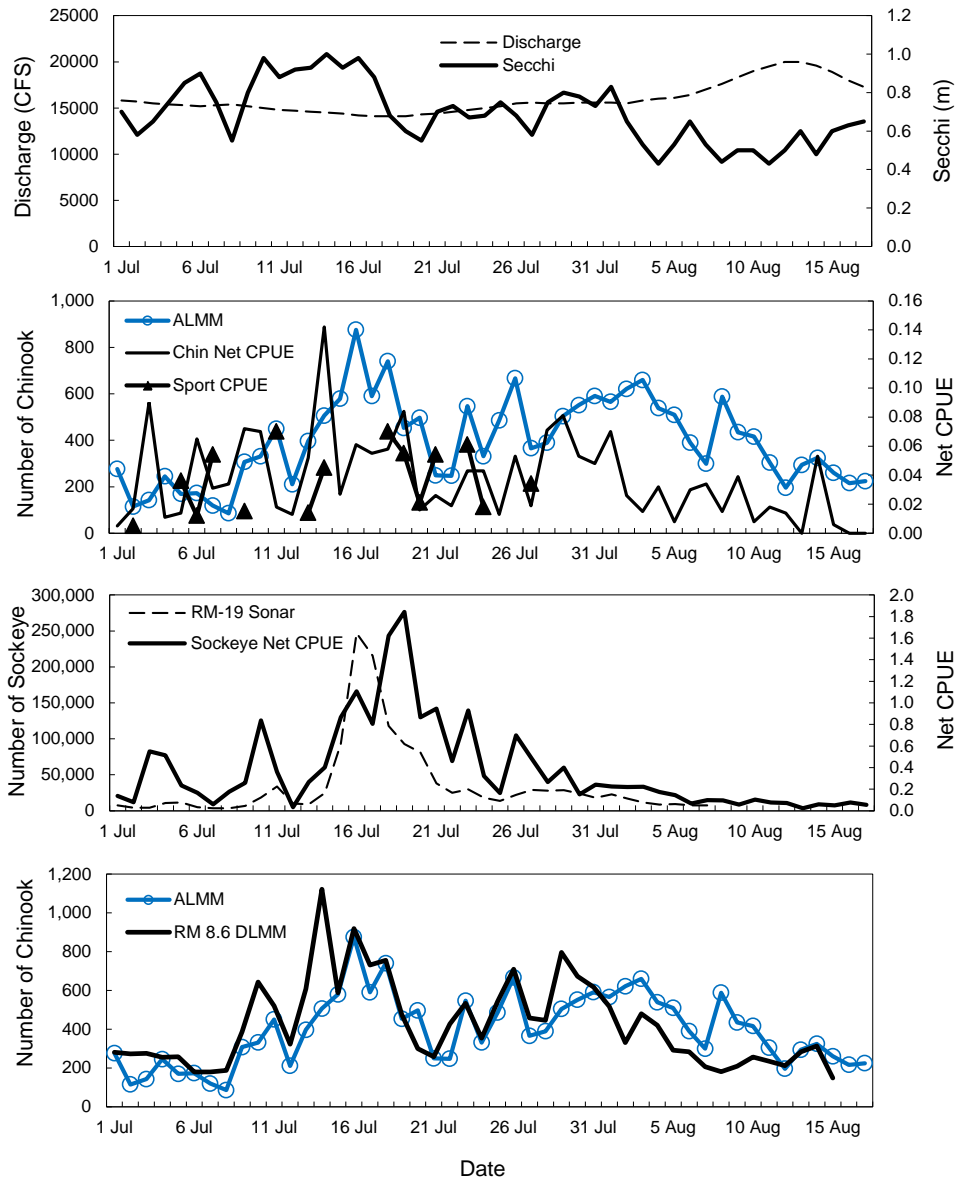


Figure 19.—Daily discharge rates collected at the Soldotna Bridge and Secchi disk readings taken at the RM 13.7 sonar site (top); ARIS-length mixture model (ALMM) estimates of net upstream Chinook salmon passage at RM 13.7, inriver gillnet Chinook salmon CPUE at RM 8.6, and Chinook salmon sport fishery CPUE (top-middle); RM 19 sockeye salmon sonar passage and inriver gillnet sockeye salmon CPUE at RM 8.6 (bottom-middle); and spatially expanded DIDSON-length mixture model (DLMM) upstream-only Chinook salmon passage at RM 8.6¹³ compared to ALMM (bottom), late run Kenai River, 2013.

Note: River discharge taken from USGS¹⁴. Net CPUE and sport fish CPUE from Perschbacher (2015). RM 19 sonar estimates from Glick and Willette (2015). DLMM estimates¹⁶ were multiplied by 1.28 to account for Chinook salmon passage shoreward of the RM 8.6 transducers. Open triangles represent days on which only unguided anglers were allowed to fish. The sport fishery closed after 27 July.

¹³ Derived by multiplying 1.28 times the daily midriver passage estimates presented in Table 5 in Key et al. (2016a).

¹⁴ USGS Water resource data, Alaska, water year 2013. Website Daily Streamflow for Alaska, Soldotna gauging station, site #15266300, accessed September 8, 2015. <http://water.usgs.gov/ak/nwis/discharge>.

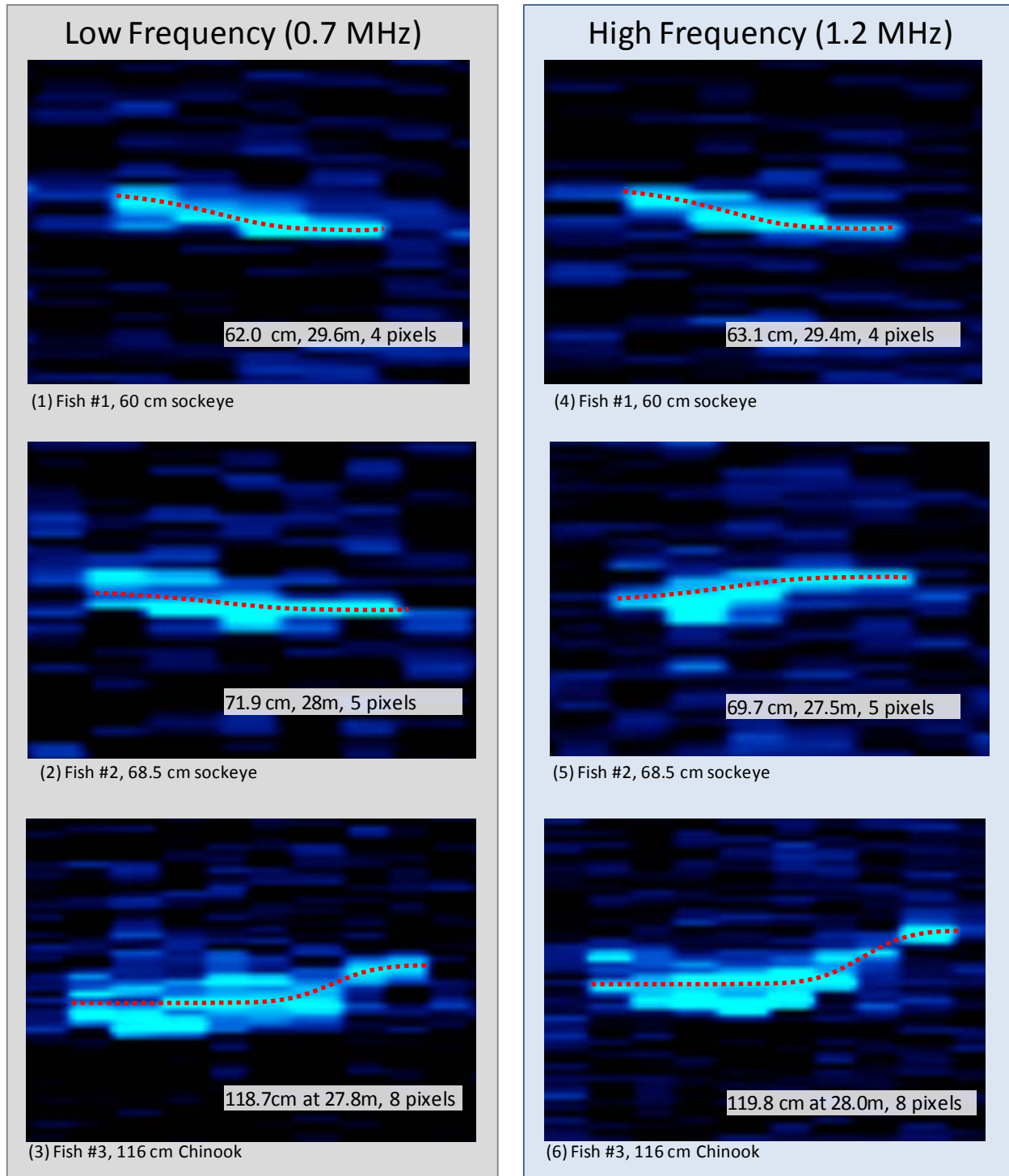


Figure 20.—Images from 3 tethered salmon: a 60 cm sockeye salmon (top panels 1 and 4), a 68.5 cm sockeye salmon (middle panels 2 and 5), and a 116 cm Chinook salmon (bottom panels 3 and 6). Data were collected in both low (left panels 1, 2, and 3) and high (right panels 4, 5, and 6) frequencies to compare length measurements at both frequencies. Images were collected at RM 8.6 Kenai River on 17 July 2013.

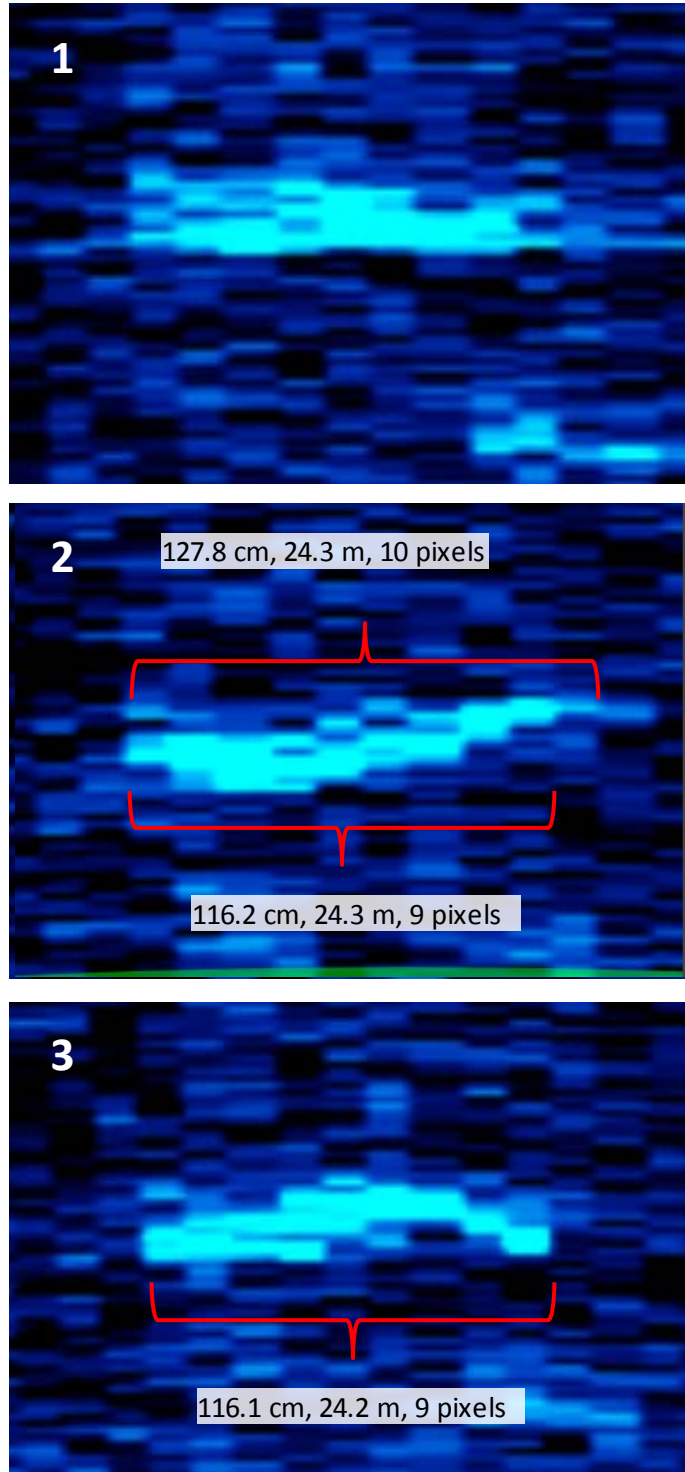


Figure 21.—Three images collected at low frequency (0.7 MHz) from a 116 cm tethered Chinook salmon. Panel 1 shows crosstalk in the beams adjacent to both the snout and tail. Panel 2 shows crosstalk adjacent to the tail that could be mistaken for an extension of the tail by 1 or even 2 pixels. Panel 3 shows an optimal image for measurement.

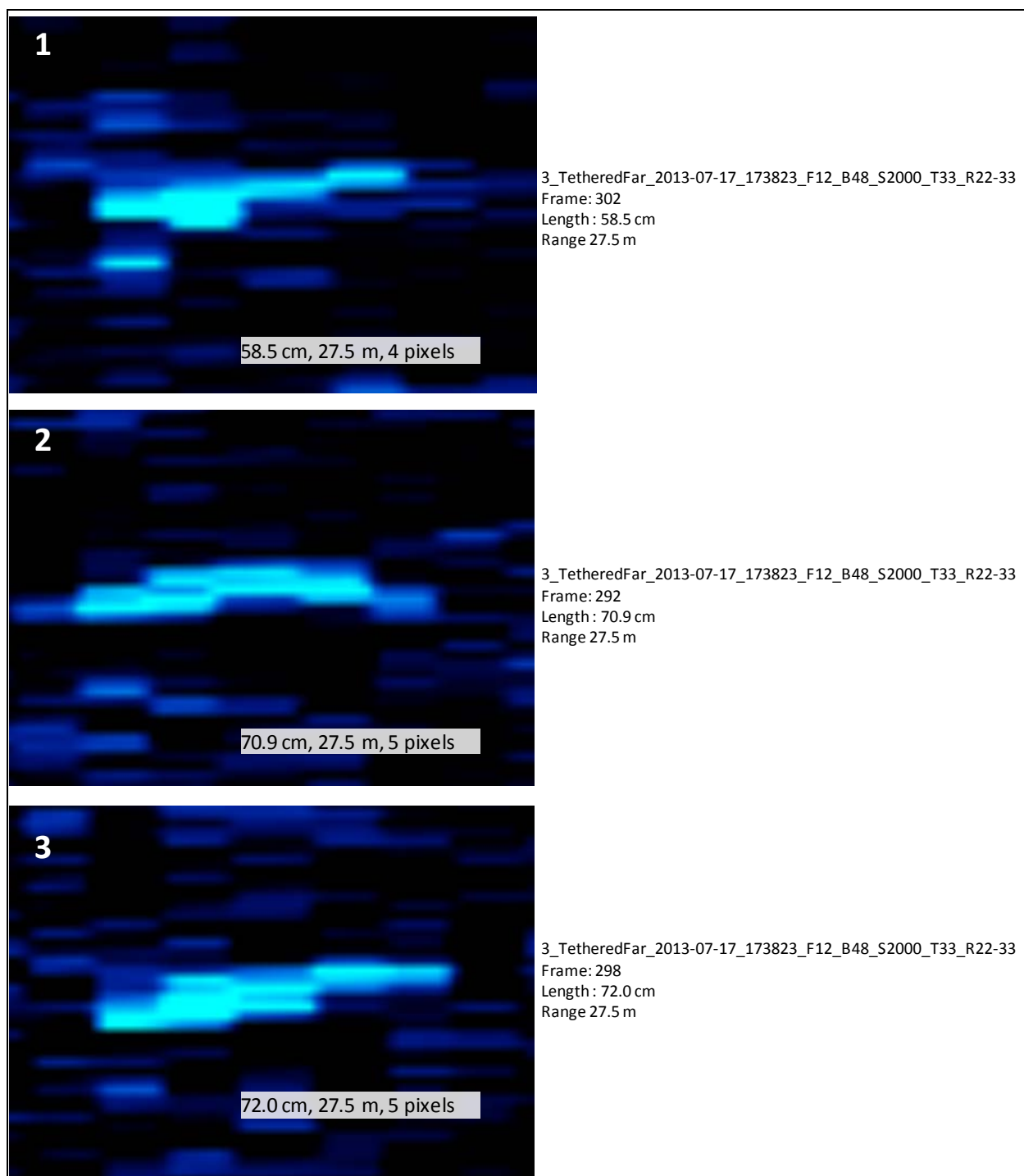
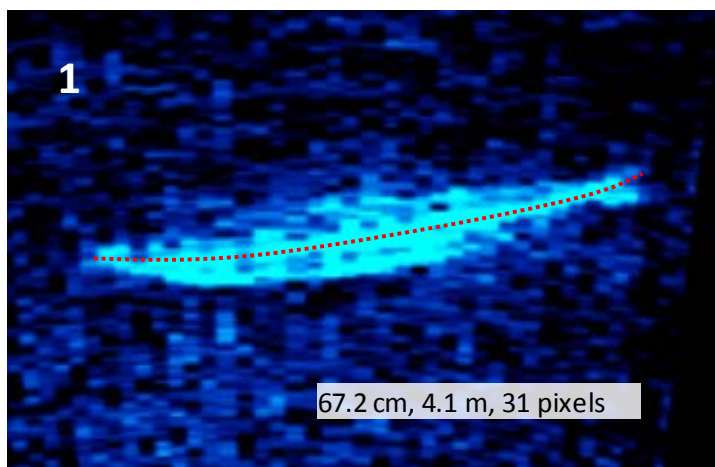
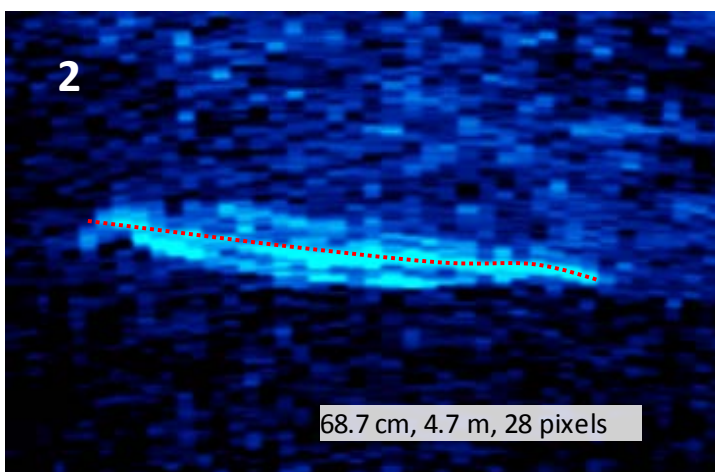


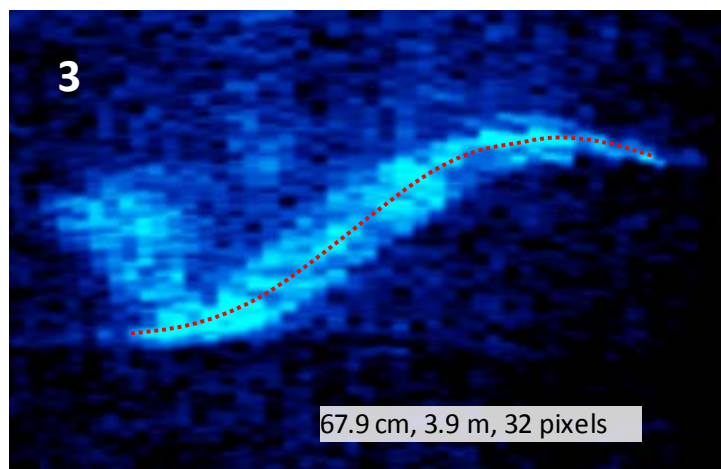
Figure 22.—Images from a 68.5 cm sockeye salmon (Fish 2 in Tables 13–14) tethered at far range that show a strong 4-pixel image (top), an ambiguous 5-pixel image where the tail is not yet distinct (middle), and a strong 5-pixel image (bottom).



3_TetheredNear_2013-07-17_182746_F12_B48_S1724_T08_R3-8.aris, Frame 5555, 68.1 cm at 4.1m



3_TetheredNear_2013-07-17_182746_F12_B48_S1724_T08_R3-8.aris, Frame 8984, 68.8 cm at 4.7m



3_TetheredNear_2013-07-17_182746_F12_B48_S1724_T08_R3-8.aris, Frame 662, 67.9 cm at 3.9m

Figure 23.—Images from a 68.5 cm sockeye salmon (Fish 2 in Tables 13–14) tethered at close range (3.9 m to 4.7 m).

Note: Images were collected at RM 8.6, Kenai River, 17 July 2013.

APPENDIX A: COMPARISON OF DIDSON AND ARIS CONFIGURATIONS

Frequency

The dual-frequency identification sonar (DIDSON) operates at 2 frequencies: a higher frequency that produces higher resolution images and a lower frequency that detects targets at farther ranges but at a reduced image resolution. Two DIDSON models are currently available based on different operating frequencies (Appendix A2). The short-range or standard model (DIDSON SV) operates at 1.8 MHz to approximately 15 m in range and at 1.1 MHz to approximately 35 m and produces higher resolution images than the long-range model. The long-range model (DIDSON LR) with a high-resolution lens operates at 1.2 MHz to approximately 30 m in range and at 0.7 MHz to ranges exceeding 100 m, but produces images with approximately half the resolution of the DIDSON SV (see explanation below).

Similar to DIDSON, adaptive resolution imaging sonar (ARIS) systems operate at 2 frequencies analogous to the DIDSON frequencies (Appendix A3). The two ARIS models used on this project, ARIS 1800 and ARIS 1200, are essentially updated versions of the DIDSON SV and DIDSON LR models (Appendices A2–A3). Both ARIS models used in the RM 13.7 study were operated in high frequency mode when possible to achieve maximum image resolution. One difference between ARIS and DIDSON with respect to low-frequency data collection is that the ARIS 1800 uses 96 beams at low frequency by default, whereas the equivalent DIDSON SV is hard-wired for 48 beams at low frequency.

Beam Dimensions and Lens Selection

Both the DIDSON LR and ARIS 1200 can be used with high-resolution lenses (+HRL) to increase the image resolution to the level achieved by the DIDSON SV and ARIS 1800 (these modifications are referred to as DIDSON LR+HRL and ARIS 1200+HRL). The high-resolution lens has a larger aperture, which increases the image resolution over the standard lens by approximately a factor of 2 by reducing the width of the individual beams and spreading them across a narrower field of view (Appendix A2). Overall nominal beam dimensions for a DIDSON LR or an ARIS 1200 with a standard lens are approximately 28° in the horizontal axis and 14° in the vertical axis. Operating at 1.2 MHz, the 28° horizontal axis is a radial array of 48 beams that are nominally 0.50° wide and spaced across the array at approximately 0.60° intervals. With the addition of the high-resolution lens, the overall nominal beam dimensions of the DIDSON LR and ARIS 1200 are reduced to approximately 15° in the horizontal axis and 3° in the vertical axis, and the 48 individual beams are reduced to approximately 0.3° wide and spaced across the array at approximately 0.3° intervals (Appendices A2 and A4). The combined concentration of horizontal and vertical beam widths also increases the returned signal from a given target by 10 dB, an effect that increases the maximum range of the sonar over the standard lens.

Four ARIS 1200 fitted with high-resolution lenses were used for most of the data collected at the RM 13.7 site. However, an ARIS 1800 with a standard lens was used on the left-bank nearshore stratum because the coverage range was shorter and because the wider beam dimensions of the ARIS 1800 are preferred for increasing the beam coverage at close range and reducing biases associated with focal resolution at close range (see below).

-continued-

Focal Resolution of DIDSON and ARIS Lenses: considerations for measurement accuracy

When sizing fish from DIDSON or ARIS images, there can be a bias beyond the geometric beam spreading issue, depending on the start range and end range of the image window. Depth of field is reduced at closer focusing ranges with the effect that defocused targets will appear smeared in the horizontal direction. The degree of bias is dependent on both the set focus range and the distance of the target from that set focus range. It is also dependent on the lens set. In general, if the focus is set to 4 m or longer for a standard lens, or 7 m or longer for a large (+HRL) lens, targets will be in good focus from there out to infinity. Inside of that range, focus will degrade significantly (Bill Hanot, Sound Metrics Corporation, Seattle Washington, personal communication). One way to minimize out-of-focus images is to create a smaller range window to insonify targets at close range. For example, we often use a 5 m range window from about 3 to 8 m for the first range stratum when using a large (high-resolution) lens.

For DIDSON, focus counts of 0–255 represent the total range of travel of the middle (focus) lens. For the ARIS 1200 and 1800, which use the same lens sets and have the same focus curves, focus counts of 0–1000 represent the total range of travel (0.1% per unit). Appendix A5 shows the ARIS lens position (indicated by the numbers in the range 0–1000) versus focus range for the ARIS +HLR. There is a nonlinear relationship between lens position and focus range, with short ranges requiring large position movements for small increments of change in focus range and long ranges having small position movements for several meters of change in focus range. Also, beyond a certain range, images are generally in focus. Based on the focus curves in Appendix A5, images are at least 75% in focus starting at 4 m for the standard lens and starting at 7 m for the large lens.

Image Resolution Basics

The resolution of a DIDSON or ARIS image is defined in terms of downrange and crossrange resolution where crossrange resolution refers to the width and downrange resolution refers to the height of the individual pixels that make up the image (Appendix A6). Each image pixel in a DIDSON or ARIS frame has (x, y) rectangular coordinates that are mapped back to a beam and sample number defined by polar coordinates. The pixel height defines the downrange resolution and the pixel width defines the crossrange resolution of the image. Appendix A6 shows that image pixels are sometimes broken down into smaller screen pixels (e.g., pixels immediately to the right of the enlarged pixels), which are an artifact of conversions between rectangular and polar coordinates.

-continued-

Crossrange Resolution

The crossrange resolution is primarily determined by the individual beam spacing and beam width, both of which are approximately 0.3° for all the sonar configurations used in this study (i.e., DIDSON LR +HRL at 1.8 MHz, ARIS 1800 at 1.8 MHz with standard lens, and ARIS 1200 +HRL at 1.2 MHz; Appendix A2). Targets at closer range are better resolved because the individual beam widths and corresponding image pixels increase with range following the formula below:

$$X = 2R \tan \frac{\theta}{2} \quad (A1)$$

where

X = width of the individual beam or “image pixel” in meters,

R = range of interest in meters, and

θ = individual beam angle in degrees (approximately 0.3°)

Optimizing Crossrange Resolution

Achieving the highest crossrange resolution is important when taking fish length measurements from images. Collecting data at high frequency with a high-resolution lens produces the highest crossrange resolution for each ARIS or DIDSON model. However, the high-resolution lens is not always used because it also decreases the vertical beam width dimension from about 14° to about 3° and the field of view from about 30° to about 15° (Appendix A2). Also, reduced focal resolution at close range must be considered. The high-resolution lens is used in this study on DIDSON LR and ARIS 1200 models, both to extend the range at which high-frequency data can be collected (~35 m) and to double the crossrange resolution. The standard lens is used on the ARIS 1800 to achieve better water column coverage over the short range.

ARIS 1800 images can attain a finer crossrange resolution than the equivalent DIDSON SV at low frequency because, as mentioned previously, ARIS 1800 can use 96 beams at low frequency whereas DIDSON is hard-wired for 48 beams at low frequency. This means the ARIS 1800 can achieve twice the resolution that a DIDSON SV can achieve at ranges requiring low frequency mode (i.e., ranges exceeding approximately 15–20 m). However, using all 96 beams will cut the maximum frame rate by half, which can be an issue when insonifying longer ranges.

Downrange Resolution

Window length, i.e., the range interval sampled by the sonar, controls the downrange resolution of the DIDSON image, which is calculated using the formula:

$$Y = W/N \quad (A2)$$

where

W = window length (cm), and

N = number of range samples (or pixels)

-continued-

With DIDSON, N is fixed at 512 samples (pixels) and images with shorter window lengths are always better resolved. The DIDSON LR+HRL “Window Length” parameter can only be set at discrete values: 2.5, 5.0, 10.0, or 20.0 m at 1.2 MHz. Although using shorter window lengths increases resolution, it also requires more individual strata to cover the desired range. Dividing the total range covered into too many discrete strata increases the data-processing time. Typically, a window length of 5 m is used for the first 2 range strata to minimize the bias associated with close-range targets (see below). A window length of 10 m is used for each subsequent range stratum sampled, a compromise that allows a relatively high resolution while allowing a reasonable distance to be covered by each stratum. The downrange resolution (or pixel height) for a 5 m range window is 1 cm (500 cm per 512 samples) and for a 10 m window length is 2 cm (1,000 cm per 512 samples).

ARIS images can attain a finer downrange resolution than DIDSON. With ARIS, N can vary from 128 to a maximum of 4,000 samples (pixels) and window length is user selectable. This allows the user to collect data over longer window lengths but increases the number of samples per beam to compensate. Appendix A6 contrasts images from a DIDSON LR+HRL with an ARIS 1200+HRL. The ARIS image in Appendix A6 has twice the downrange resolution of the DIDSON image because it was collected at 2,000 samples (pixels) per beam with a 20 m range window yielding a downrange resolution of 1 cm (2,000 cm per 2,000 samples) compared to a downrange resolution of 2 cm for the DIDSON image, which was collected at 512 samples with a 10 m range window (1,000 cm per 512 samples). Note that the pixels composing the ARIS image in Appendix A6 appear less well defined because a smoothing algorithm has been applied.

Setting the Downrange Resolution in ARIS

Data acquisition parameters affecting downrange resolution, or image pixel height, can be selected using the “Detail” parameter (measured in millimeters) from the ARIScope Sonar Control menu or by fixing the “Sample Period” parameter (measured in microseconds) in the Advanced Sonar Settings menu (Appendix A7). Decreasing the detail or sample period (or increasing resolution) will automatically increase the number of samples per beam. Additionally, if the window length parameter is changed, the number of samples per beam will automatically increase or decrease to maintain the selected sample period or detail setting. These parameters are described in Appendix A8.

Some General Rules for Better Measurements

When sampling at close range (less than ~8 m with a long-range lens or less than ~4 m with a standard lens; Appendix A5), a shorter range window is used for the first range stratum to minimize the effect of poor focal resolution at close range (Appendix A9).

We find that a 5 m range window is adequate for sampling a 3.5–8.5 m stratum using a long-range lens, and we do not generally sample at less than 3.5 m when using a long-range lens to avoid range-related size bias due to poor focal resolution (Appendix A10).

Tethered fish studies showed that a 10 μ s sample period (SP) is a good compromise yielding high-resolution images at manageable file sizes.

Sound Metrics Corporation (SMC) recommends using a transmit pulse width (PW) that is long enough to get a minimum of 2 samples within the transmit pulse at further ranges (e.g., for a constant SP = 10 μ s, at 20 m use PW \approx 20 μ s, and at 30 m use PW \approx 30 μ s). This maintains a better downrange-to-crossrange ratio and should provide a better image for “beam-edge-to-beam-edge” measurements. At closer ranges less than about 10 m, a PW that is long enough to get 1 sample within the transmit pulse is acceptable (e.g., PW = 10–15 μ s). Poor images can result when the SP is equal to or greater than the transmit pulse (Appendix A11: Panel 3).

Avoid aiming the sonar too far into the bottom. It’s a common mistake to optimize the image of the bottom, using the logic that the fish should be optimally insonified too. But, as shown in Appendix A12, aiming the sonar farther into the bottom than required to cover the near-bottom region can cause unnecessary loss of vertical beam width and water column coverage and degrade the image quality. This can be a problem especially when using a long-range lens accessory because the beam width has been reduced from about 12° to about 3°; unless the river is extremely shallow, losing more vertical beam width than necessary is undesirable.

Appendix A2.—Summary of manufacturer specifications for maximum range, individual beam dimensions, and spacing for DIDSON SV, DIDSON LR, ARIS 1800, and ARIS 1200 systems at 2 frequencies, with and without the addition of a high-resolution lens (specifications from Sound Metrics Corporation).

System	Frequency	Maximum range (m) ^a	Horizontal beam width	Vertical beam width	Number of beams	Individual beam width ^{b,c}	Individual beam spacing ^{b,c}
DIDSON SV or ARIS 1800	1.8 MHz	15	28°	14°	96	0.30°	0.30°
	1.1 MHz ^d	35	28°	14°	48	0.50°	0.60°
	1.8 MHz + high-resolution lens	20	15°	3°	96	0.17°	0.15°
	1.1 MHz + high-resolution lens	40+	15°	3°	48	0.22°	0.30°
DIDSON LR or ARIS 1200	1.2 MHz	25	28°	14°	48	0.50°	0.60°
	0.7 MHz	80	28°	14°	48	0.80°	0.60°
	1.2 MHz + high-resolution lens	30	15°	3°	48	0.27°	0.30°
	0.7 MHz + high-resolution lens	100+	15°	3°	48	0.33°	0.30°

Note: A more complete summary is given in Appendix A3.

^a Actual range will vary depending on site and water characteristics.

^b Beam width values are for 2-way transmission at –3 dB points.

^c Values for beam spacing and beam width are approximate. Beam widths are slightly wider near the edges of the beam and the beam spacing is slightly narrower. Conversely, beams are slightly narrower near the center of the beam, and the beam spacing is slightly wider (e.g., the center beam spacing is closer to 0.34°, and the beam width is 0.27° for a DIDSON SV at 1.8 MHz; Bill Hanot, Sound Metrics Corporation, personal communication). Nonlinear corrections are applied by the manufacturer in software to correct for these effects in the DIDSON with standard lens but not with the high-resolution lens. Nonlinear corrections are applied in software to correct for these effects in the ARIS with both the standard and high-resolution lenses.

^d ARIS 1800 uses 96 beams at low frequency by default, whereas DIDSON is hard-wired for 48 beams at low frequency. If ARIS 1800 is set for 96 beams then beam spacing is 0.3° at both low frequency and high frequency. If ARIS 1800 is set for 48 beams then beam spacing is 0.6° at both low frequency and high frequency.

ARIS 1800 Specifications

Detection Mode

Operating Frequency 1.1 MHz
Beamwidth (2-way) 0.5° H by 14° V
Source Level (average) ~204 dB re 1 µPa at 1 m
Nominal Effective Range 35 m

Identification Mode

Operating Frequency 1.8 MHz
Beamwidth (2-way) 0.3° H by 14° V
Source Level (average) ~195 dB re 1 µPa at 1 m
Nominal Effective Range 15 m

Both Modes

Number of beams 96 or 48
Beam Spacing 0.3° nominal
Horizontal Field-of-View 28°
Max frame rate (96 beams) 3–15 frames/s (6–15 frames/sec w/48 beams)
Minimum Range Start 0.7 m
Downrange Resolution 3 mm to 10 cm
Transmit Pulse Length 4 µs to 100 µs
Remote Focus 0.7 m to max range
Power Consumption 15 Watts typical
Weight in Air 5.5 kg (12.1 lb)
Weight in Water *TBD*, ~1.4kg (3 lb)
Dimensions 31 cm × 17 cm × 14 cm
Depth rating 300 m
Data Comm Link 100BaseT Ethernet or HomePlug
Maximum cable length (Ethernet) 90 m (300 ft)
Maximum cable length (HomePlug) 300 m (1000 ft)

ARIS 1200 Specifications

Detection Mode

Operating Frequency 0.7 MHz
Beamwidth (2-way) 0.8° H by 14° V
Source Level (average) ~216 dB re 1 µPa at 1 m
Nominal Effective Range 80 m

Identification Mode

Operating Frequency 1.2 MHz
Beamwidth (2-way) 0.5° H by 14° V
Source Level (average) ~206 dB re 1 µPa at 1 m
Nominal Effective Range 25 m

-continued-

ARIS 1200 Specifications (continued)

Both Modes

Number of beams 48
Beam Spacing 0.6° nominal
Horizontal Field-of-View 28°
Max frame rate (range dependent) 2.5–15 frames/s
Minimum Range Start 0.7 m
Downrange Resolution 3 mm to 10 cm
Transmit Pulse Length 4 µs to 100 µs
Remote Focus 0.7 m to max range
Power Consumption 18 Watts typical
Weight in Air 5.5 kg (12.1 lb)
Weight in Water ~1.4 kg (3 lb)
Dimensions 31 cm × 17 cm × 14 cm
Depth rating 300 m
Data Comm Link 100BaseT Ethernet or HomePlug
Maximum cable length (Ethernet) 90 m (300 ft)
Maximum cable length (HomePlug) 300 m (1000 ft)

DIDSON SV Specifications

Detection Mode

Operating Frequency 1.1 MHz
Beamwidth (2-way) 0.4° H by 14° V
Source Level (average) ~204 dB re 1 µPa at 1 m
Number of Beams 48
Beam Spacing 0.6°
(Extended) Window Start 0.83 m to 52.3 m in 0.83 m steps
(Extended) Window Length 5 m, 10 m, 20 m, 40 m
Range Bin Size (relative to window length) 10 mm, 20 mm, 40 mm, 80 mm
Pulse Length (relative to window length) 18 µs, 36 µs, 72 µs, 144 µs

Identification Mode

Operating Frequency 1.8 MHz
Beamwidth (2-way) 0.3° H by 14 ° V
Source Level (average) ~195 dB re 1 µPa at 1 m
Number of Beams 96
Beam Spacing 0.3°
(Extended) Window Start 0.42 m to 26.1 m in 0.42 m steps
(Extended) Window Length 1.25 m, 2.5 m, 5 m, 10 m
Range Bin Size (relative to window length) 2.5 mm, 5 mm, 10 mm, 20 mm
Pulse Length (relative to window length) 4.5 µs, 9 µs, 18 µs, 36 µs

-continued-

DIDSON SV Specifications (continued)

Both Modes

Max Frame Rate (range dependent) 4–21 frames/s
Field-of-view 29°
Remote Focus 1 m to Infinity
Control & Data Interface UDP Ethernet
Aux Display NTSC Video
Max cable length (100/10BaseT) 61m/152 m (200 ft/500 ft)
Max cable length (twisted pair, Patton Extender) 1220 m (4000 ft)
Power Consumption 25 Watts typical
Weight in Air 7.9 kg (17.4 lb)
Weight in Sea Water 1.0 kg (2.2 lb)
Dimensions 31.0 cm × 20.6 cm × 17.1 cm
Topside PC Requirements Windows (XP, Vista, 7), Ethernet
Optional NTSC video monitor

DIDSON LR Specifications

Detection Mode

Operating Frequency 0.7 MHz
Beamwidth (2-way) 0.8° H by 14° V
Source Level (average) ~216 dB re 1 µPa at 1 m
Number of Beams 48
Beam Spacing 0.6°
Extended Range Settings
(Extended) Window Start 0.83 m to 52.3 m in 0.83 m steps
(Extended) Window Length 10 m, 20 m, 40 m, 80 m
Range Bin Size (relative to window length) 20 mm, 40 mm, 80 mm, 160 mm
Pulse Length (relative to window length) 23 µs, 46 µs, 92 µs, 184 µs

Identification Mode

Operating Frequency 1.2 MHz
Beamwidth (2-way) 0.5° H by 14 ° V
Source Level (average) ~206 dB re 1 µPa at 1 m
Number of Beams 48
Beam Spacing 0.3° nominal
Extended Range Settings
(Extended) Window Start 0.42 m to 26.1 m in 0.42 m steps
(Extended) Window Length 2.5 m, 5 m, 10 m, 20 m
Range Bin Size (relative to window length) 5 mm, 10 mm, 20 mm, 40 mm
Pulse Length (relative to window length) 7 µs, 13 µs, 27 µs, 54 µs

-continued-

DIDSON LR Specifications (continued)

Both Modes

Max Frame Rate (range dependent) 2–21 frames/s

Field-of-view 29°

Remote Focus 1 m to Infinity

Control & Data Interface UDP Ethernet

Aux Display NTSC Video

Max cable length (100/10BaseT) 61 m/152 m (200 ft/500 ft)

Max cable length (twisted pair, Patton Extender) 1220 m (4000 ft)

Power Consumption 25 Watts typical

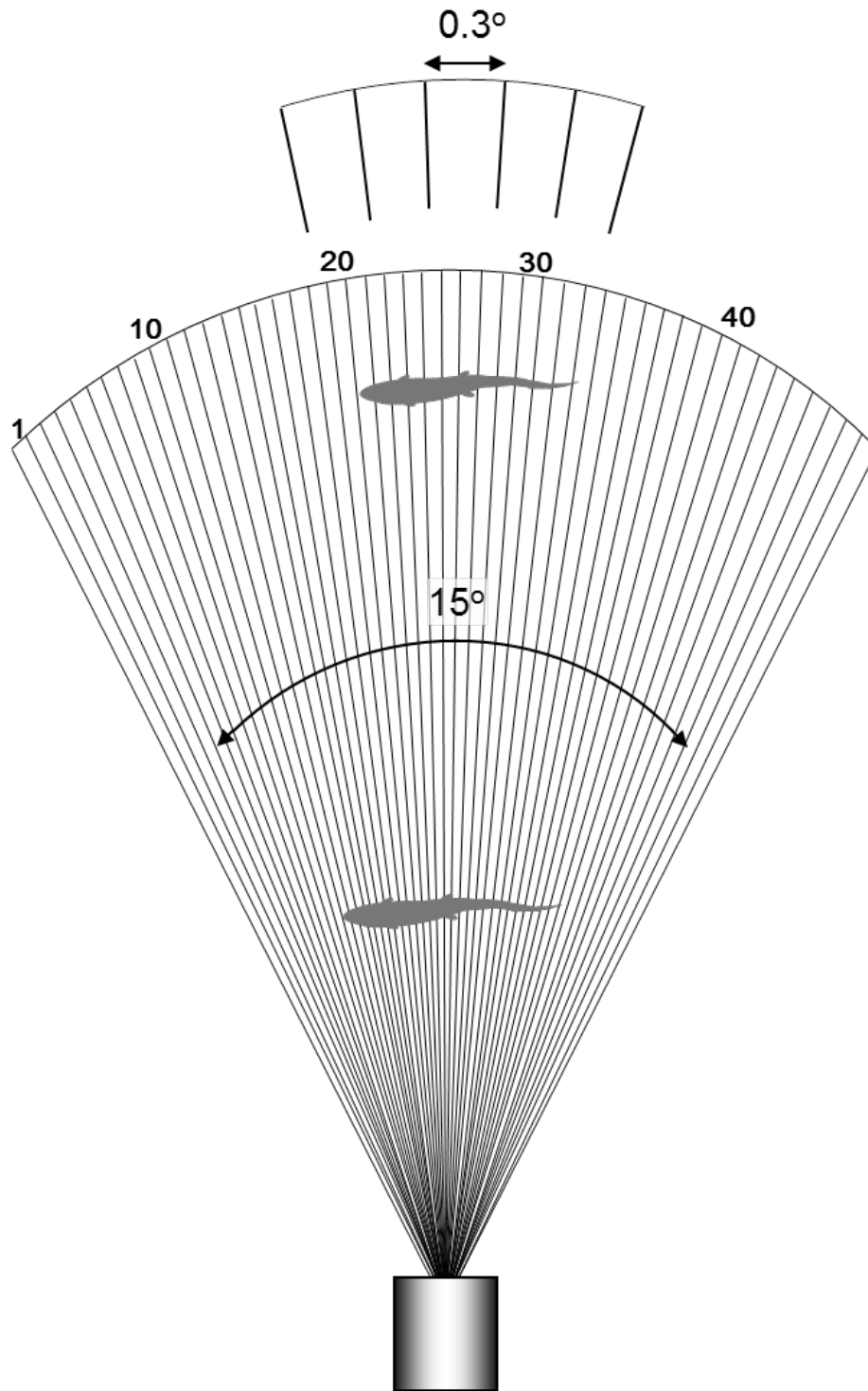
Weight in Air 7.9 kg (17.4 lb)

Weight in Sea Water 1.0 kg (2.2 lb)

Dimensions 31.0 cm × 20.6 cm × 17.1 cm

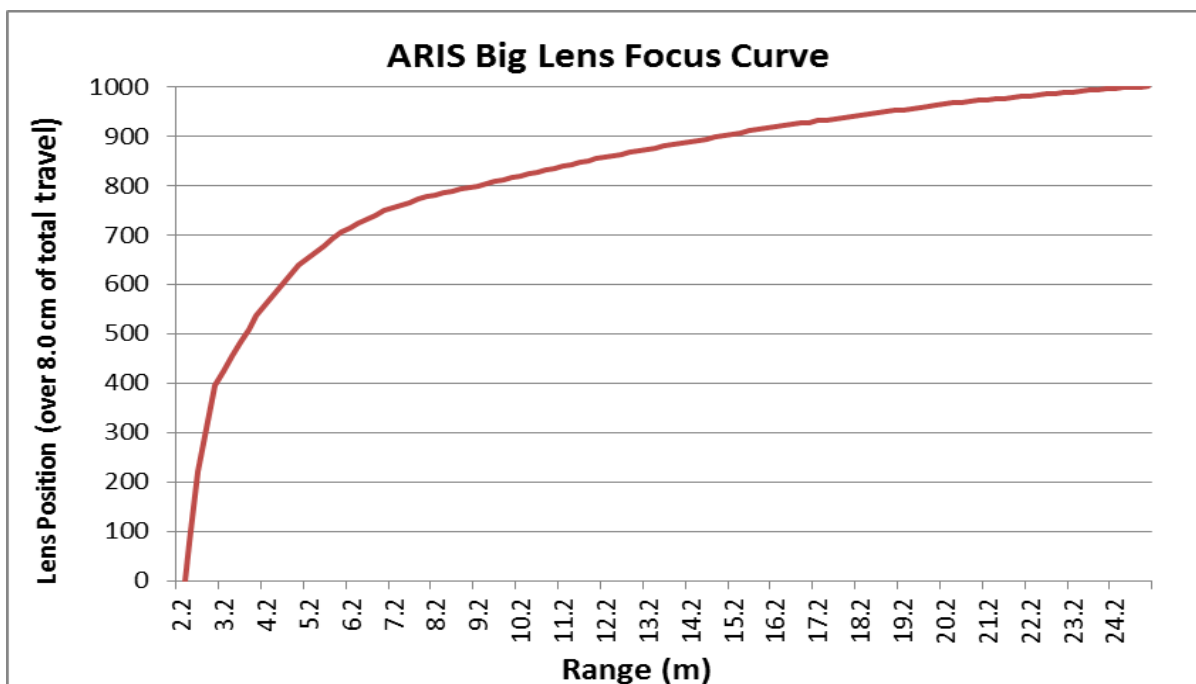
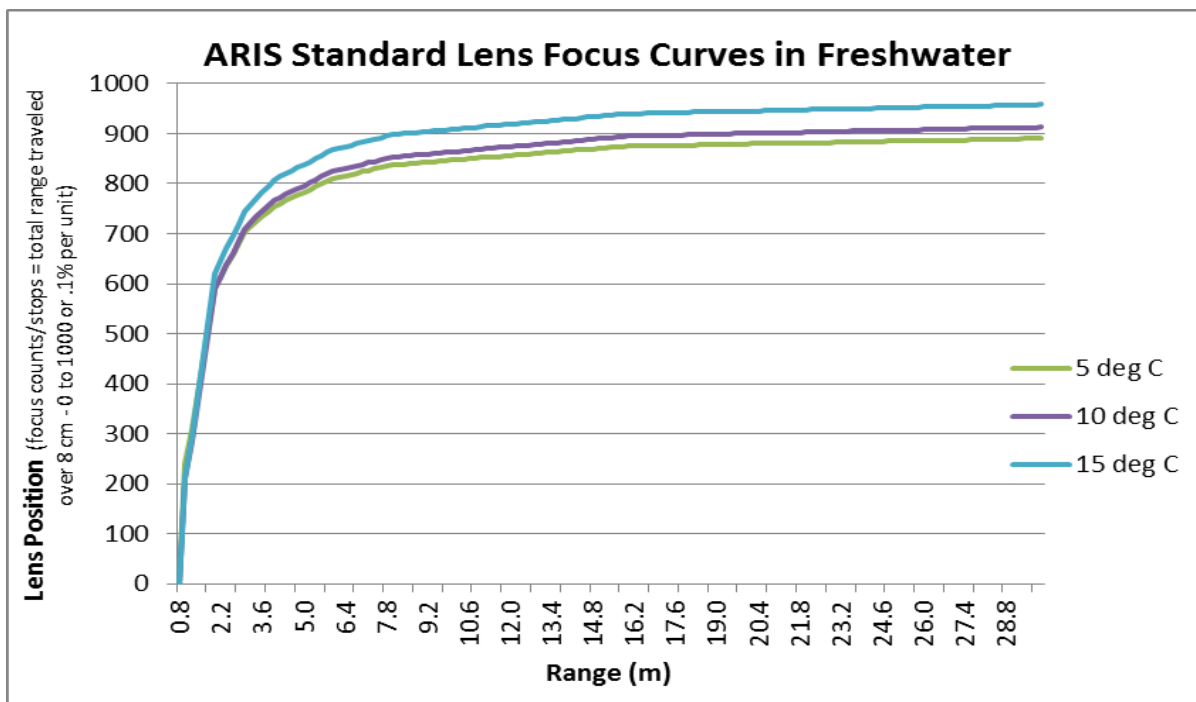
Topside PC Requirements Windows (XP, Vista, 7), Ethernet

Optional NTSC video monitor



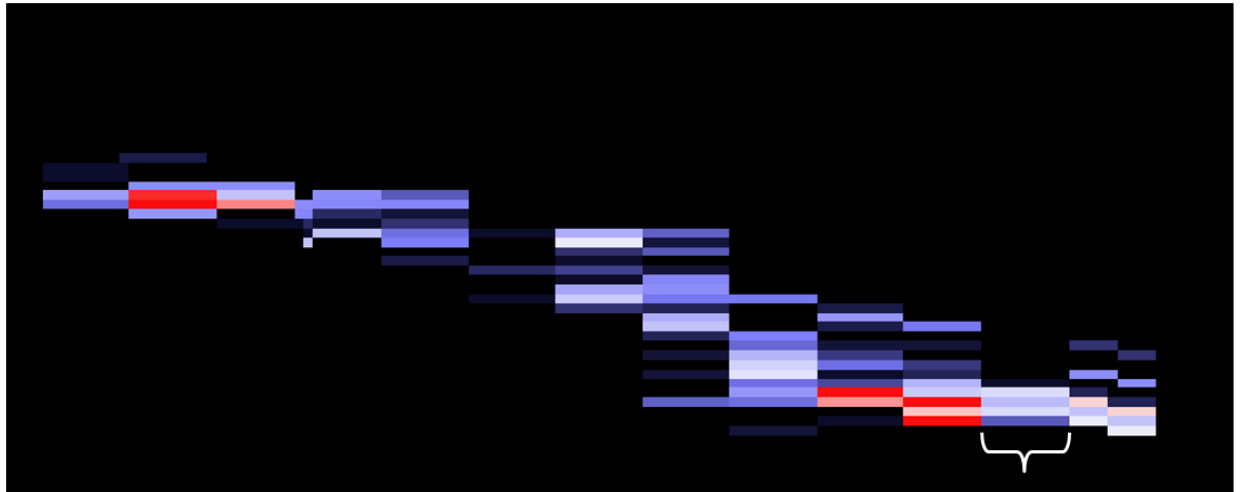
Appendix A4.—Diagram showing the horizontal plane of a DIDSON LR or ARIS 1200 with a high-resolution lens.

Note: The overall horizontal beam width of 15° is composed of 48 sub-beams with approximately 0.3° beam widths. Because sub-beams grow wider with range, fish at close range are better resolved than fish at far range (adapted from Burwen et al. [2007]).

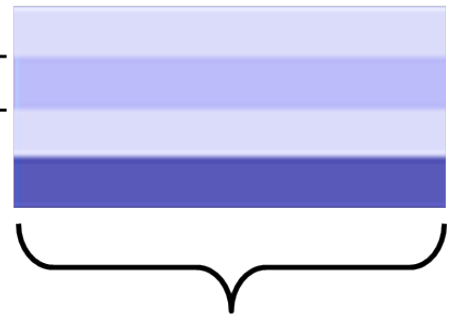


Appendix A5.—Relationships between focal length and lens position for ARIS.

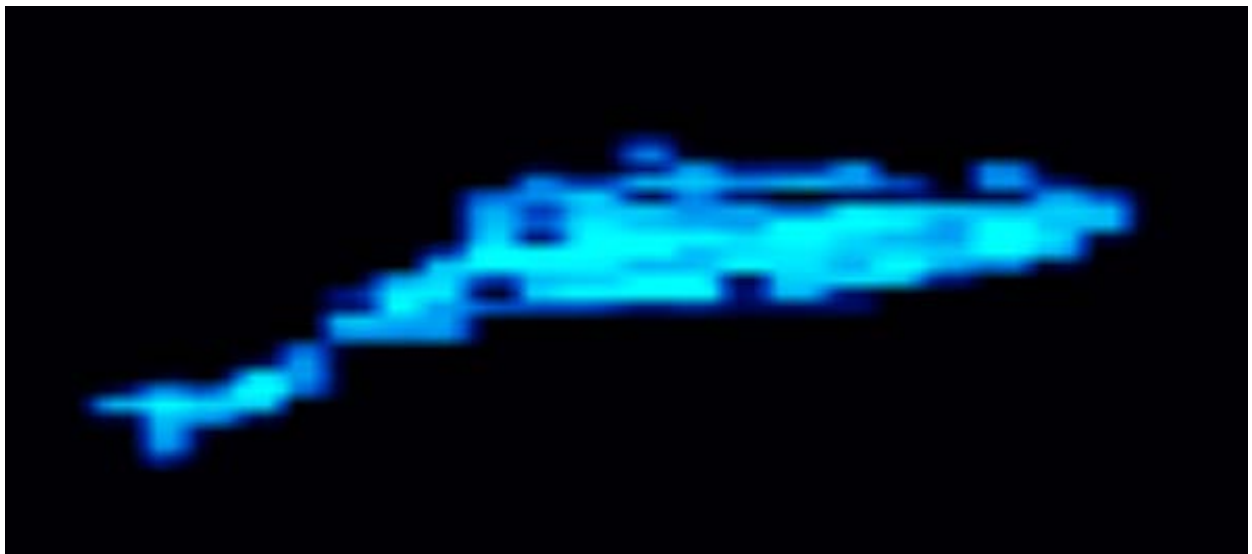
Note: “Big Lens” refers to the high-resolution lens.



Pixel Height {



Pixel width



Appendix A6.—An enlargement of a tethered Chinook salmon showing the individual pixels that compose a DIDSON image (top) contrasted with an ARIS image of a free-swimming Chinook salmon (bottom).

Control Panel Menu

Expanded Sonar Control Window

Advanced Settings dialog

The *Advance Settings* dialog allows direct access to all sonar data acquisition parameters, sample start and end range, and fine manual focus control.

In practice, we have found it easiest to set certain parameters in the *Advance Settings* dialog rather than using the sliders in other control windows (e.g. Sample Period versus Detail). The sliders are useful for exploring the best parameters during initial sonar set up. Once the approximate range and resolution have been selected using sliders, more exact values can be set in the *Advance Settings* dialog.

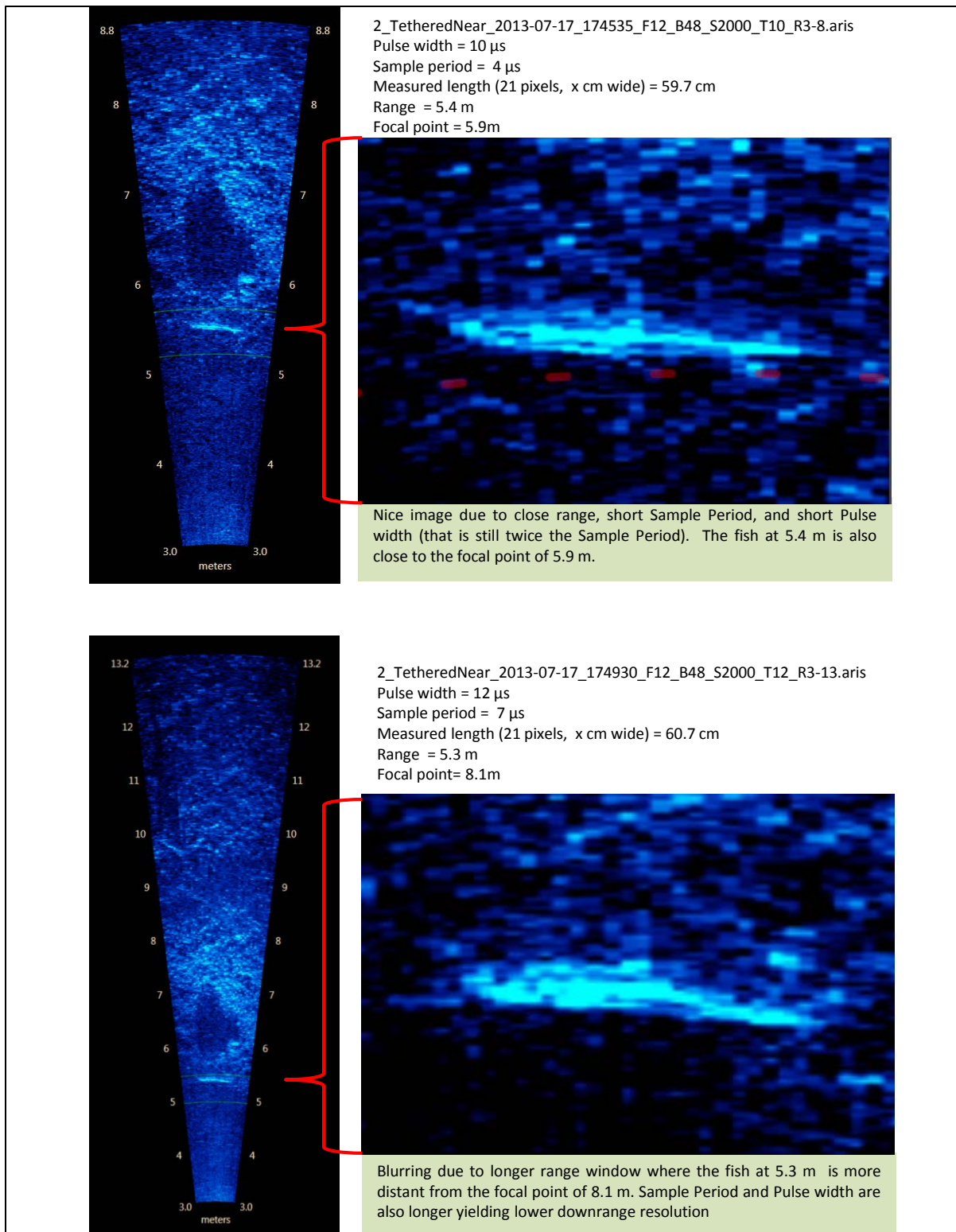
Appendix A7.–Downrange resolution for ARIS images is set using the “Detail” slider under the expanded “Sonar Control” dialog window or by setting the “Sample Period” under the “Advanced Sonar Settings” dialog window.

Appendix A8.–Summary of ARIScope data acquisition parameters that affect downrange resolution.

Parameter	Description
Detail (mm)	<p>Downrange resolution refers to the “height” of the ARIS image pixel and can be set in ARIScope using the <Detail> or <Sample Period> parameters. Setting the <Detail> parameter, measured in millimeters, in turn sets the data for <Sample Period>, which is the equivalent parameter in microseconds. The downrange resolution can be set using the <Detail> slider in the <i>Sonar Control</i> dialog window under ECHOScope’s <i>Control Panel</i> (Appendix A7), which then automatically sets the <Sample Period>. Downrange resolution can also be set more exactly and directly by entering a value for <Sample Period> in the <i>Advanced Sonar Settings</i> dialog window (Appendix A7). These parameters, in combination with the transmit pulse width, control downrange resolution.</p> <p>Slide the <Detail> control to the left for less detail (longer sample period) or to the right for more detail (shorter sample period). Images with greater detail have more samples per beam, leading to larger frame sizes. As a consequence, file sizes will be larger and frame rates may need to be reduced to handle the data throughput. This may also be a consideration when transmitting data via wireless radio where bandwidth may limit frame size and frame rate. <Samples/Beam> has a limit of 4096, so at maximum <Detail> that translates to about 12 m (39 ft) maximum range (2.9 mm maximum downrange resolution × 4096 samples ≈ 12 m).</p> <p>Using <Auto> (<Detail>):</p> <p>Checking the <Auto> box (default) will attempt to provide a good balance between <Detail> and file size and frame rate. For our purposes, we find that using <Auto> does not provide the level of resolution we prefer, particularly at farther ranges.</p> <p>Also note that when the <Auto> box is checked, the number for <Samples/Beam> is automatically fixed at the current number when starting to record a file. Checking the <Auto> box automatically unchecks the <Fixed> (<Samples/Beam>) box in the <i>Advanced Sonar Settings</i> dialog window.</p>
Pulse (μs)	<p>Transmit <Pulse> width determines the downrange resolution and brightness of the image. Shorter pulses make for better resolution but put less energy into the water, reducing the brightness of the image and the maximum effective range. Longer pulses will reduce downrange resolution but make the image brighter with a longer maximum effective range. In general, choosing between narrow, medium, and wide settings in the <i>Sonar Control</i> window will give you sufficient control over the tradeoff between maximum range and resolution. Transmit <Pulse> width can be manually set in the <i>Advanced Sonar Setting</i> dialog window (Appendix A7).</p> <p><Pulse> width settings:</p> <ul style="list-style-type: none"> • Narrow (default) transmit <Pulse> width is set to ~1.2× the <Sample Period>. • Medium transmit <Pulse> width is set to ~2.0× the <Sample Period>. • Wide transmit <Pulse> width is set to ~3.3× the <Sample Period>. • Auto transmit <Pulse> width is set to approximately the end range in microseconds (μs). • Custom settings in μs can be selected in the <i>Advanced Sonar Settings</i> dialog window (Appendix A7).

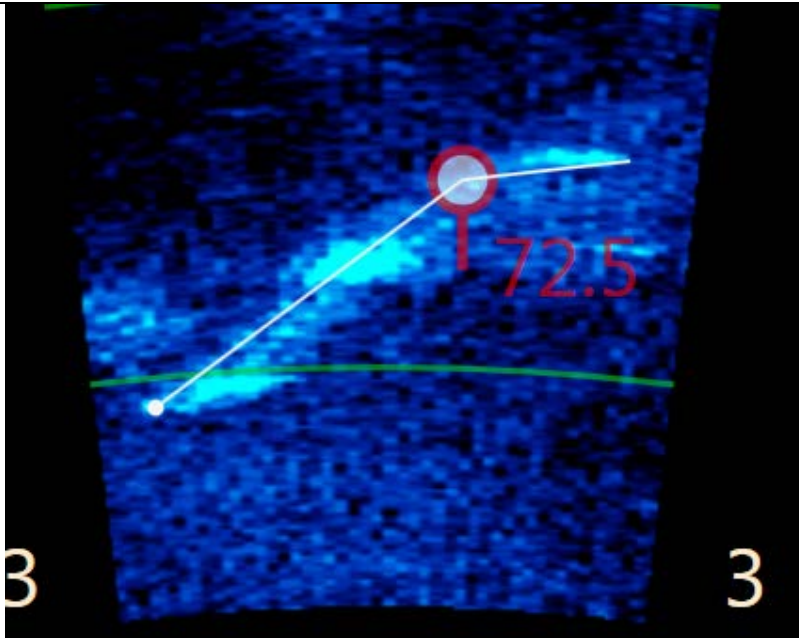
-continued-

Parameter	Description
Sample Period (μs)	The < Sample Period > parameter sets the image data sample period within a beam in microseconds. Shorter values provide higher downrange resolution at the expense of larger frame sizes and potentially restricted frame rates. < Sample Period > can be set with the Sonar Control < Detail > slider or < Auto > checkbox or in the <i>Advanced Sonar Settings</i> dialog window.
Samples/Beam	<p>The <Samples/Beam> parameter is the number of data samples in a sonar beam, from 128 to 4096. Changing this value manually to a larger number will increase the image window end range and decrease the end range to a smaller number. Check the <Fixed> box to force a fixed number in <Samples/Beam>. This allows changing the range start and the range end of the image window while recording without starting a new output file. Checking the <Fixed> box automatically unchecks the <Auto> (<Detail>) box in the <i>Advanced Sonar Settings</i> window (if the <Auto> box is checked when <Fixed> is unchecked, then the number for <Samples/Beam> is automatically fixed at the current number while recording a file).</p> <p>Avoid trying to set the resolution using the <Samples/Beam> parameter because increasing the number for <Samples/Beam> will automatically increase the window end range rather than increase <Sample Period> or <Detail> parameters.</p>
<p><i>Note:</i> Parameters can be found in Appendix A7. Names of parameters that can be set in ARIScope are listed in <bold>; names of dialog windows are shown in <i>bold italics</i>.</p>	

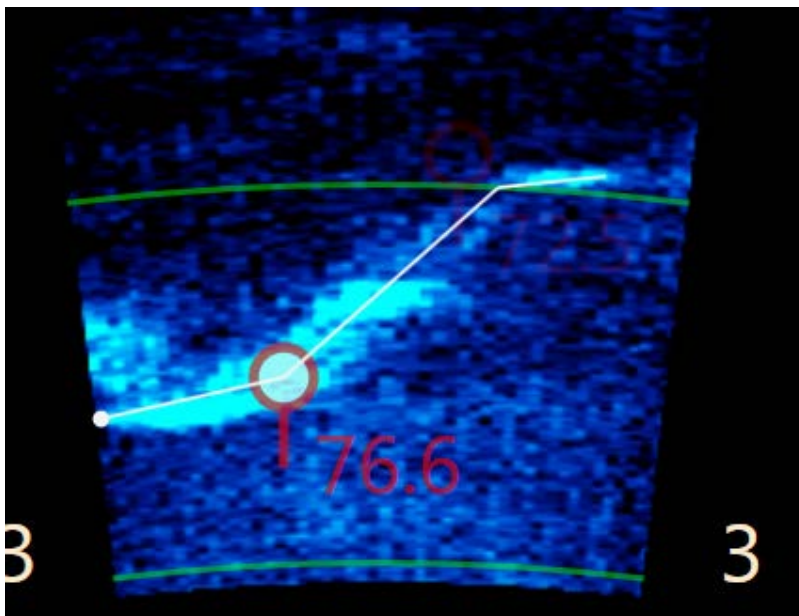


Appendix A9.—Images from a close-range tethered fish at 2 different range windows demonstrate the advantage of a shorter range window and higher sample period for close-range sampling.

Note: The top image has better resolution because of the shorter range window with better focal resolution and a higher sample period than the bottom image.

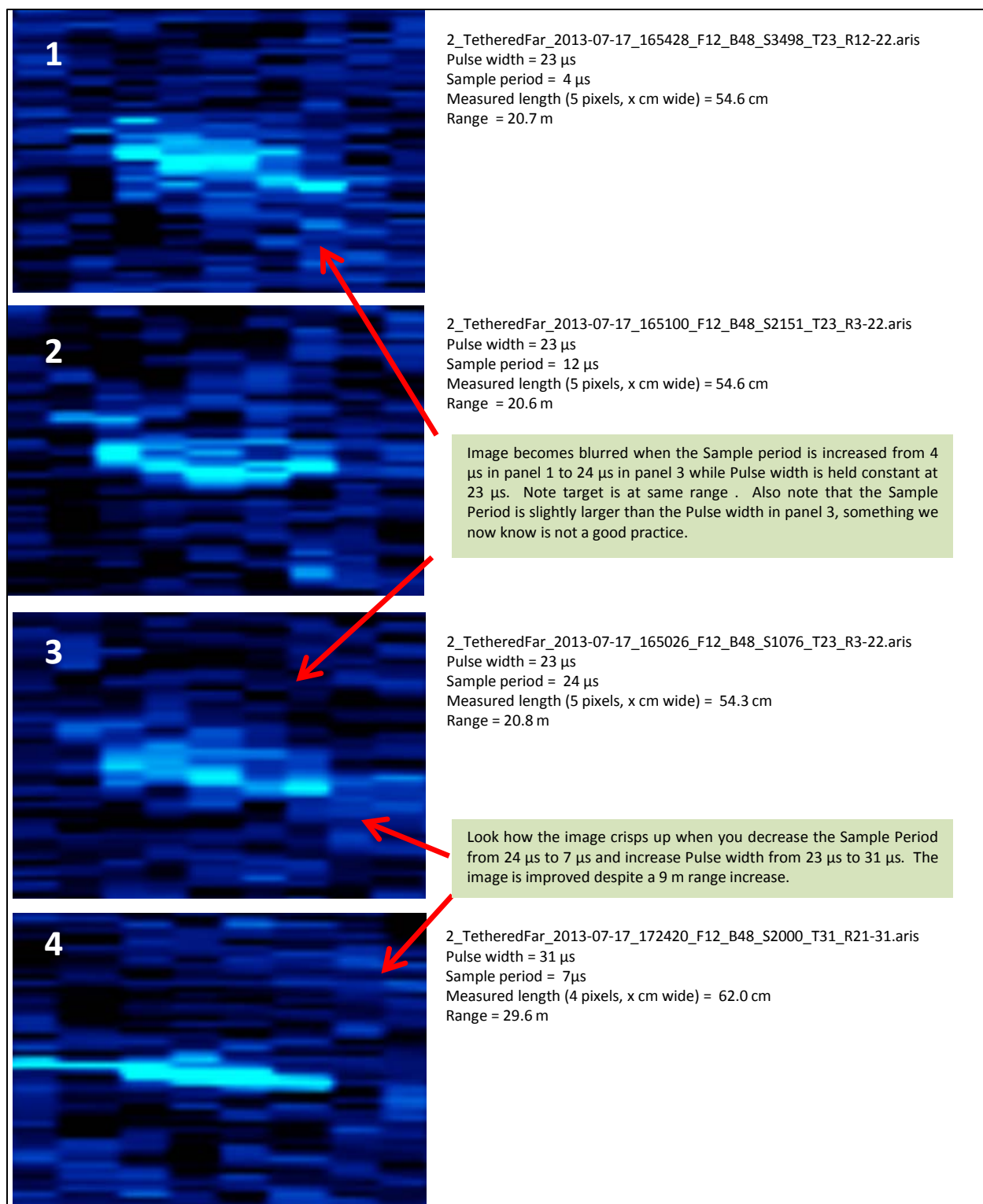


3_TetheredNear_2013-07-17_182746_F12_B48_S1724_T08_R3-8.aris
 Fish Range: 3.35 m
 Frame 2498
 Fish size 72.5 cm



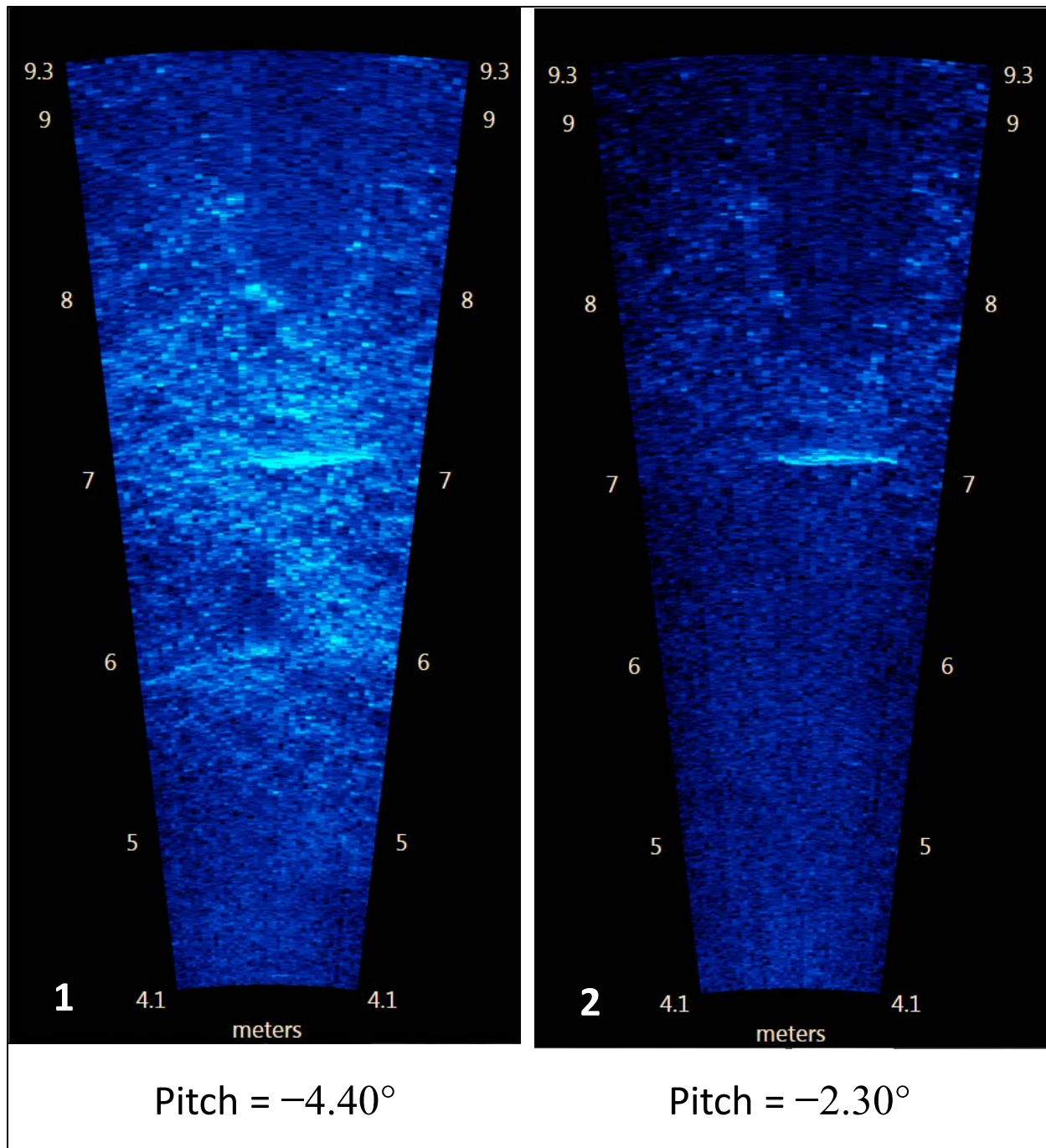
3_TetheredNear_2013-07-17_182746_F12_B48_S1724_T08_R3-8.aris
 Fish Range: 3.17 m
 Frame 1896
 Fish size 76.6 cm

Appendix A10.–Images from a 68.5 cm sockeye salmon (Fish 2 in Table 14) demonstrate a measurement bias at ranges less than 3.5 m, even with the short 5 m range window.



Appendix A11.–Data collected from tethered fish provided the opportunity to compare the effects and interrelationship between 2 parameters affecting image resolution: transmitted pulse length and sample period.

Note: This is a 60 cm sockeye salmon.



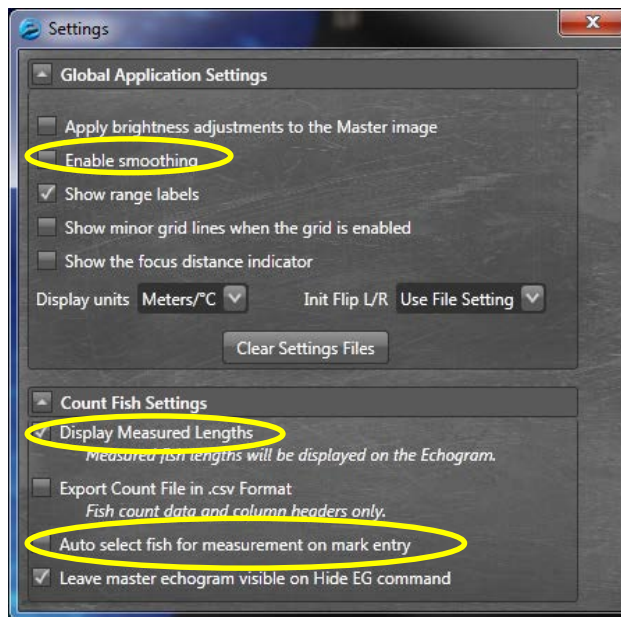
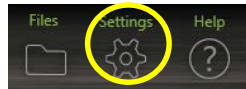
Appendix A12.—Images of a tethered fish taken at 2 different aims: Panel 1, where the bottom is better defined but measuring the fish is actually more difficult against the bright background, and Panel 2, where the sonar pitch is raised 2° and the fish outline is better defined for easier measuring and bottom structures still show at all ranges.

Note: Aiming the sonar farther into the bottom than required to cover the near-bottom region can cause unnecessary loss of vertical beam width and water column coverage and degrade the fish image.

APPENDIX B: INSTRUCTIONS AND SETTINGS FOR MANUAL FISH LENGTH MEASUREMENTS

Set Global Settings after a new installation of ARISFish

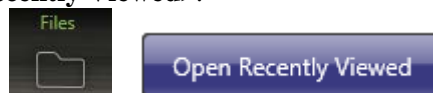
1. Open the ARISFish <Global Application Settings> menu (using the <Settings> cog in the upper right hand corner) and use the following settings:



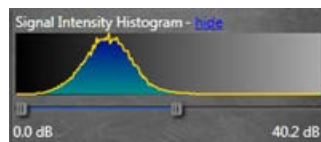
2. <Enable smoothing> is off.
3. <Display Measured Lengths> is on.
4. <Auto select fish for measurement> can be either on or off, as desired.

Set processing parameters for a new set of files for a new day or stratum

1. Select <Files> <Open Recently Viewed>.

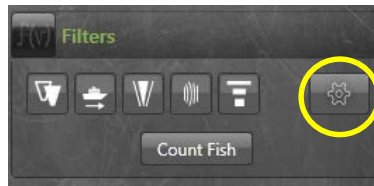


2. Navigate to the appropriate directory and open file (or simply <double click> on the file).
3. Set <Signal Intensity Histogram> sliders to 0.0 and 40.2 dB (or other recommended values for a specific stratum).



-continued-

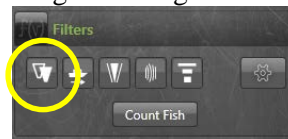
4. Select the **<Settings>** cog from the **<Filters>** menu.



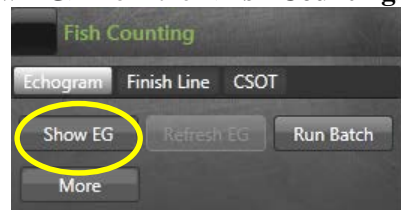
5. Select **<SMC adaptive background>** and set **<Remove speckles smaller than>** to 30 cm².



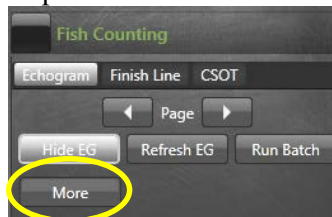
6. Select the **<Background Subtraction>** icon on the **<Filters>** menu (toggle); this will enable background subtraction for producing the echogram.



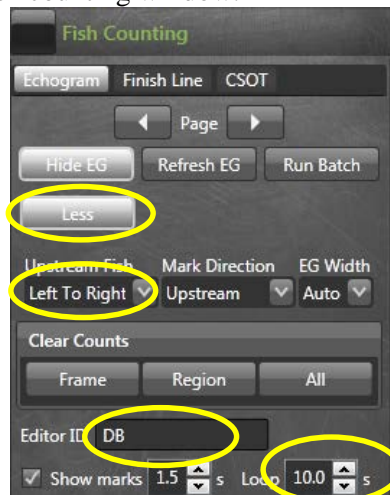
7. Select **<Echogram>** **<Show EG>** from the **<Fish Counting>** menu to display the echogram.



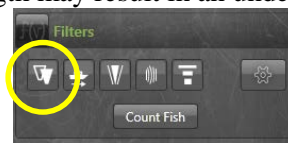
8. Select **<More>** to get expanded options in the **<Fish Counting>** menu.



9. *Increase <Loop> length to at least 8 seconds.
*Enter initials for <Editor ID>.
*set <Mark Direction> “upstream” and <Upstream Fish> direction parameter (usually “left to right” for left bank sonar files and “right to left” for right bank sonar files).
*Select <Less> to shrink fish counting window.



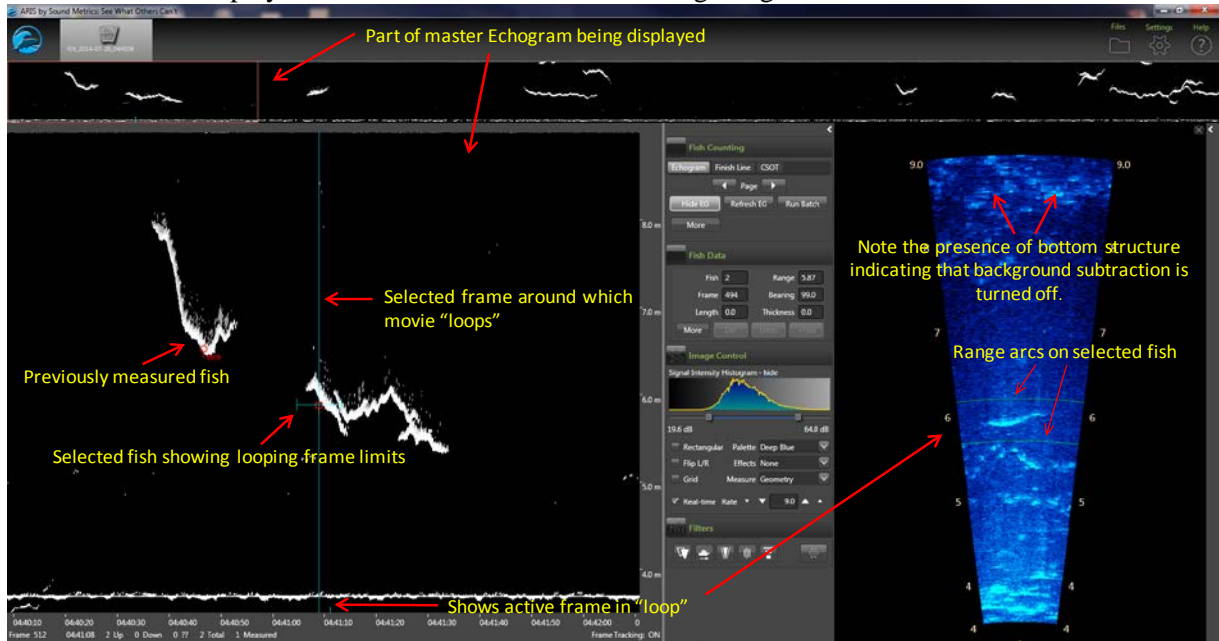
10. Now select the <Background Subtraction> icon on the <Filters> menu (toggle) to turn the background subtraction “off” on the video image. Failing to turn background subtraction off prior to measuring the fish image length may result in an underestimate of actual fish length.¹⁵



-continued-

¹⁵ Unlike with DIDSON data, we do not usually use the background subtraction (BS) option while measuring ARIS fish image lengths. The new SMC ARISFish BS algorithm is more aggressive than the DIDSON algorithm and unless one is very careful in selecting a frame, it is easy to underestimate fish length. Toggling between BS mode and the raw image can sometimes be helpful in determining the end of a tail or snout. If BS is used, we generally take BS off before finalizing a measurement. A well-selected frame will give the same length measurement with or without BS.

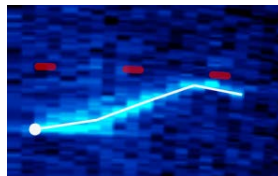
11. The overall display should look similar to the following image:



12. Select <Alt><right arrow> to advance to the next file when needed; all parameter settings and the display configuration should be preserved.
13. Individual fish may be measured at this point.
14. When switching banks, reset <Upstream Fish> direction of travel in Step 9.
15. When switching strata, use Windows Explorer to find the first file and <double click> it.

Instructions for manual fish length measurements using SMC ARISFish software version 1.5 in 2013.

1. Ensure <Background Subtraction> is toggled “off” as described in Step 10 above.
2. <Left click> on the echogram fish to be measured (puts red marker on fish).
3. <Right click> inside the red circle (a blue line with loop limits will appear).
4. Press <space bar> to start movie showing fish bounded by range arcs (see figure in Step 11 above).
5. <Right click drag> on the movie image to zoom in for measurement.
6. Press <space bar> to pause the movie.
7. Use <right arrow> and <left arrow> to step through movie 1 frame at a time to find a frame that displays the entire fish length well (e.g., Appendix B3).
8. <Left click drag> if necessary to center the movie window prior to measuring.
9. <Left click> on the fish snout and continue to <left click> along the midline of the fish to create a “segmented measurement.” The segments should follow the midline of the body of the fish, ending with the tail.



-continued-

10. Select the **<f>** key to add the measurement to the .txt file (“fish it”). The measurement will appear in red (**<left click>** on echogram inside mark, to delete measurement and start over).
11. Select the **<v>** key to “unzoom” the movie window (this not necessary if there is another fish nearby to measure).
12. Repeat steps 1–8 for each fish, or **<left click>** on the master echogram to advance to a new echogram section, or **<alt><right arrow>** to advance to the next file.

Hot keys

- <e>** to “save” all echogram measurements to file
- <f>** to “fish it” (to accept the measurement and display it on the echogram)
- <u>** to “undo” the last segment
- <d>** to “delete” the all segments
- <v>** to “unzoom” the movie window
- <space bar>** to pause in movie mode
- <right arrow>** forward direction when playing a movie or advances frame 1 at a time if the movie is paused.
- <left arrow>** opposite of above
- <left click drag>** to show movie over the selected time
- <right click drag>** zooms the selected area

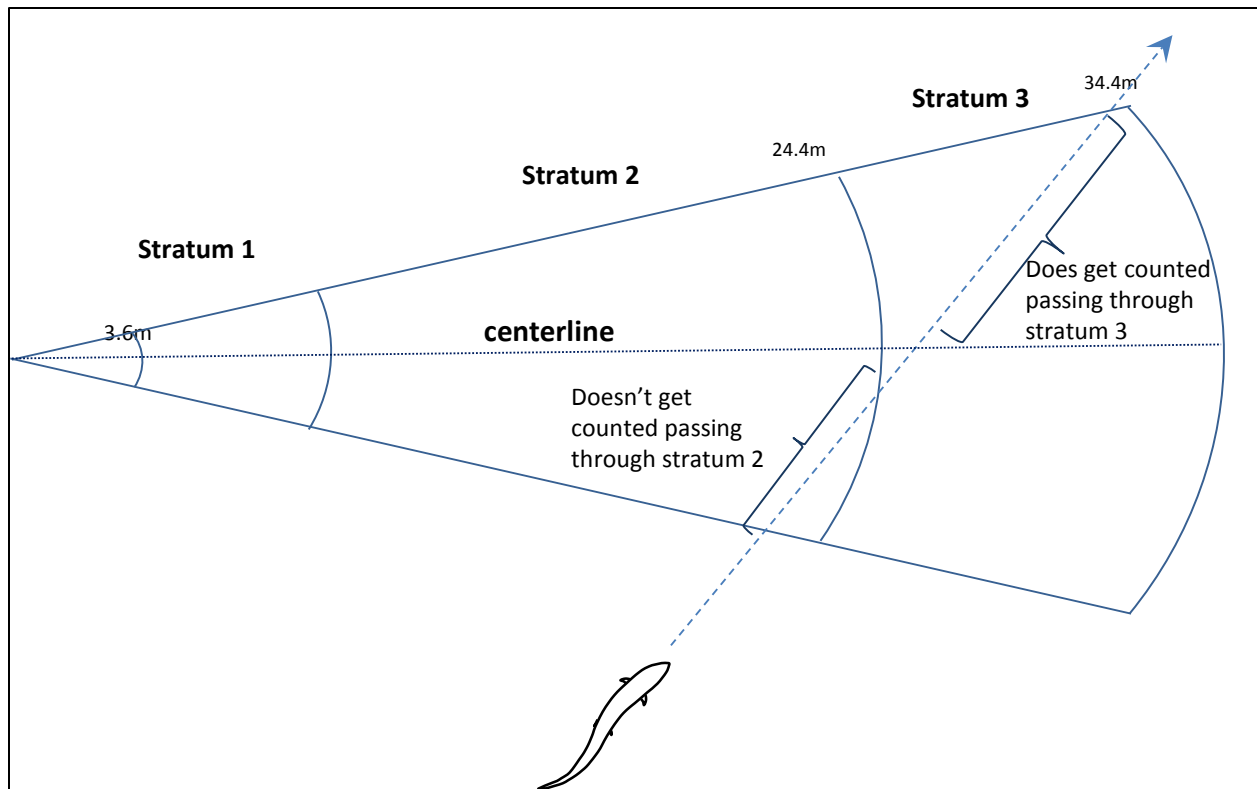
Instructions for including or excluding fish to be counted and measured

In order to optimize the aim of the sonar beams relative to the river bottom, the insonified zone is often divided into individual range strata that are sampled separately. In order to avoid overcounting fish as they cross stratum boundaries, we apply the “centerline rule” where a fish is not counted unless it crosses the centerline of the sonar beam. Appendix B2 demonstrates the potential for overcounting without applying this criterion. Additional examples are given in Appendix B3.

Summary of fish measurement rules

1. For a fish to be considered valid for measurement, it must cross the centerline.
 - a) If a fish enters or exits the beam on the near- or far-range boundary (beginning or end range), the snout of the fish must cross the centerline before it can be considered a valid fish to measure.
 - b) If the snout of the fish enters the near- or far-range boundary right on the centerline, the fish should be considered valid for measurement.
2. Exclude fish that “hold” throughout the length of the sample.

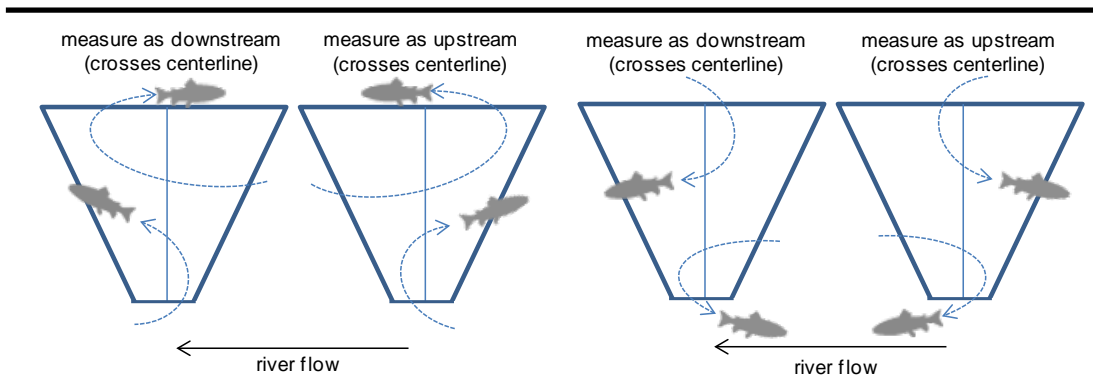
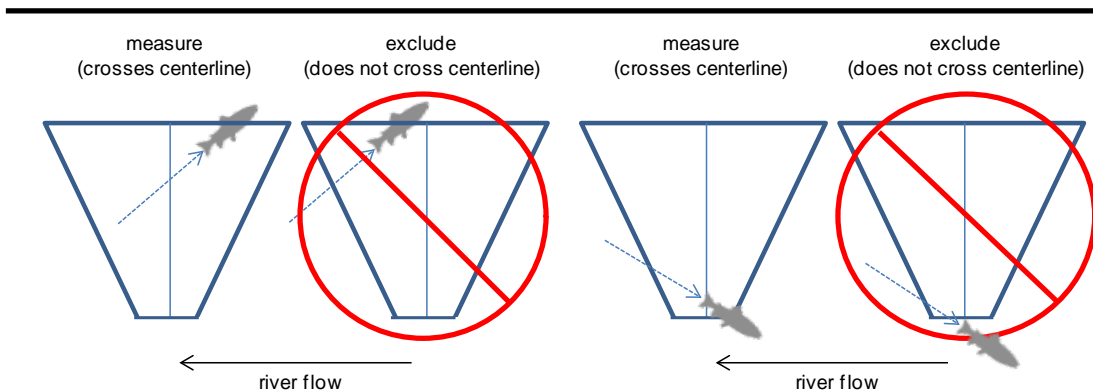
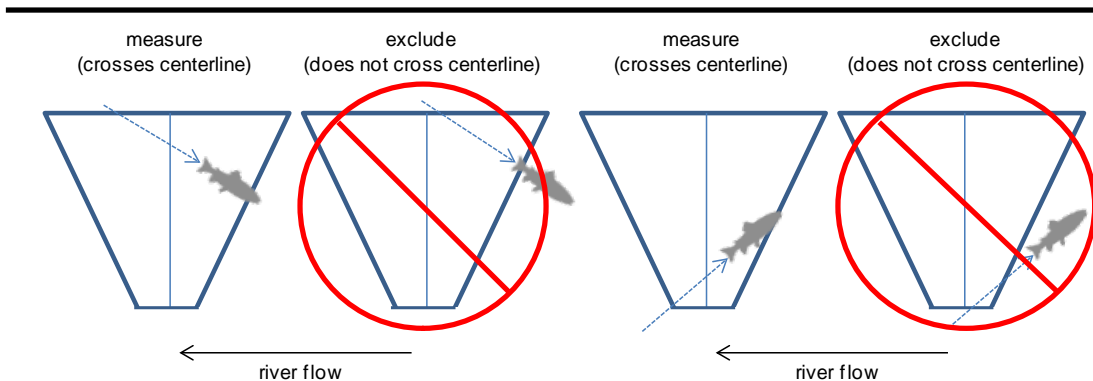
3. Exclude fish that are “holding” at either the beginning or the end of the sample. Fish that are actively migrating (not holding) as the sample begins or ends should be considered valid targets for measurement as long as they cross the centerline.
4. Exclude fish that enter the beam from upstream and then exit the beam upstream (do not measure even if they cross the centerline).
5. Exclude fish that enter the beam from downstream and then exit the beam downstream (do not measure even if they cross the centerline).
6. Exclude fish that enter the beam from either upstream or downstream and then disappear from the image (unless there is evidence to suggest direction of travel).
7. Use the video image to identify actively migrating fish when several holding fish are present. If several fish are holding throughout the sample, use the video mode or run the cursor across the echogram while watching the ARIS image to observe fish that are actively transiting the image. Measure fish that are actively transiting the image and that meet all criteria listed above.
8. Consulting with others is recommended if there is a questionable trace or fish or if the rules listed above are unclear.



Appendix B2.—To avoid counting this fish in both Stratum 2 and Stratum 3, the fish will only be counted in Stratum 3 where it crosses the centerline of the beam.

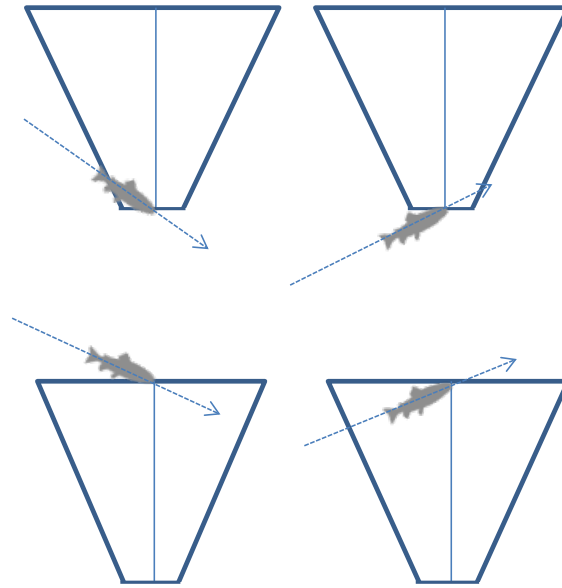
Appendix B3.—Specific examples for applying the “centerline” rule when selecting fish for counting and measurements.

For a fish to be considered valid for measurement (either upstream or downstream), the snout must cross the centerline.

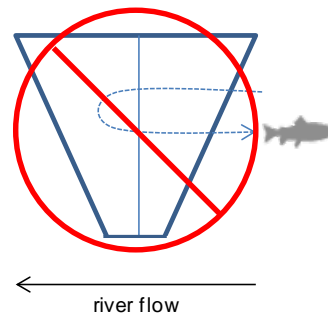


-continued-

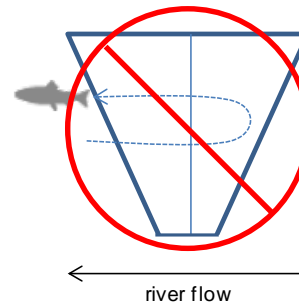
If the snout of the fish enters the near- or far-range boundary right on the centerline, the fish should be considered valid for measurement.



Exclude fish that enter the beam from upstream, then exit the beam upstream (do not measure even if they cross the centerline).

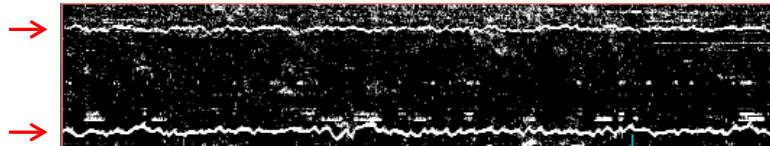


Exclude fish that enter the beam from downstream, then exit the beam downstream (do not measure even if they cross the centerline).



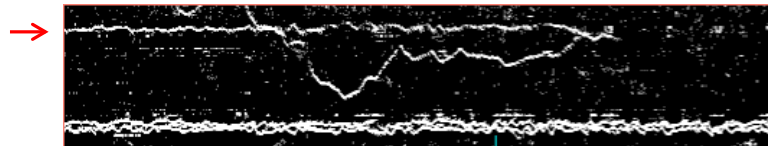
-continued-

Exclude fish that hold throughout the length of the sample.

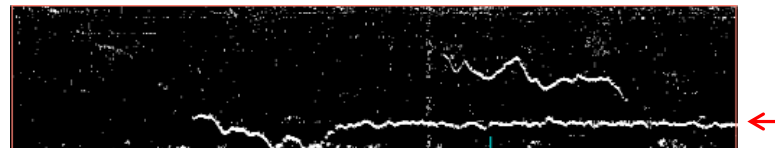


Two fish hold throughout the entire file.
Exclude both fish.

Exclude fish that hold at either the beginning or end of the sample.



Fish holding as sample begins, then exits the beam about ¾ of the way through the sample. Exclude this fish.



Fish enters the beam mid sample, then holds through the end of the sample. Exclude this fish

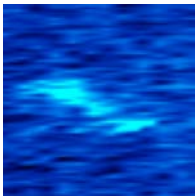
Fish that are actively migrating (not holding) as the sample begins or ends should be considered valid targets for measurement as long as they cross the centerline.



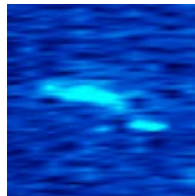
Fish is actively migrating through the beam as the sample starts. It crosses the center line and exits upstream so should be measured.

-continued-

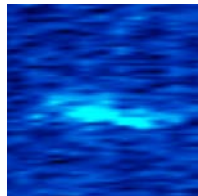
A fish passing through the beam that turns perpendicular to the axis and disappears should be excluded unless there is other evidence to indicate direction of travel.



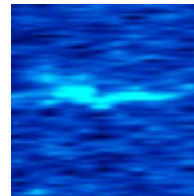
Frame #2353



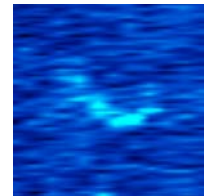
Frame #2354



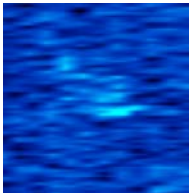
Frame #2355



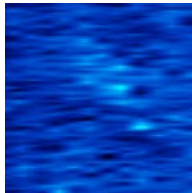
Frame #2356



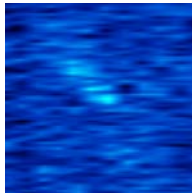
Frame #2357



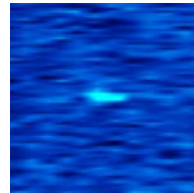
Frame #2358



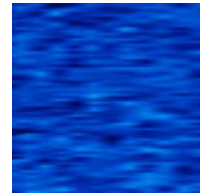
Frame #2359



Frame #2360



Frame #2361



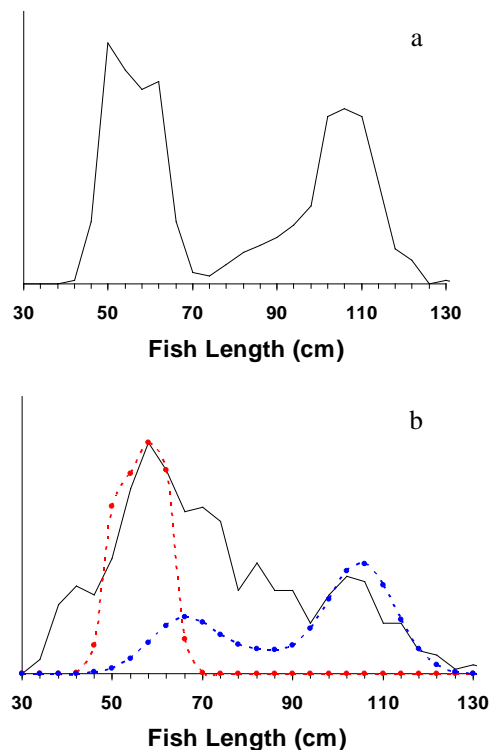
Frame #2362

APPENDIX C: ARIS LENGTH MIXTURE MODEL AND ASSOCIATED BUGS PROGRAM CODE

Appendix C1.–Mixture model description.

Mixture models are useful for extracting information from the observed frequency distribution of a carefully selected measurement. For example, if the exact length, but not the species of every fish passing the sonar were known, the distribution of such measurements might resemble graph “a” in the figure below. With auxiliary information about sockeye and Chinook salmon size, the shape of such a distribution can reveal much about the relative abundance of sockeye and Chinook salmon. For instance, if sockeye salmon were known not to exceed 70 cm, and small Chinook salmon were known to be rare, one could conclude that the left hand mode of the distribution is almost all sockeye salmon and that the species composition is perhaps 50:50 sockeye salmon to Chinook salmon. Mixture model analysis is a quantitative version of this assessment in which the shape of the overall frequency distribution is modeled and “fitted” until it best approximates the data. Uncertainty is assessed by providing a range of plausible species compositions that could have resulted in the observed frequency distribution.

The mixture model analysis is sensitive to and accounts for measurement error. For example, if many Chinook salmon are small and there is error in the length measurements, the effect of the measurement error is to cause the modes of the distribution to overlap, reducing the ability to detect detail in the length distribution and reducing the precision of the estimates (e.g., graph “b” of the figure below). Under this scenario, it is more difficult to interpret the data, but a mixture model approach can provide objective estimates with objective assessments of uncertainty.



Note: True length distributions of sockeye salmon (red dashed line) and Chinook salmon (blue dashed line) are shown along with hypothetical distributions of fish length measurements (black dashed line).

-continued-

The mixture model approach explicitly incorporates the expected variability in hydroacoustic measurements (known from tethered fish experiments), as well as current information about fish size distributions (from the RM 8.6 netting program).

The probability density function (PDF) of ARIS length measurements w was modeled as a weighted mixture of 2 component distributions arising from sockeye salmon and Chinook salmon:

$$f(w) = \pi_s f_s(w) + \pi_c f_c(w) \quad (C1)$$

where $f_s(w)$ and $f_c(w)$ are the PDFs of the sockeye salmon and Chinook salmon component distributions, and the weights π_s and π_c are the proportions of sockeye salmon and Chinook salmon in the population. See also the flow chart in Appendix C2.

Individual observations of w for fish i were modeled as normal random variables whose mean is a linear function of true fish length x :

$$w_i = \beta_0 + \beta_1 x_i + \varepsilon_i \quad (C2)$$

where β_0 is the intercept, β_1 is the slope, and the error ε_i is normally distributed with mean 0 and variance σ^2 .

Thus, the component distributions $f_s(w)$ and $f_c(w)$ are functions of the length distributions $f_s(x)$ and $f_c(x)$ (see Equations C3–C4) and the linear model parameters β_0 , β_1 , and σ^2 . The species proportions π_s and π_c are the parameters of interest.

Length measurements were obtained from fish captured by gillnets immediately downstream of the RM 8.6 sonar site in a midriver corridor corresponding approximately to the portion of the river insonified by DIDSON. Multiple days of length data from the nets were paired with hydroacoustic data from a single day.

Sockeye and Chinook salmon return from the sea to spawn at several discrete ages. We modeled sockeye and Chinook salmon length distributions ($f_s(x)$ and $f_c(x)$, respectively) as 3-component normal age mixtures:

$$f_s(x) = \theta_{s1} f_{s1}(x) + \theta_{s2} f_{s2}(x) + \theta_{s3} f_{s3}(x) \text{ and} \quad (C3)$$

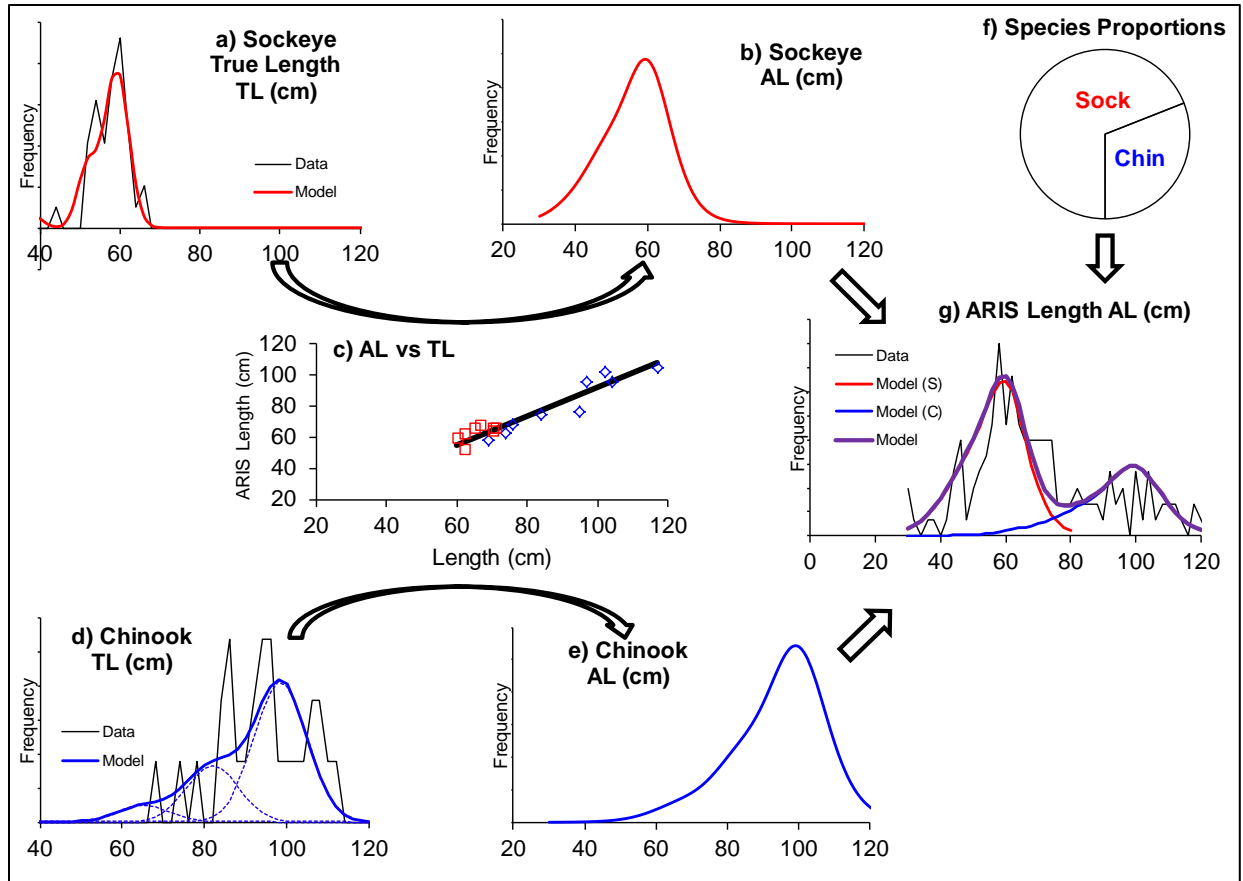
$$f_c(x) = \theta_{c1} f_{c1}(x) + \theta_{c2} f_{c2}(x) + \theta_{c3} f_{c3}(x) \quad (C4)$$

where θ_{Ca} and θ_{Sa} are the proportions of Chinook and sockeye salmon belonging to age component a and the distributions

$$f_{Sa}(x) \sim N(\mu_{Sa}, \tau_{Sa}^2), \text{ and} \quad (C5)$$

$$f_{Ca}(x) \sim N(\mu_{Ca}, \tau_{Ca}^2) \quad (C6)$$

where μ is mean length-at-age and τ is the standard deviation. The overall design is therefore a mixture of (transformed) mixtures. That is, the observed hydroacoustic data are modeled as a 2-component mixture (sockeye salmon and Chinook salmon) of ARIS length (w), each component of which is transformed from a 3-component normal age mixture of fish length (x).



Appendix C2.—Flow chart of a mixture model.

Note: The frequency distribution of ARIS length (AL, Panel g) is modeled as a weighted mixture of species-specific AL distributions (Panels b and e), which in turn are the products of species-specific size distributions (Panels a and d) and the relationship between AL and true fish length (Panel c). The weights (species proportions, Panel f) are the parameters of interest.

Bayesian statistical methods were employed to fit the mixture model to the data. Bayesian methods were chosen because they provide realistic estimates of uncertainty and the ability to incorporate diverse sources of auxiliary information. We implemented the Bayesian mixture model in WinBUGS (Bayes Using Gibbs Sampler; Gilks et al. 1994) (Appendix C4). Bayesian methods require that prior probability distributions be formulated for all unknowns in the model (Gelman et al. 2004). Species proportions π_S and π_C (Equation C1) were assigned a mildly informative Dirichlet (0.1,0.9) prior. Likewise, informative normal priors based on historical data were used for the length-at-age means μ and standard deviations τ (Appendix C4). A linear statistical model of tethered fish data (Burwen et al. 2003) was integrated into the mixture model (Appendix C5) to provide information on regression parameters β_0 , β_1 , and σ^2 .

The end product of a Bayesian analysis is the joint posterior probability distribution of all unknowns in the model. For point estimates, posterior means were used. Posterior standard deviations were reported as analogues to the standard error of an estimate from a classical (non-Bayesian) statistical analysis.

Mixture model results were more robust to length measurement error if only a minimal number of tethered fish data points were used, so a subset of tethered fish data from 2007 DIDSON experiments (Burwen et al. 2010) provided a mildly informative prior for the β_0 and β_1 parameters (Equation C2). Species proportions π_C and π_S were assigned a Dirichlet (0.1,0.9) prior. Prior distributions for age proportions $\{\theta_{ca}\}$ and $\{\theta_{sa}\}$ were constructed with nested beta (0.5,0.5) distributions. Netting probability of capture was assumed to be equal for all 3 age classes. Netting length data from days $d-6$ through d were paired with ARIS length data from day d .

WinBUGS uses Markov chain Monte Carlo methods to sample from the joint posterior distribution of all unknown quantities in the model. A single Markov chain¹⁶ was initiated for each daily run of the ARIS length mixture model, samples were thinned 10 to 1, and history plots were monitored to confirm convergence and mixing. The first 5,000 or more “burn-in” samples were discarded, and at least 10,000 additional samples were drawn from the posterior distribution.

See Fleischman and Burwen (2003) for an application of these methods to split-beam sonar data. Some of the methodological details used to produce the estimates in this report differ from those used to produce preliminary 2010–2012 mixture model estimates that were reported elsewhere (Fleischman and McKinley 2013: Table 4; and McKinley and Fleischman 2013: Table 5). These modifications are summarized in Appendix C6.

¹⁶ During initial development of the model, multiple chains were used to assess convergence (Gelman et al. 2004). This was not necessary during production of daily estimates.

```

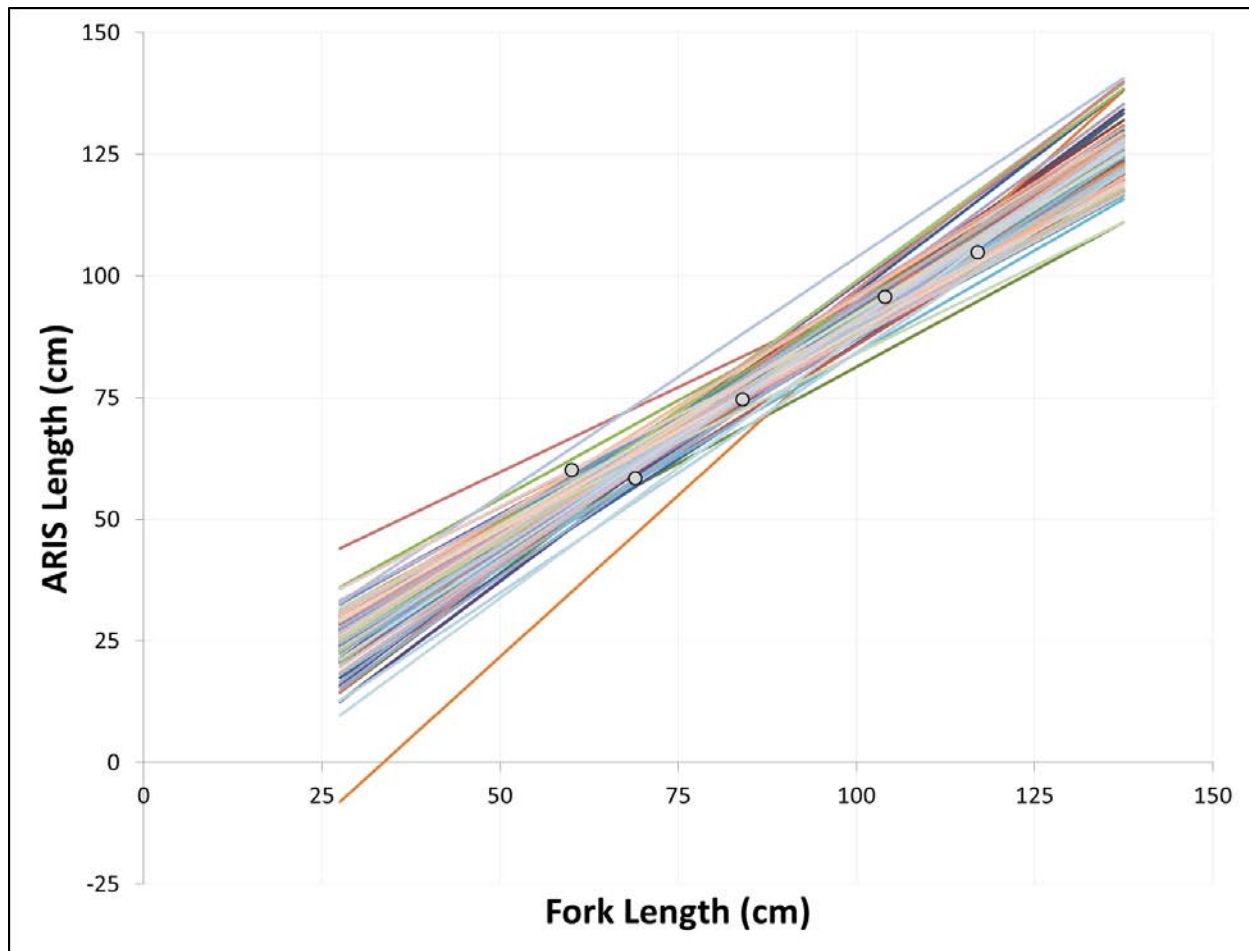
model{
  beta0 ~ dnorm(75,0.0025)
  beta1 ~ dnorm(1,25)
  sigma.AL ~ dunif(0,20)
  tau.AL <- 1 / sigma.AL / sigma.AL
  ps[1:2] ~ ddirch(D.species[])
  pa[1,1] ~ dbeta(0.5,0.5)
  theta1 ~ dbeta(0.5,0.5)
  pa[1,2] <- theta1 * (1 - pa[1,1])
  pa[1,3] <- 1 - pa[1,1] - pa[1,2]
  pa[2,1] ~ dbeta(0.5,0.5)
  theta2 ~ dbeta(0.5,0.5)
  pa[2,2] <- theta2 * (1 - pa[2,1])
  pa[2,3] <- 1 - pa[2,1] - pa[2,2]

  n.chin <- ps[1] * n_meas
  p.large <- ps[1] * (1 - pa[1,1] - pa[1,2])
  n.large <- p.large * n_meas

  Lsig[1,1] <- 78
  Lsig[1,2] <- 70
  Lsig[1,3] <- 74
  Lsig[2,1] <- 25
  Lsig[2,2] <- 25
  Lsig[2,3] <- 25
  for (s in 1:2) {for (a in 1:3) {Ltau[s,a] <- 1 / Lsig[s,a] / Lsig[s,a] }}
  mu[1,1] ~ dnorm(621,0.0076)
  mu[1,2] ~ dnorm(825,0.0021)
  mu[1,3] ~ dnorm(1020,0.0047)
  mu[2,1] ~ dnorm(380,0.0004)
  mu[2,2] ~ dnorm(500,0.0004)
  mu[2,3] ~ dnorm(580,0.0004)
  for (a in 1:3) {
    pa.effective[1,a] <- pa[1,a] * q1.a[a] / inprod(pa[1,],q1.a[])
    pa.effective[2,a] <- pa[2,a]
  }
  for (k in 1:5) {
    TL.cm.75[k] <- TL.cm[k] - 75
    mu.AL1[k] <- beta0 + beta1 * TL.cm.75[k]
    DL1[k] ~ dnorm(mu.AL1[k],tau.AL)
  }
  for (i in 1:n_fish) {
    age[i] ~ dcat(pa.effective[species[i],1:3])
    mefl.mm[i] ~ dnorm(mu[species[i],age[i]],Ltau[species[i],age[i]])
  }
  for (j in 1:n_meas) {
    species2[j] ~ dcat(ps[])
    age2[j] ~ dcat(pa[species2[j],1:3])
    mefl.mm.2[j] ~ dnorm(mu[species2[j],age2[j]],Ltau[species2[j],age2[j]])
    TL2.cm.75[j] <- (1.1*mefl.mm.2[j] + 2) / 10 - 75
    mu.AL2[j] <- beta0 + beta1 * TL2.cm.75[j]
    AL2[j] ~ dnorm(mu.AL2[j],tau.AL)I(40,)
  }
}

```

Note: Prior distributions are shown in green font, likelihoods in blue.



Appendix C5.—Abridged tethered fish data set (symbols) used to provide a mildly informative prior distribution for the relationship between fork length (FL) and ARIS length (AL). Plausible relationships (lines) are plotted using 100 random samples of the slope and intercept from the prior distribution.

Appendix C6.—Methodological details of ARIS length mixture models compared to DIDSON length mixture models at RM 8.6, Kenai River, 2013.

	Inseason	Final	Final
	DIDSON RM 8.6		
Modification	ARIS RM 13.7	DIDSON RM 8.6 ^a	ARIS RM 13.7 ^b
Age composition prior	informative ^c	noninformative ^d	noninformative ^d
Species composition prior	Dirichlet(0.5,0.5)	Dirichlet(0.1,0.9)	Dirichlet(0.1,0.9)
Days of netting data pooled and paired with day d of sonar data	$d-6$ to d	$d-3$ to $d+3$	$d-6$ to d
Chinook salmon size selectivity by age class	0.61, 0.57, 0.41	1, 1, 1	1, 1, 1
Tethered fish data	Abridged $n = 5$ ^e	Abridged $n = 5$ ^e	Abridged $n = 5$ ^e

^a Key et al. (Key et al. 2016a, 2016b)

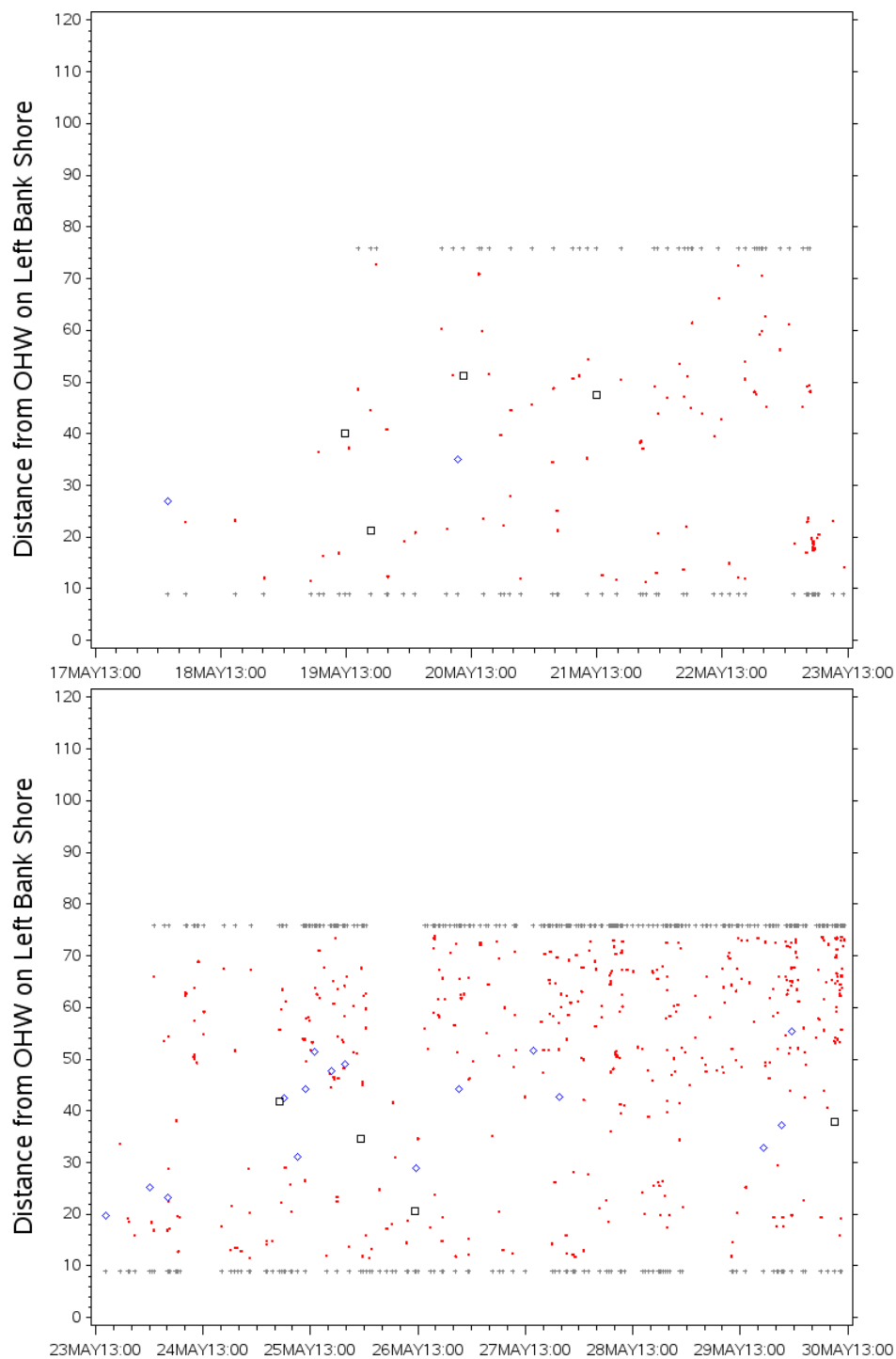
^b This report.

^c Informative priors differed by week, as developed from an hierarchical age composition model.

^d Noninformative nested beta priors (see Appendix C4).

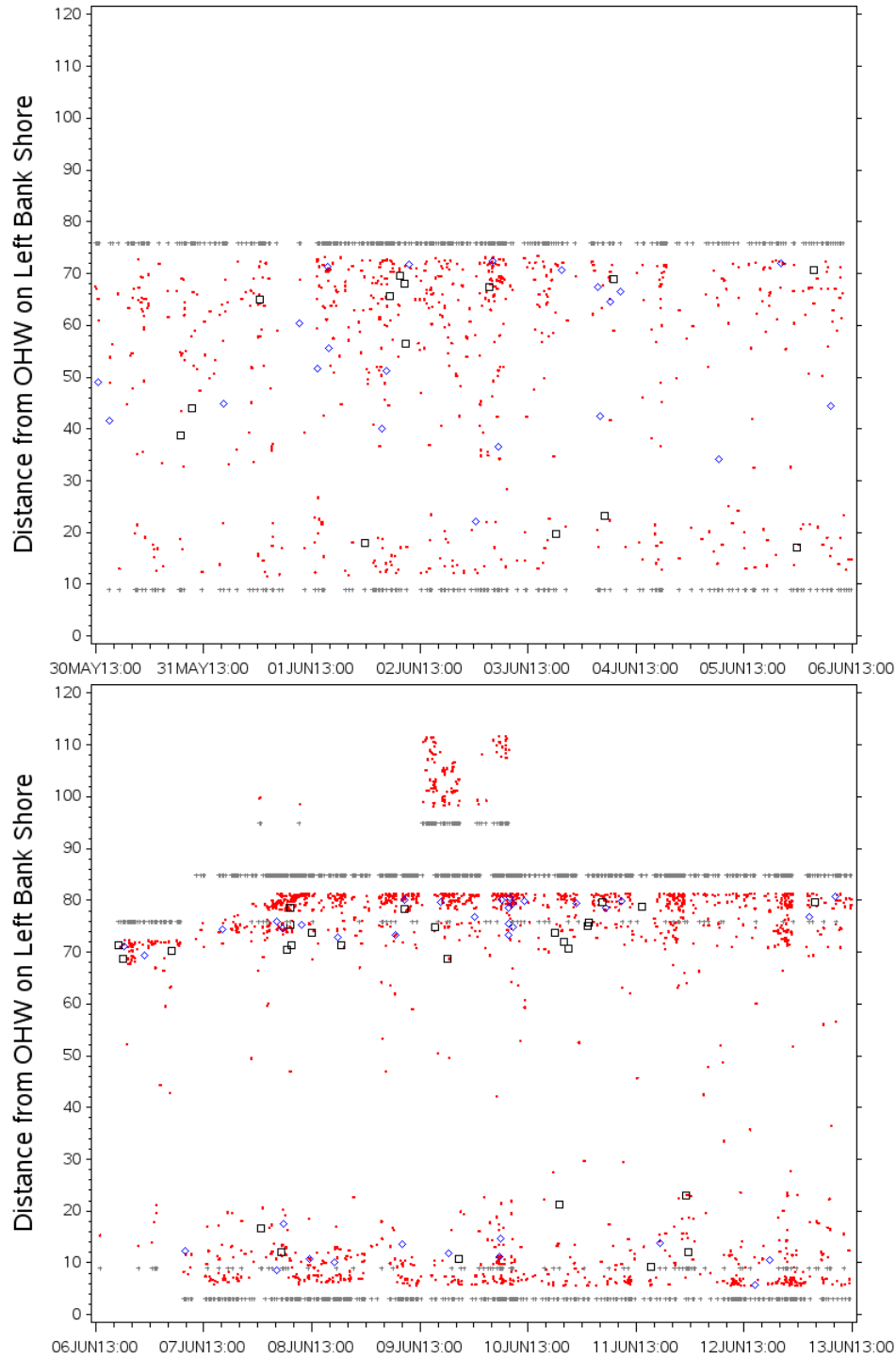
^e See Appendix C5.

**APPENDIX D: SPATIAL AND TEMPORAL DISTRIBUTION
OF FISH BY SIZE AS MEASURED BY ARIS, RM 13.7
KENAI RIVER, 2013**



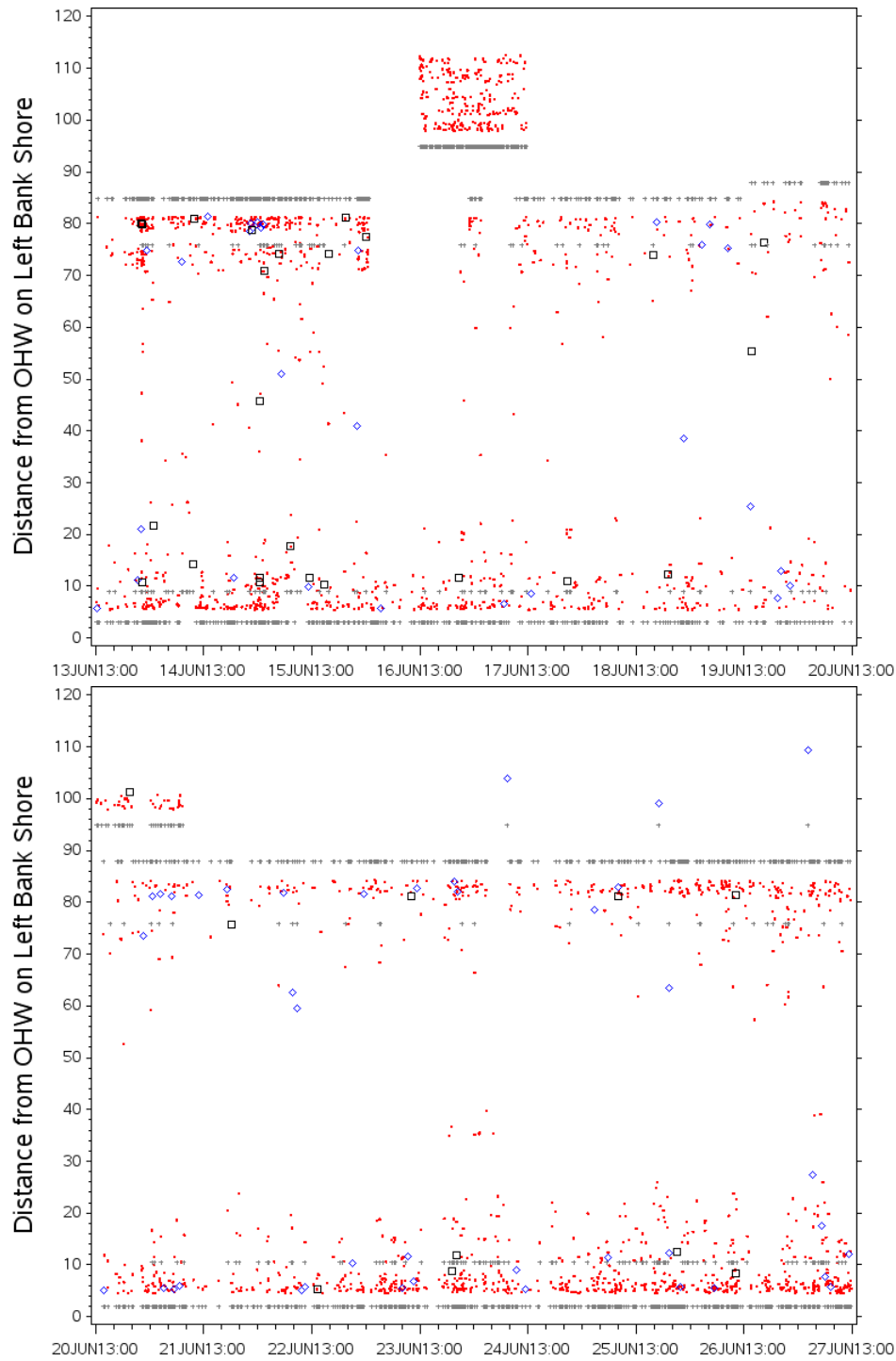
Appendix D1.—Spatial and temporal distribution of small (ARIS length [AL] < 75 cm; small red dots), medium (75 cm ≤ AL < 90 cm; larger blue diamonds), and large fish (AL ≥ 90 cm; large black squares), RM 13.7 Kenai River, 17–29 May 2013.

Note: Small fish can be underrepresented in the sample. Transducer locations are plotted as small grey crosses, one per fish. For the main channel, the vertical axis is the distance from a reference point near the ordinary high water level (OHW) on the left bank.



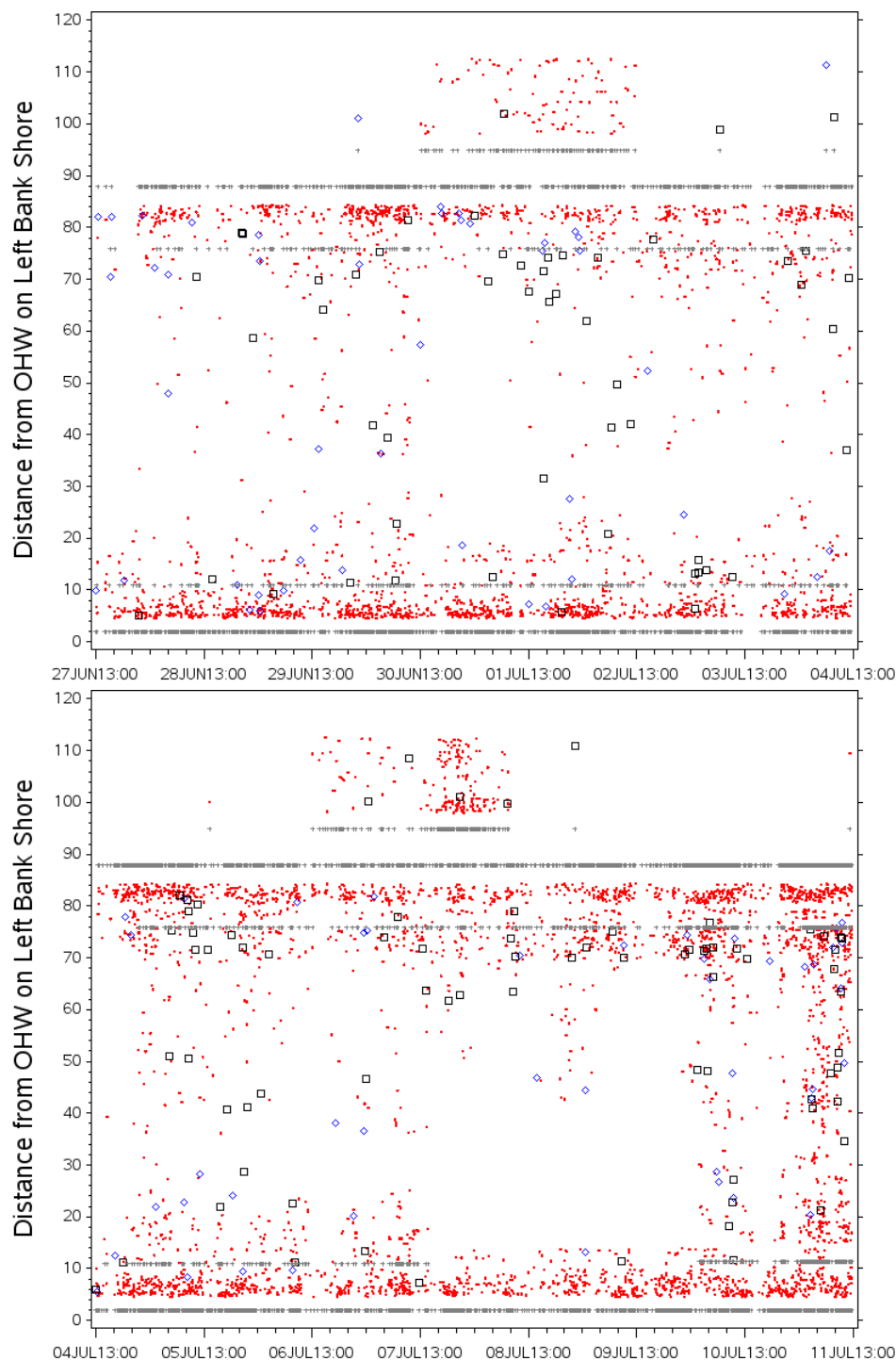
Appendix D2.—Spatial and temporal distribution of small (ARIS length [AL] < 75 cm; small red dots), medium (75 cm ≤ AL < 90 cm; larger blue diamonds), and large fish (AL ≥ 90 cm; large black squares), RM 13.7 Kenai River, 30 May–12 June 2013.

Note: Small fish can be underrepresented in the sample. Transducer locations are plotted as small grey crosses, one per fish. For the main channel, the vertical axis is the distance from a reference point near the ordinary high water level on the left bank. The side channel transducer was arbitrarily set to 95 m for graphical convenience.



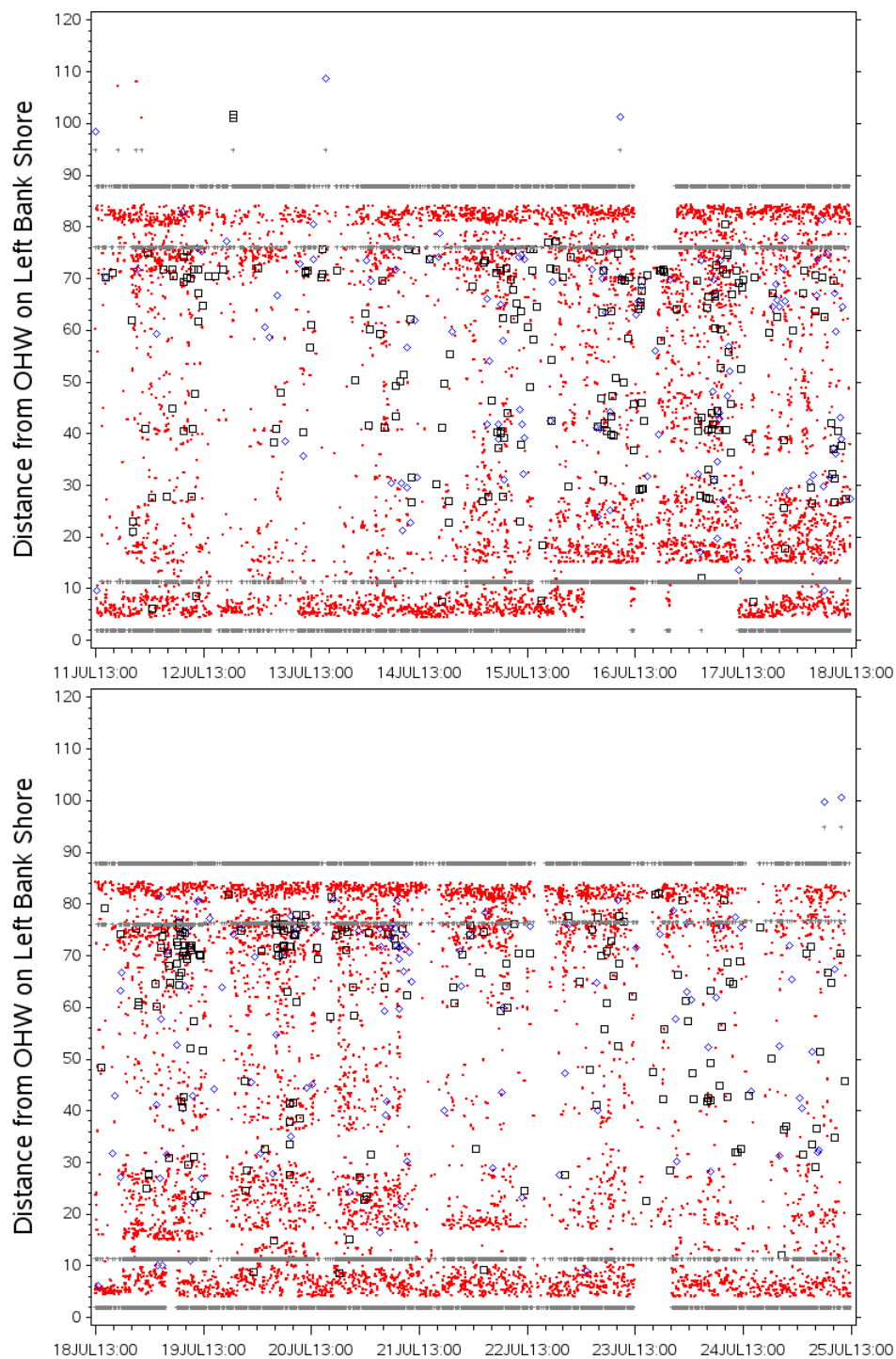
Appendix D3.—Spatial and temporal distribution of small (ARIS length [AL] < 75 cm; small red dots), medium ($75 \text{ cm} \leq \text{AL} < 90 \text{ cm}$; larger blue triangles), and large fish ($\text{AL} \geq 90 \text{ cm}$; large black squares), RM 13.7 Kenai River, 13–26 June 2013.

Note: Small fish can be underrepresented in the sample. Transducer locations are plotted as small grey crosses, one per fish. For the main channel, the vertical axis is the distance from a reference point near the ordinary high water level on the left bank. The side channel transducer was arbitrarily set to 95 m for graphical convenience.



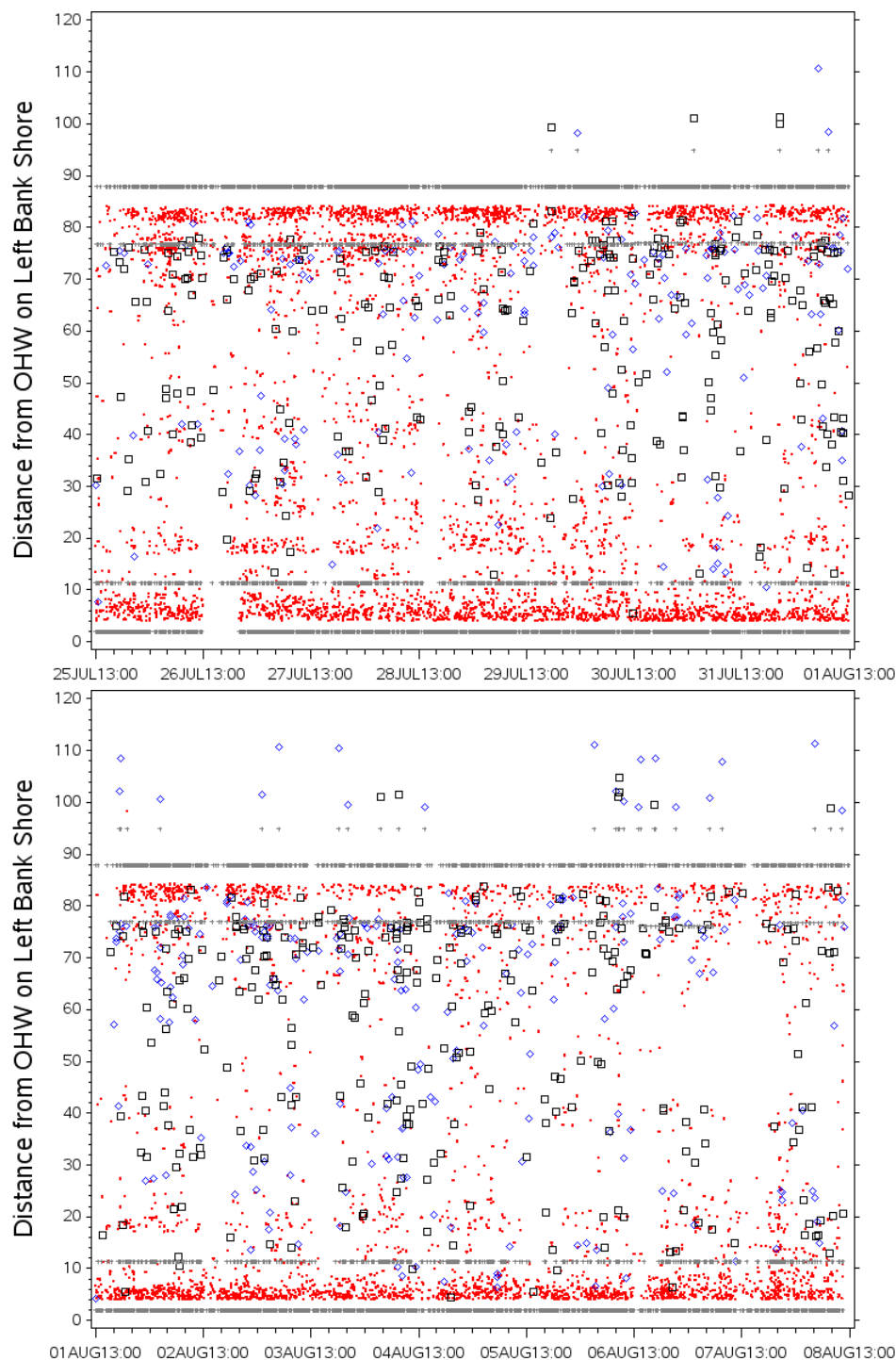
Appendix D4.—Spatial and temporal distribution of small (ARIS length [AL] < 75 cm; small red dots), medium ($75 \text{ cm} \leq \text{AL} < 90 \text{ cm}$; larger blue diamonds), and large fish ($\text{AL} \geq 90 \text{ cm}$; large black squares), RM 13.7 Kenai River, 27 June–10 July 2013.

Note: Small fish can be underrepresented in the sample. Transducer locations are plotted as small grey crosses, one per fish. For the main channel, the vertical axis is the distance from a reference point near the ordinary high water level on the left bank. The side channel transducer was arbitrarily set to 95 m for graphical convenience.



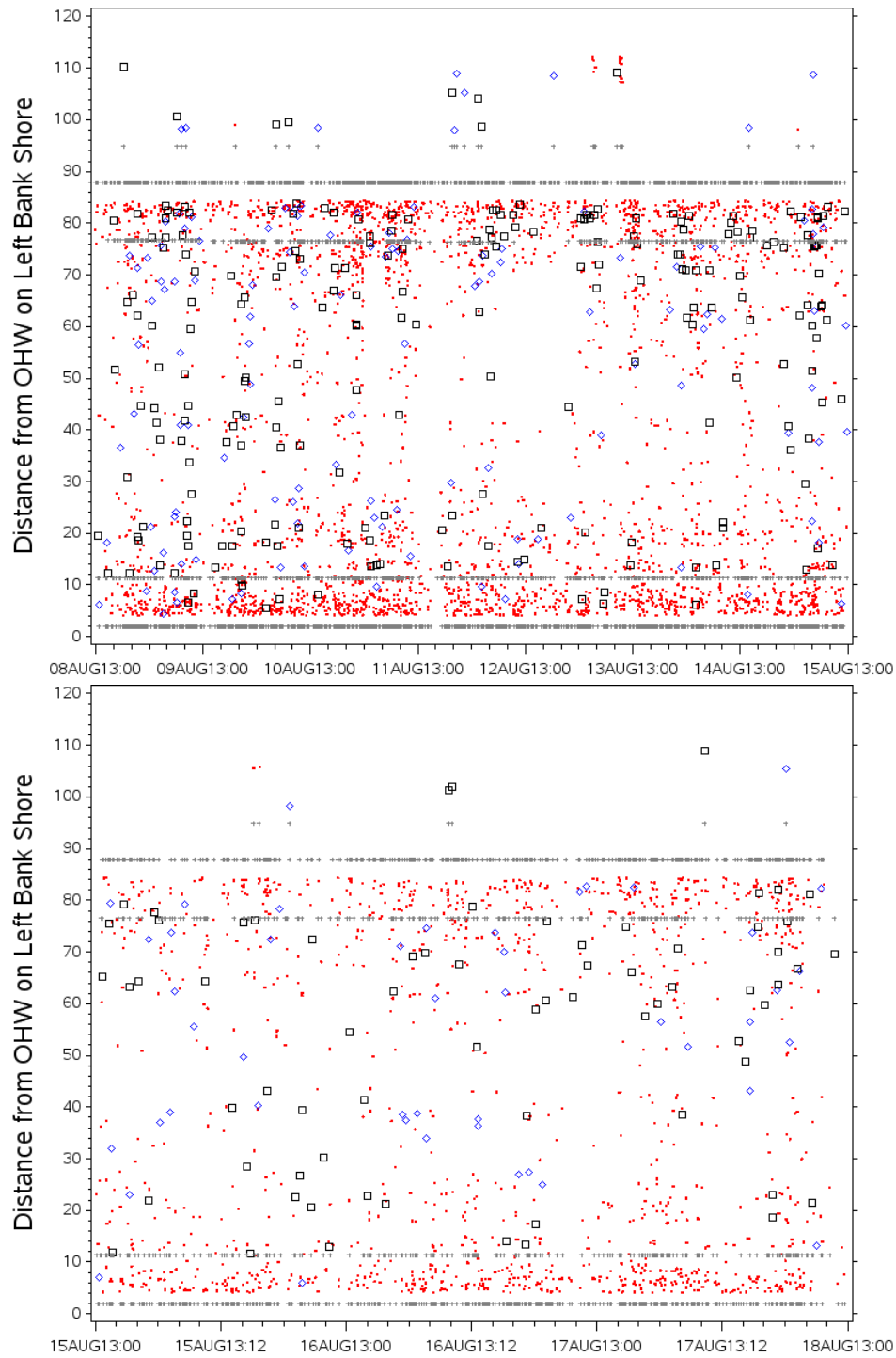
Appendix D5.—Spatial and temporal distribution of small (ARIS length [AL] < 75 cm; small red dots), medium (75 cm ≤ AL < 90 cm; larger blue diamonds), and large fish (AL ≥ 90 cm; large black squares), RM 13.7 Kenai River, 11–24 July 2013.

Note: Small fish can be underrepresented in the sample. Transducer locations are plotted as small grey crosses, one per fish. For the main channel, the vertical axis is distance from a reference point near the ordinary high water level on the left bank. The side channel transducer was arbitrarily set to 95 m for graphical convenience.



Appendix D6.—Spatial and temporal distribution of small (ARIS length [AL] < 75 cm; small red dots), medium (75 cm ≤ AL < 90 cm; larger blue diamonds), and large fish (AL ≥ 90 cm; large black squares), RM 13.7 Kenai River, 25 July–7 August 2013.

Note: Small fish can be underrepresented in the sample. Transducer locations are plotted as small grey crosses, one per fish. For the main channel, vertical axis is the distance from a reference point near the ordinary high water level on the left bank. The side channel transducer was arbitrarily set to 95 m for graphical convenience.



Appendix D7.—Spatial and temporal distribution of small (ARIS length [AL] < 75 cm; small red dots), medium (75 cm ≤ AL < 90 cm; larger blue diamonds), and large fish (AL ≥ 90 cm; large black squares), RM 13.7 Kenai River, 8–17 August 2013.

Note: Small fish can be underrepresented in the sample. Transducer locations are plotted as small grey crosses, one per fish. For the main channel, the vertical axis is distance from a reference point near the ordinary high water level on the left bank. The side channel transducer was arbitrarily set to 95 m for graphical convenience.

**APPENDIX E: DIRECTION OF TRAVEL OF MEDIUM AND
LARGE FISH DETECTED BY ARIS, RM 13.7 KENAI
RIVER, 2013**

Appendix E1.—Daily count and proportion of fish greater than or equal to 75 cm ARIS length moving upstream and downstream for the early run, RM 13.7 Kenai River, 2013.

Date	Downstream		Upstream		Total number sampled
	Number	Percent	Number	Percent	
17 May	0		0		0
18 May	0	0%	1	100%	1
19 May	0	0%	3	100%	3
20 May	0		0		0
21 May	1	50%	1	50%	2
22 May	0		0		0
23 May	1	33%	2	67%	3
24 May	1	20%	4	80%	5
25 May	0	0%	6	100%	6
26 May	0	0%	1	100%	1
27 May	0	0%	2	100%	2
28 May	0		0		0
29 May	0	0%	4	100%	4
30 May	0	0%	3	100%	3
31 May	0	0%	3	100%	3
1 Jun	0	0%	11	100%	11
2 Jun	0	0%	4	100%	4
3 Jun	0	0%	8	100%	8
4 Jun	0	0%	1	100%	1
5 Jun	0	0%	4	100%	4
6 Jun	0	0%	5	100%	5
7 Jun	0	0%	13	100%	13
8 Jun	1	11%	8	89%	9
9 Jun	0	0%	16	100%	16
10 Jun	0	0%	10	100%	10
11 Jun	0	0%	5	100%	5
12 Jun	0	0%	5	100%	5
13 Jun	0	0%	10	100%	10
14 Jun	0	0%	18	100%	18
15 Jun	0	0%	7	100%	7
16 Jun	0	0%	2	100%	2
17 Jun	0	0%	2	100%	2
18 Jun	1	13%	7	88%	8
19 Jun	0	0%	6	100%	6
20 Jun	1	10%	9	90%	10
21 Jun	0	0%	7	100%	7
22 Jun	0	0%	8	100%	8

-continued-

Appendix E1.–Page 2 of 2.

Date	Downstream		Upstream		Total number sampled
	Number	Percent	Number	Percent	
23 Jun	0	0%	7	100%	7
24 Jun	0	0%	4	100%	4
25 Jun	0	0%	8	100%	8
26 Jun	0	0%	6	100%	6
27 Jun	1	8%	11	92%	12
28 Jun	0	0%	13	100%	13
29 Jun	0	0%	16	100%	16
30 Jun	0	0%	13	100%	13
Total	7	2.5%	274	97.5%	281

Appendix E2.—Daily count and proportion of fish greater than or equal to 75 cm ARIS length moving upstream and downstream for the late run, RM 13.7 Kenai River, 2013.

Date	Downstream		Upstream		Total number sampled
	Number	Percent	Number	Percent	
1 Jul	2	8%	23	92%	25
2 Jul	0	0%	10	100%	10
3 Jul	1	8%	11	92%	12
4 Jul	2	10%	19	90%	21
5 Jul	2	12%	15	88%	17
6 Jul	0	0%	13	100%	13
7 Jul	2	15%	11	85%	13
8 Jul	0	0%	10	100%	10
9 Jul	1	4%	22	96%	23
10 Jul	0	0%	29	100%	29
11 Jul	1	3%	36	97%	37
12 Jul	2	8%	22	92%	24
13 Jul	0	0%	34	100%	34
14 Jul	3	5%	54	95%	57
15 Jul	2	4%	55	96%	57
16 Jul	5	6%	80	94%	85
17 Jul	3	5%	54	95%	57
18 Jul	5	6%	75	94%	80
19 Jul	6	10%	55	90%	61
20 Jul	0	0%	52	100%	52
21 Jul	6	19%	26	81%	32
22 Jul	2	7%	27	93%	29
23 Jul	3	7%	43	93%	46
24 Jul	7	18%	31	82%	38
25 Jul	3	6%	46	94%	49
26 Jul	3	5%	57	95%	60
27 Jul	6	11%	48	89%	54
28 Jul	1	2%	52	98%	53
29 Jul	4	6%	62	94%	66
30 Jul	7	8%	78	92%	85
31 Jul	4	5%	82	95%	86
1 Aug	3	4%	79	96%	82
2 Aug	5	5%	87	95%	92
3 Aug	11	10%	96	90%	107
4 Aug	9	11%	74	89%	83
5 Aug	10	11%	77	89%	87

-continued-

Appendix E2.–Page 2 of 2.

Date	Downstream		Upstream		Total number sampled
	Number	Percent	Number	Percent	
6 Aug	3	5%	52	95%	55
7 Aug	9	16%	46	84%	55
8 Aug	3	3%	83	97%	86
9 Aug	2	3%	58	97%	60
10 Aug	4	7%	52	93%	56
11 Aug	2	5%	39	95%	41
12 Aug	2	7%	27	93%	29
13 Aug	0	0%	40	100%	40
14 Aug	7	11%	56	89%	63
15 Aug	3	7%	39	93%	42
16 Aug	11	22%	39	78%	50
17 Aug	3	8%	36	92%	39
Total	170	7.1%	2,212	92.9%	2,382